IMPROVED METHODS TO ENHANCE THE COLOR PERCEPTION FOR PEOPLE WITH COLOR VISION DEFICIENCY

MOHD FIKREE BIN HASSAN

FACULTY OF ENGINEERING
UNIVERSITY OF MALAYA
KUALA LUMPUR

2018

IMPROVED METHODS TO ENHANCE THE COLOR PERCEPTION FOR PEOPLE WITH COLOR VISION DEFICIENCY

MOHD FIKREE BIN HASSAN

THESIS SUBMITTED IN FULFILMENT OF THE REQUIREMENTS FOR THE DEGREE OF DOCTOR OF PHILOSOPHY

FACULTY OF ENGINEERING
UNIVERSITY OF MALAYA
KUALA LUMPUR

2018

UNIVERSITI MALAYA

ORIGINAL LITERARY WORK DECLARATION

Name of Candidate: Mohd Fikree bin Hassan

Registration/Matric No.: KHA150003

Name of Degree: Doctor of Philosophy (Engineering)

Title of Thesis ("this Work"): Improved Methods to Enhance the Color Perception for People with Color Vision Deficiency

Field of Study: Signal and Systems

I do solemnly and sincerely declare that:

(1) I am the sole author/writer of this Work;
(2) This work is original;
(3) Any use of any work in which copyright exists was done by way of fair dealing and for permitted purposes and any excerpt or extract from, or reference to or reproduction of any copyright work has been disclosed expressly and sufficiently and the title of the Work and its authorship have been acknowledged in this Work;
(4) I do not have any actual knowledge nor do I ought reasonably to know that the making of this work constitutes an infringement of any copyright work;
(5) I hereby assign all and every rights in the copyright to this Work to the University of Malaya ("UM"), who henceforth shall be owner of the copyright in this Work and that any reproduction or use in any form or by any means whatsoever is prohibited without the written consent of UM having been first had and obtained;
(6) I am fully aware that if in the course of making this Work I have infringed any copyright whether intentionally or otherwise, I may be subject to legal action or any other action as may be determined by UM.

Candidate's Signature Date:

Subscribed and solemnly declared before,

Witness's Signature Date:

Name:
Designation:

IMPROVED METHODS TO ENHANCE THE COLOR PERCEPTION FOR PEOPLE WITH COLOR VISION DEFICIENCY

ABSTRACT

Color images are widely used to disseminate information in public places, on Web sites, and on smartphone applications. Moreover, millions of color images are also shared and used as a medium of communication among people. However, people with color vision deficiency are not able to discriminate certain colors and may thus misinterpret information. Elderly people also suffer from loss of color perception as a result of age. In this thesis, both color perception loss among the elderly people as well as those with red-green deficiency are studied.

Recent clinical studies of color perception of the elderly show that as humans age, uniform yellowing pigmentation occurs on the human lens. In order to understand the effect of the uniform yellowing pigmentation, a mathematical formulation has been proposed in this thesis. The mathematical formulation uses the measured transmittance functions of the liquid-crystal display (LCD) and the spectral transmission factor of the human lens. Based on the values, three effective tristimulus ratios are computed, and the uniform yellowing pigmentation is simulated. The simulated uniform yellowing pigmentation is compared with the results of recent clinical studies for validation. The comparison shows that the simulated uniform yellowing pigmentation is in agreement with the results from these clinical studies. Using the uniform yellowing pigmentation, color perception of the elderly is simulated to three different types of images; MacBeth ColorCheckers color patches, synthesized and real images. The results of the simulated images show that as humans age, the images lose their bluish element and become yellowish. Furthermore, comparison with the non-uniform yellowing pigmentation methods show that the results from the proposed

method are closer to the clinical data.

Various image recoloring methods have been proposed by researchers to improve the color perception of people with red-green deficiency. However, the recolored images may look non-pleasing to people with normal color vision. Moreover, the recolored images may lose their naturalness. In addition, some of the recoloring methods utilize complex and iterative processes that may not be suitable for practical usage. This thesis proposes a much simpler and efficient recoloring method that enhances the color perception of people with red-green deficiency while maintaining the naturalness of the original images as much as possible. The proposed method utilizes the error and rotation parameters to recolor the images. Using this process, the recolored images have the same luminance and hue as the original images. Objective evaluation shows that the recolored images maintain the naturalness better than three other existing methods. A total of twenty six people, which includes fifteen people with normal color vision and eleven red-green deficients, took part in the paired comparison test. The results of the paired comparison test show that the proposed method achieves higher preference scores in terms of naturalness preservation and the overall preference.

Keywords: Color vision deficiency, uniform yellowing pigmentation, color perception of the elderly, red-green deficients, naturalness preservation.

KAEDAH-KAEDAH PENAMBAHBAIKAN UNTUK MENINGKATKAN PERSEPSI WARNA BAGI ORANG YANG MEMPUNYAI KEKURANGAN PENGLIHATAN BERWARNA

ABSTRAK

Imej berwarna digunakan secara meluas untuk menyebarkan maklumat di tempat awam, di laman web, dan pada aplikasi telefon pintar. Malahan, jutaan imej berwarna juga dikongsi dan digunakan sebagai medium komunikasi di kalangan orang ramai. Walau bagaimanapun, orang yang mempunyai kekurangan penglihatan warna tidak dapat membezakan antara warna-warna tertentu dan oleh kerana itu, kesalahan dalam mentafsir maklumat mungkin berlaku. Orang tua juga mengalami kehilangan persepsi warna akibat peningkatan usia. Dalam tesis ini, kajian terhadap kehilangan persepsi warna orang tua, dan mereka yang mengalami kekurangan penglihatan merah-hijau telah dijalankan.

Kajian klinikal terkini mengenai persepsi warna orang tua menunjukkan bahawa apabila usia manusia meningkat, pigmentasi kuning seragam terbentuk pada lensa mata manusia. Untuk memahami kesan pigmentasi kuning seragam, satu formulasi matematik telah dicadangkan di dalam tesis ini. Formulasi matematik ini menggunakan fungsi transmisi yang diukur dari paparan kristal cecair (LCD) dan faktor transmisi spektrum lensa manusia. Berdasarkan nilai-nilai ini, tiga nilai tristimulus berkesan dikira dan digunakan untuk menghasilkan simulasi pigmentasi kuning seragam. Untuk pengesahan, pigmentasi kuning seragam yang dihasilkan telah dibandingkan dengan hasil kajian klinikal terkini. Hasil perbandingan menunjukkan pigmentasi kuning seragam yang terhasil adalah seiring dengan hasil kajian klinikal. Dengan menggunakan pigmentasi kuning seragam ini, persepsi warna orang tua telah disimulasi kepada tiga jenis imej; keratan warna daripada MacBeth ColorCheckers, imej sintetik, dan imej semulajadi. Keputusan simulasi menunjukkan apabila usia manusia meningkat, imej yang terhasil hilang unsur kebiruan dan menjadi kekuningan. Tambahan pula, perbandingan antara kaedah yang dicadangkan dan kaedah pigmentasi kuning tidak seragam menunjukkan bahawa keputusan daripada kaedah yang dicadangkan adalah lebih hampir dengan keputusan daripada data klinikal. Pelbagai kaedah pewarnaan semula imej telah dicadangkan oleh para penyelidik untuk meningkatkan persepsi warna bagi orang yang mempunyai kekurangan penglihatan merah-hijau. Walaubagaimanapun, imej yang dihasilkan kelihatan tidak menyenangkan kepada penglihatan manusia biasa. Malahan, imej yang terhasil mungkin akan kehilangan ciri-ciri semulajadi. Di samping itu, beberapa kaedah pewarnaan semula imej menggunakan proses yang kompleks and pengiraan berulang yang mungkin tidak sesuai untuk kegunaan praktikal. Tesis ini mencadangkan kaedah pewarnaan semula yang lebih mudah dan cekap untuk meningkatkan persepsi warna bagi orang yang mempunyai kekurangan penglihatan merah-hijau di samping mengekalkan keaslian imej aslinya sebanyak yang mungkin. Kaedah yang dicadangkan menggunakan parameter ralat dan parameter putaran untuk mewarnakan semula imej. Dengan menggunakan proses ini, imej yang terhasil mempunyai ciri-ciri cahaya dan warna yang sama dengan imej asal. Penilaian objektif menunjukkan bahawa imej yang terhasil berjaya mengekalkan ciri-ciri semulajadi yang lebih baik daripada tiga kaedah sedia ada yang lain. Seramai dua puluh enam orang yang terdiri daripada lima belas orang dengan penglihatan warna yang normal dan sebelas orang dengan kekurangan penglihatan merah-hijau mengambil bahagian di dalam ujian perbandingan berpasangan. Hasil ujian ini menunjukkan bahawa kaedah yang dicadangkan mendapat skor keutamaan yang lebih tinggi dari segi pemeliharaan ciri-ciri semulajadi imej asal dan keseluruhan pilihan.

Katakunci: Kekurangan penglihatan warna, pigmentasi kuning seragam, persepsi warna orang tua, kekurangan penglihatan merah-hijau, pemeliharaan keaslian imej.

ACKNOWLEDGEMENTS

This thesis has benefited greatly from the support of many people, some of whom I would sincerely like to thank here:

My thesis supervisor, Professor Dr. Raveendran Paramesran for offering me such an interesting topic of investigation. His continuous guidance, constant support and invaluable suggestions and advice have given me the confidence to complete this research work.

Present and past members of the Center for Signal and Image Processing (CISIP) of University of Malaya, for their direct and indirect contribution to the constructive ideas and the time together in the lab.

All the authors of the color vision deficiencies, who shared their source codes and results of the tests. Without their unselfish sharing of knowledge and data, the comparison studies would not be possible.

All the people behind the offices of the Department of Electrical Engineering and Faculty of Engineering for giving me the opportunity to pursue my education.

Last but not least, I would like to thank my family and friends for their constant support and encouragement throughout the difficult times. Not forgotten is my gratitude to those who have helped me but not mentioned here.

Mohd Fikree bin Hassan

Department of Electrical Engineering

Faculty of Engineering

University of Malaya

September 2018

TABLE OF CONTENTS

LIST OF FIGURES

LIST OF TABLES

LIST OF SYMBOLS AND ABBREVIATIONS

CIE : International Commission on Illumination

EM : Expectation-Maximization

FSIMc : Feature Similarity chrominance

GMM : Gaussian Mixture Model

HSV : Hue-Saturation-Value

HVS : Human Visual System

IEC : International Electrotechnical Commission

LCD : Liquid Crystal Display

RGB : Red Green Blue

SPP : Standard Pseudoisochromatic Plates

sRGB : standard Red Green Blue

LIST OF APPENDICES

CHAPTER 1: INTRODUCTION

1.1 Overview

An image is an object that portrays visual perception. It can be two-dimensional, such as a photograph and a map, and it can also be three-dimensional, such as a hologram. In the current world of digital information technology that we live in, two-dimensional color images play an important role in human lives. Color images not only embody information but are also used as a medium of communication among people. Hence, the usage of color images in distributing information via websites and smartphone applications has increased in the 21st century. Electronic devices such as laptops and smartphones have become essential items as millions of color images are shared on Facebook (Thomas, 2012) and Instagram (DesMarais, 2013) everyday. Moreover, color images are also utilized in advertisement boards, traffic maps, and signboards in public places such as airports, shopping malls, and train stations.

Color is an attribute of visual sensation and the color appearance of an object depends on the interaction between three main components; light sources, objects and the human visual system (Fairchild, 2005). The interaction between the light sources and the physical and chemical properties of an object creates a modulated energy that will be processed by the human visual system to produce the perceptions of color. The ability to distinguish the set of signals that are produced by the modulated energy is known as human color perception (Fairchild, 2005). The modulated energy reacts with the three types of cone photoreceptors in the human eye. Each of the cone photoreceptors is sensitive to either short (S), medium (M), and long (L) wavelength light, and each wavelength light exhibits bluish, greenish, and reddish sensitivity respectively (Hunt, 2004; Pascale, 2003).

However, a percentage of people have some kind of color vision deficiency that arise from differences in the pigmentation of the cone photoreceptors in their eyes (Wandell, 1995). Thus, they are unable to distinguish certain shades of colors. This inability may create barriers in terms of physical capabilities (Hassan & Paramesran, 2017). Some of them may have difficulty finding goods in stores, and some may even bump into a glass door due to the confusion that occurs to their color perception (K. Ishihara, Ishihara, Nagamachi, Hiramatsu, & Osaki, 2001). Moreover, the reaction time and cognitive time of the elderly are slower compared to younger people (T. Suzuki, Okajima, & Funai, 2012; T. Suzuki, Yi, Sakuragawa, Tamura, & Okajima, 2005). In addition, their social life and even their career may be affected due to their inability to discriminate colors (Cole, 2007; Tagarelli et al., 2004).

Color vision deficiency can be categorized as acquired and inherited (Simunovic, 2016; Verriest, 1963). In acquired color vision deficiency, color perception loss is due to medication, aging, disease, or accidents. As reported by the Department of Statistics, there are about 2.5 million people over the age of 60 in Malaysia (Hassan, Kugimiya, Tanaka, Tanaka, & Paramesran, 2015), and this number is expected to grow by 2020 (Chua, Chang, & Lim, 2015). This trend is also reflected globally (Hegde & Bishop, 2018). Hence, it is important to understand the difficulties experienced by the elderly in order to provide various support systems to assist them during their daily activities (Bright & Egger, 2008; Hegde & Bishop, 2018).

Thus, much has been conducted on acquired color vision deficiencies due to aging. Earlier studies have confirmed that as human age increases, the thickness of the lens continues to grow and the accumulation of yellow pigmentation occurs (Artigas, Felipe, Navea, Fandino, & Artigas, 2012; Norren & Vos, 1974; Pokorny, Smith, & Lutze, 1986; Romano et al., 2011; Ruddock, 1965a; Said & Weale, 1959; Weale, 1961a). This yellowing pigmentation effects the transparency of the human crystalline lens (Alio, Schimchak, Negri, & Montes-Mico, 2005). Apart from the yellowing pigmentation, the size of human pupil also reduces with age (Applegate, Donnelly, Marsack, & Koenig, 2007; Birren, Casperson, & Botwinick, 1950; Bitsios, Prettyman, & Szabadi, 1996; Kadlecova, Peleska, & Vasko, 1958; Ortiz, Bowyer, & Flynn, 2013; Said & Sawires, 1972; Winn, Whitaker, Elliott, & Phillips, 1994) which causes the reduction of the effective light reaching the retina (Sloan, 1939; Weale, 1961a, 1961b; Werner, Peterzell, & Scheetz, 1990). Due to these reasons, elderly people experience yellowish and darker color perception than younger people.

A lot of effort has been poured into research on the elderly color perception model. The effect of yellowing pigmentation to the human lens-density spectrum has been studied in Pokorny et al. (1986), Savage, Haegerstrom-Portnoy, Adams, and Hewlett (1993), Weale (1988), and Xu, Pokorny, and Smith (1997) while the investigation of pupil size has been studied in Birren et al. (1950), Said and Sawires (1972), and Winn et al. (1994). To replicate the experience of elderly color perception, experimental studies using artificial uniform yellowing filter have been conducted in K. Ishihara et al. (2001), Schneck, Adams, Huie, and Lee (1993), and Yoshida and Sakuraba (1996). Computerized simulations of elderly color perception have also been conducted in Okajima and Takase (2001) and Tanaka et al. (2011). Based on the non-uniform yellowing pigmentation method by Tanaka et al. (2011), several image enhancement methods to improve the elderly color perception have been proposed in R. Suzuki et al. (2012), Ueda, Azetsu, Suetake, and Uchino (2015a), Ueda, Azetsu, Suetake, and Uchino (2015b, 2016), and Ueda et al. (2016).

Meanwhile, for inherited color vision deficiency, color loss occurs due to the changes of the cone photoreceptors in the human eyes. About eight percent of the male population is color vision deficient (Ching & Sabudin, 2010; Lee & dos Santos, 2011; Semary & Marey, 2014). One type of inherited color vision deficiency is dichromacy, which occurs when one type of cone photoreceptors is absent or not functioning. People with dichromacy are also known as dichromats. Dichromacy can be classified into three categories: protanopia, deuteranopia, or tritanopia depending on whether the missing cone is the L-cone, M-cone, or S-cone respectively (Neitz & Neitz, 2011). Protanopia and deuteranopia are also called red-green deficiencies (Moreira, Alvaro, Melnikova, & Lillo, 2018). People with either protanopia and deuteranopia have difficulty in distinguishing between these two colors (Ching & Sabudin, 2010; Judd, 1949). Another type of dichromacy is called tritanopia with which people have difficulty distinguishing shades of blue and yellow. However, people with tritanopia constitute less than one percent of the male population (Moreira et al., 2018).

To simulate dichromatic color perception, various algorithms have been proposed in Brettel, Vienot, and Mollon (1997), Capilla, Diez-Ajenjo, Luque, and Malo (2004), Capilla, Luque, and Diez-Ajenjo (2004), Lee and dos Santos (2011), Machado, Oliveira, and Fernandes (2009), Meyer and Greenberg (1988), Rodriquez-Pardo and Sharma (2011), Vienot, Brettel, and Mollon (1999), and Wachtler, Dohrmann, and Hertel (2004). Due to its mathematical simplicity and its usability in expressing color discrimination of the people with dichromacy, Brettel's algorithm (Brettel et al., 1997; Vienot et al., 1999) is the most accepted model in modeling dichromatic color perception.

Based on Brettel's algorithm, researchers have proposed image recoloring methods to improve the color perception of people with dichromacy, in particular, red-green deficiency. Many strategies have been utilized for the image recoloring and these methods have been presented in Anagnostopoulos, Tsekouras, Anagnostopoulos, and Kalloniatis (2007), Doliotis, Tsekouras, Anagnostopoulos, and Athitsos (2009), Huang, Chen, Jen, and Wang (2009), Huang, Tseng, Wu, and Wang (2007), Ichikawa et al. (2003), Jefferson and Harvey (2006), Kuhn, Oliviera, and Fernandes (2008), Ma, Gu, and Wang (2006), Machado and

Oliveira (2010), Rasche, Geist, and Westall (2005a), Rasche, Geist, and Westall (2005b), Ribeiro and Gomes (2013), Rigden (1999), Suetake, Tanaka, Hashii, and Uchino (2012), Wakita and Shimamura (2005), and Yang and Ro (2003).

Although all the aforementioned methods for elderly and red-green deficients color perception enable us to understand more about their color perception, there are certain issues that need to be addressed.

1.2 Problem Statement

In the field of elderly color perception, non-uniform yellowing pigmentation has been utilized to simulate their color perception. Recently, results in clinical studies (Artigas et al., 2012; Romano et al., 2011) of elderly color perception confirm that uniform yellowing pigmentation occurs on human crystalline lenses. However, the uniform yellowing pigmentation has not been represented mathematically, and this creates a gap in the research of elderly color perception. Hence, it has becomes a motivation to develop a mathematical model of the uniform yellowing pigmentation and assess the color perception experienced by the elderly.

Meanwhile, most of the recolored images for red-green deficients lose their naturalness when viewed by those with normal color vision (Huang et al., 2007; Jeong, Kim, Wang, & Yoon, 2011). Thus, the recolored images are not suitable for use in advertisements, signboards, and maps in public places such as airports, shopping malls, and train stations. Some of the image recoloring methods may also change all the colors of the original image. As consequence, the recolored images tend to look unnatural to the red-green deficients as well (Kuhn et al., 2008).

In addition, apart from lack of naturalness preservation, several of the recoloring algorithms for red-green deficiency may not be suitable for practical use due to complex and iterative algorithms (Doliotis et al., 2009; Ichikawa et al., 2003), high computational time (Rasche et al., 2005a, 2005b), recoloring process performed in the reduced color space of dichromats (Kuhn et al., 2008), and limited color options in their recoloring process (Rigden, 1999; Wakita & Shimamura, 2005). Hence, there are opportunities for improvement for the enhancement of the color perception for people with color vision deficiency, in particular the elderly people and the red-green deficients.

1.3 Objectives

The main aim of this research is to enhance the color perception for people with color vision deficiency. In order to achieve this aim, this thesis has two objectives. The objectives of this thesis are:

1. *To improve the computerized simulation method of elderly color perception by introducing a mathematical representation of the uniform yellowing pigmentation to mimic elderly color perception*

   It is shown in medical reports that elderly people suffer from certain degrees of color perception loss. Previous works on elderly color perception utilized a non-uniform yellowing pigmentation method. However, results from recent medical studies show that uniform yellowing pigmentation occurs on human crystalline lens as human age increases. This provides motivation and new opportunities to expand the research work in elderly color perception. Thus, a mathematical representation of the uniform yellowing pigmentation is formulated to improve the computerized simulation method of elderly color perception. The simulated uniform yellowing pigmentation is used to mimic the color perception of elderly (Chapter 3).

2. *To improve the image recoloring method for the red-green deficients by proposing a naturalness preservation image recoloring method*

   Although there are various image recoloring methods that enhance the visual details and improve the color perception of the red-green deficients, the recolored images may look non-pleasing to people with normal color vision. This may happen in public places such as airports, shopping malls, and train stations where color images used in maps and advertisements are viewed by everyone. Moreover, the recolored images may look unnatural to the red-green deficients as well since all the colors of the original images are changed during the recoloring process. To overcome this issue, a naturalness preservation image recoloring method is introduced which enhances visual details while maintaining the naturalness of the recolored images as much as possible (Chapter 4).

1.4 Organization of the Thesis

This thesis, as was pointed out earlier in this chapter, describes improved methods to enhance the color perception for people with color vision deficiency. A uniform yellowing pigmentation method is introduced to simulate the color perception of the elderly. An image recoloring method that enhances the color perception of the red-green deficients and also maintains the naturalness of the image is also introduced.

The following is a summary of the content of each chapter.

Chapter 2: Human Color Vision. This chapter presents an overview of human color vision. Information on the human visual system is described here. The developments of the CIE color matching functions that corresponds to the response of the human eye are presented. Based on the CIE color matching functions, *XYZ* color space was formulated. The basic formulation of the *XYZ* tristimulus values and its chromaticity diagram are described in this chapter. *XYZ* color space is utilized as the main working domain for the methods proposed in this thesis. Moreover, the mathematical relationship between *XYZ* and *RGB* color spaces is also presented in this chapter. This information is essential as all color images utilized in the proposed methods are transformed from *RGB* color space to

XYZ color space. The types of color vision deficiencies are also described in this chapter.

Chapter 3: Color Perception of the Elderly. This chapter discusses the research developments in elderly color perception. Findings from earlier research works show that the color perception of the elderly people is degraded due to yellowing pigmentation that occurs on the human crystalline lens. In addition, reduction in the human pupil size also affects the ability of elderly people to differentiate colors. To mimic color perception of the elderly, previous works utilized the non-uniform yellowing pigmentation method. However, results from recent clinical studies have shown that uniform yellowing pigmentation occurs on the human crystalline lens. To study the effects of the uniform yellowing pigmentation on the color perception of the elderly, a mathematical method representing the uniform yellowing pigmentation is proposed. Using the uniform yellowing pigmentation, color perception of the elderly is simulated, and the experimental results are compared with the results from medical studies for validation. In addition, results from experimental studies show that the proposed method produces images that are closer to the results from medical studies and perform better than the results from the non-uniform yellowing pigmentation method.

Chapter 4: Color Perception of Red-green Deficients. This chapter presents an overview of the color perception of red-green deficients. A simulation method to reproduce their color perception is described in this chapter. Some of the research done with the specific aim of improving the color perception of the red-green deficients is briefly discussed in this chapter. Although previous works enhance the color perception of red-green deficients, the recolored images lose their naturalness. These color images used in advertisements in public places may look non-pleasing to the people with normal color vision as well as to red-green deficients. Thus, the chapter proposes a naturalness preserving recoloring method that enhances the color perception of the red-green deficients and also maintains the naturalness of the recolored images to both parties. Experimental results are presented to validate this claim, and a comparison between the state-of-the-art method and two other existing methods show that the proposed recoloring method achieves better objective and subjective scores.

Chapter 5: Conclusion. The thesis is concluded, summarizing the contents of the thesis and discussing the possibilities of future work in this direction.

1.5 Contributions

One of the contributions of this thesis is that it proposes a mathematical representation of the uniform yellowing pigmentation that occurs on the human crystalline lens. The simulated uniform yellowing pigmentation is utilized to model the color perception of the elderly. This work has been published in Hassan, Paramesran, Tanaka, and Tanaka (2018). The proposed method is essential in order for us to really understand the difficulties faced by the elderly. Moreover, it is imperative to consider a good visual presentation through color in order to enable the elderly to experience the surrounding environment safely and with confidence. Based on the proposed method, improvements such as the usage of better color schemes to represent information can be considered, thus avoiding miscommunication and misinterpretation. This, in turn, can improve the quality of life of the elderly. Therefore, the proposed method contributes to the development of the field of color perception of the elderly.

Some of the current image recoloring methods for red-green deficients may potentially change all the colors of the original image. As a result, the recolored image may look non-pleasing to both red-green deficients as well as people with normal color vision. Therefore, the second contribution of this thesis is the construction of a naturalness preserving recoloring method for red-green deficients. This work has been published in Hassan and Paramesran (2017). The proposed method takes into consideration the needs of red-green deficients as well as people with normal color vision. By maintaining the luminance and the hue of the original image, the proposed method enhances the color perception of the red-green deficients and maintains the naturalness of the recolored images to both parties. This is important for images used in public places such as airports, shopping malls, and train stations where color images such as maps and advertisements are viewed by everyone.

CHAPTER 2: HUMAN COLOR VISION

This chapter presents an overview of human color vision. A description of the human visual system is briefly represented. Research developments on color matching functions that correspond to the response of the human eyes are also discussed. All the color sensations that a human perceives can be encompassed using *XYZ* color space. Thus, information on the *XYZ* color space and its chromaticity diagram are also described in this chapter. However, due to the non-uniformity of the *XYZ* color space, for color reproduction in digital world, transformation to *RGB* color space is required. Hence, the chapter describes the *RGB* color space and the mathematical transformation process between the two color spaces. Lastly, the chapter presents the types of color vision deficiencies.

2.1 Introduction

The human visual system (HVS) consists of the human eyes, part of the brain, and the pathway connecting them. It is part of the human central nervous system which interprets information from the visible light spectrum to form a visual perception of the surrounding world. The human eye can be thought of as an optical path and is the main recipient of the visible light spectrum. Thus, human visual perception is initiated and strongly influenced by the anatomical structure of the human eyes. Figure 2.1 shows a schematic illustration of the optical structure of the human eye.

Some of the key components of the human eye shown in Figure 2.1 are briefly described below (Fairchild, 2005; Malacara, 2011):

1. The Cornea

   The cornea is the transparent outer surface in front of the eye through which light passes. Its normal ideal shape is nearly spherical.

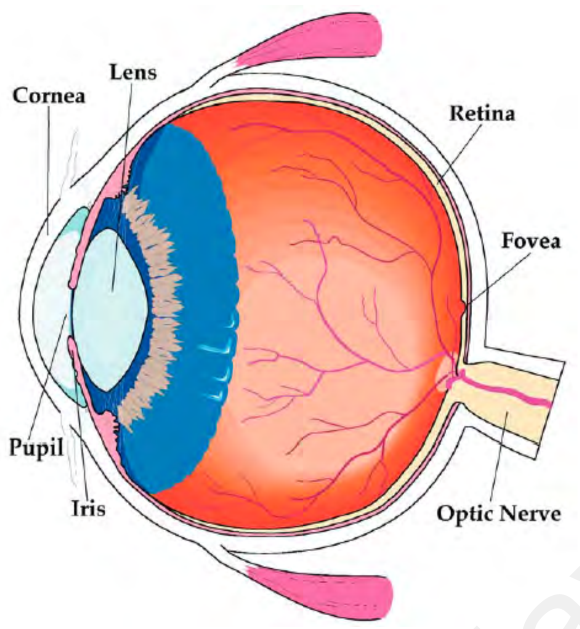

Figure 2.1: Schematic diagram of the human eye (Fairchild, 2005)

2. The Pupil

   This is the circular opening in front of the eye, which is surrounded by the iris. The pupil increases or decreases its diameter to control the amount of light entering the eye. The maximum diameter of the pupil, with low illumination levels, is around 6–8 mm, and the minimum diameter, with high illumination levels, is between 1 and 2 mm. Its average diameter is about 3.5–4 mm.

3. The Iris

   The iris is the sphincter muscle that controls pupil size. The iris is pigmented, giving us our specific eye color.

4. The Lens

   Also called the crystalline lens, the flexible lens varies in index of refraction. The shape and its optical power can be modified by means of the ciliary muscles. The ciliary muscles increase the power (accommodation) to focus on near objects and relaxes its shape to focus on distant objects. The crystalline lens contains a yellow pigment with strong absorption in the ultraviolet region, near a wavelength of 365 nm, with almost perfect transparency 550–650 nm.

5. The Retina

   The optical image formed by the eye is projected onto the retina. The retina is formed by several layers: cell and fiber nerves are in the internal layer while rods and cones are in the last layer. Rods and cones are photoreceptors that serve to transduce the information present in the optical image into chemical and electrical signals. These signals are then transmitted to the later stages of the HVS.

6. The Fovea

   The fovea is the arc on the retina where we have the best spatial and color visions. The fovea contains only cones in a dense random array. Outside the fovea the main light-sensitive elements are the rods, which are responsible for scotopic vision.

7. The Optic Nerve

   The optic nerve is made up of the axons of the ganglion cells, the last level of neural processing in the retina.

As mentioned above, the retina includes several layers of neural cells. Among the cells, there are two photoreceptors: the rods and the cones. The names are derived from their prototypical shapes. There are about 100 million rods and 5 million cones in each human eye (Wandell, 1995). There is only one type of rod receptor with a peak spectral responsivity at approximately 510 nm (Fairchild, 2005). There are three types of cones that are denoted as long (L), medium (M), and short (S) cones. Each cone is sensitive to red, green, and blue stimulation respectively. The three cones enable color vision while the rods are incapable of color vision. Thus, at low luminance levels (< 0.003 cd/m^2), the rods are active; this is referred to as scotopic vision. When the cones are active in high luminance levels (> 3 cd/m^2), vision is referred to as photopic vision. In intermediate luminance levels, both rods and cones are active, and this is referred to as mesopic vision.

The different types of visions and their respective luminance levels are illustrated in Fig 2.2.

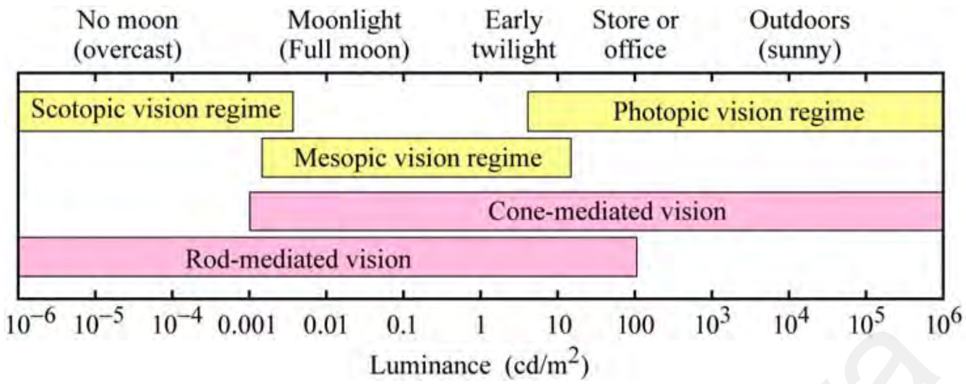

Figure 2.2: Type of visions and its respective luminance levels (Schubert, 1996)

The rest of the chapter is organized as follows. Section 2.2 describes the developments of color matching functions. Section 2.3 and 2.4 describe the XYZ and RGB color spaces respectively and the mathematical transformation process between the two color spaces. The types of color vision deficiencies are presented in Section 2.5. Section 2.6 concludes the chapter.

2.2 Trichromacy and Color Matching Functions

Trichromacy is a condition in which the HVS has three independent channels to convey information about color. These three independent channels are the three types of cones in the human eye. Humans with trichromacy vision are called trichromats. With the establishment of a standardized system of colorimetry, it is necessary to obtain a reliable estimate of the average color matching functions that correspond to the response of the human eye.

Thus, two sets of independent experiments (Wright, 1928; Guild, 1932) were completed to estimate the average color matching functions. These experiments employed the 2° field of view as the viewing condition of standard observers. 2° was chosen as they believed that all the color-sensing cones of the human eyes are located within a 2° arc of the fovea.

The color matching experiments were conducted in a dark room environment where a white screen was divided into two regions: test and reference regions. Red, green, and blue lights of different primary wavelengths were placed in the test region. Meanwhile, in the reference region, a light source of equal energy monochromatic light covering the visible spectrum was placed. This is illustrated in Figure 2.3.

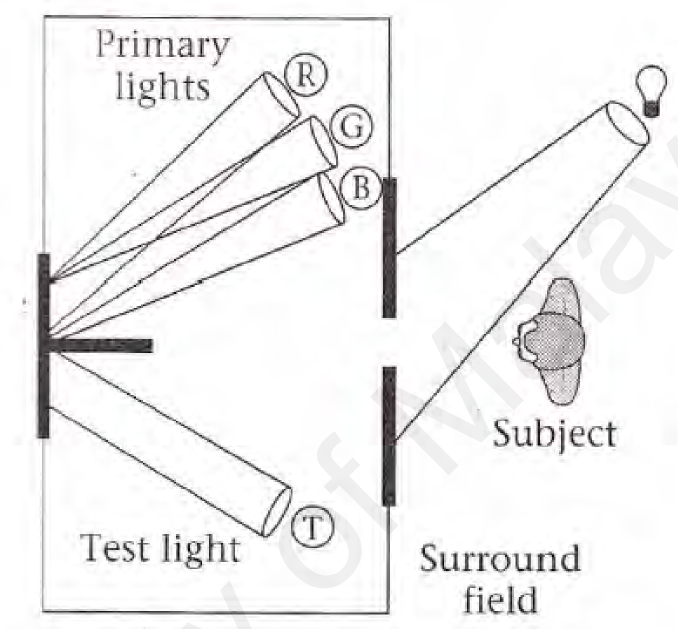

Figure 2.3: Color matching experiment (Wandell, 1995)

During the experiment, the observers had to adjust the red, green, and blue lights until they produced the same light as in the reference region. If the observers could not get a match, the same set of primaries were used in the reference field, and the observers used them to find a match. In this case, negative coefficients of the primaries were obtained. The results from both set of experiments (Wright, 1928; Guild, 1932) were adopted by the International Commission on Illumination (CIE) and are called the color matching functions $\bar{r}(\lambda)$, $\bar{g}(\lambda)$, and $\bar{b}(\lambda)$ for CIE 2° Standard Observer. However, since negative values could not be physically implemented, a set of all positive functions were obtained through a series of transformations and these functions are called the CIE1931 color matching functions $\bar{x}(\lambda)$, $\bar{y}(\lambda)$, and $\bar{z}(\lambda)$.

However, by the 1960s, it was realized that the cones were present in a larger area of the eye than previously believed, and so in 1964, the 10° Standard Observer was developed. The difference between the two viewing angles is that at a viewing distance of 50 cm, a 2° field of view would be a circle with diameter equal to approximately 1.7 cm while a 10° field of view would be a circle with diameter equal to approximately 8.8 cm.

Thus, another color matching functions experiment based the 10° Standard Observer was conducted by Stiles and Burch (Stiles & Burch, 1959, 1955a). From this experiment, CIE adopted another set of color matching functions $\bar{x}_{10}(\lambda)$, $\bar{y}_{10}(\lambda)$, and $\bar{z}_{10}(\lambda)$ for 10° Standard Observer also known as CIE1964 color matching functions. Both sets of color matching functions are illustrated in Figure 2.4.

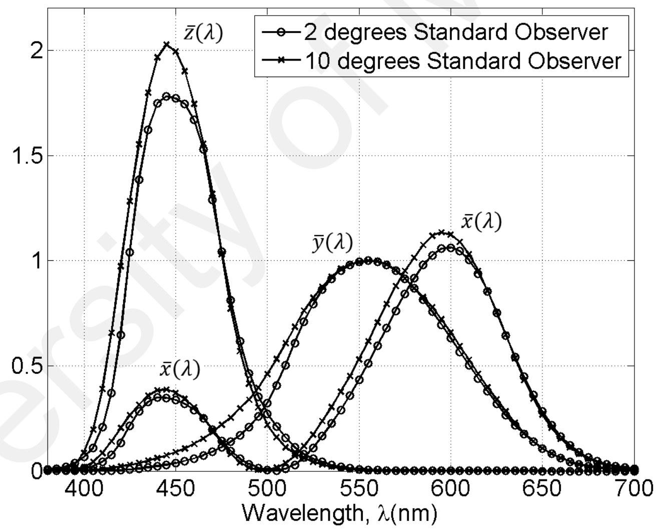

Figure 2.4: CIE color matching functions

Since the color matching functions are intended to correspond to the response of the human eye, both the CIE1931 and CIE1964 color matching functions have profoundly affected the development of modern imaging systems and applications. The CIE1931 color matching functions are used, almost exclusively in color appearance models (Fairchild, 2005).

2.3 *XYZ* Tristimulus Values and Chromaticity Diagram

Utilizing the color matching functions, *XYZ* tristimulus values were formulated. The *XYZ* tristimulus values were formulated so that the *Y* value has a spectral sensitivity that corresponds to the lightness sensitivity of human vision (Poynton, 1995). When the *Y* value is augmented with the *X* and *Z* values, they embed the spectral properties of human color vision (Poynton, 1995).

The *XYZ* tristimulus values for colored stimuli are calculated generally using the equations below (Fairchild, 2005)

$$X = k \int_{\lambda} \Phi(\lambda)\bar{x}(\lambda)d\lambda \tag{2.1}$$

$$Y = k \int_{\lambda} \Phi(\lambda)\bar{y}(\lambda)d\lambda \tag{2.2}$$

$$Z = k \int_{\lambda} \Phi(\lambda)\bar{z}(\lambda)d\lambda \tag{2.3}$$

where $\Phi(\lambda)$ is the spectral power distribution of the stimulus, $\bar{x}(\lambda)$, $\bar{y}(\lambda)$, and $\bar{z}(\lambda)$are the color matching functions, and k is a normalizing constant which is defined as

$$k = \frac{100}{\int_{\lambda} E(\lambda)\bar{y}(\lambda)d\lambda} \tag{2.4}$$

where $E(\lambda)$ is the relative spectral power distribution of the light source or illuminant (Fairchild, 2005).

For reflective objects, the *XYZ* tristimulus values are represented as

$$X = k \int_{\lambda} E(\lambda)\rho(\lambda)\bar{x}(\lambda)d\lambda \tag{2.5}$$

$$Y = k \int_{\lambda} E(\lambda)\rho(\lambda)\bar{y}(\lambda)d\lambda \tag{2.6}$$

$$Z = k \int_{\lambda} E(\lambda)\rho(\lambda)\bar{z}(\lambda)d\lambda \tag{2.7}$$

where $\Phi(\lambda)$ from Eqs. (2.1) to (2.3) is defined as the product of the spectral reflectance factor of the object, $\rho(\lambda)$ and the relative spectral power distribution of the light source or illuminant, $E(\lambda)$ (Fairchild, 2005). The most common illuminant used in colorimetric application is the CIE Illuminant D65 which represents average daylight with a correlated color temperature of 6504 K.

Utilizing the *XYZ* tristimulus values, the color of a stimulus can be represented. However, to provide a convenient two-dimensional representation of colors in term of conceptual understanding and computation, a chromaticity diagram was developed (Fairchild, 2005; Poynton, 1995). To accomplish this, a standardized procedure for normalizing the *XYZ* tristimulus values were performed using the projective transformation shown below.

$$x = \frac{X}{X + Y + Z} \tag{2.8}$$

$$y = \frac{Y}{X + Y + Z} \tag{2.9}$$

$$z = 1 - x - y \tag{2.10}$$

To form the chromaticity diagram, only the x and y values are needed. Thus, the representation of colors is simplified from 3-dimensional to 2-dimensional values. However, the transformation process from *XYZ* tristimulus values to *xyz* representation removes the luminance information represented by the *Y* value (Pascale, 2003). Therefore, it is common practice to report the Y value when dealing with the chromaticity diagram. The xyY chromaticity diagram with Y equal to 100 is illustrated below.

Moreover, using the Y value and the chromaticity coordinates, the other two tristimulus

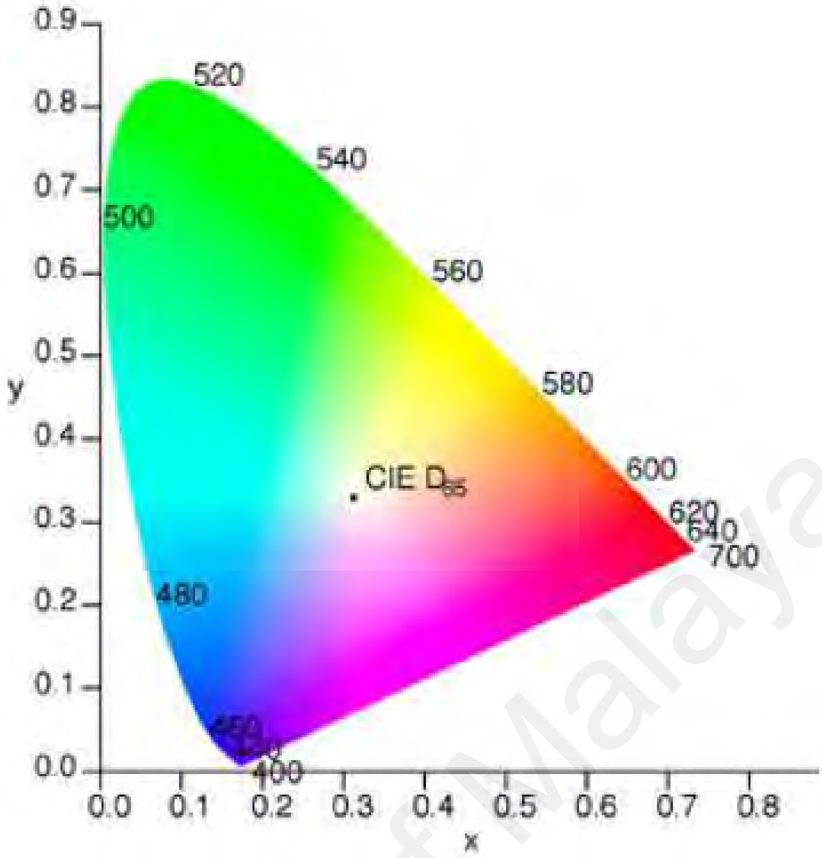

Figure 2.5: Chromaticity diagram with Y equal to 100. (Colantoni, 2004)

values can be obtained using these equations.

$$X = \frac{xY}{y} \tag{2.11}$$

$$Z = \frac{(1 - x - y)Y}{y} \tag{2.12}$$

2.4 *RGB* Color Space and Transformation Matrix

As described in the previous section, the color of stimuli can be represented by the *XYZ* tristimulus values. However, *XYZ* tristimulus values are not realizable in practice since they are not visually uniform (Broadbent, 2017). Therefore, to achieve color reproduction, *XYZ* tristimulus values need to be transformed into a mathematical domain in which physical realizability is not a constraint (Poynton, 1995).

To solve this problem, a mathematical transformation process to *RGB* color space was proposed. The *RGB* color space is an addictive color system in which red, green, and blue lights are added together to reproduce a broad array of colors. This color space is based on human color perception, and the main objective is for the representation and display of images in electronic systems such as televisions and computers. Thus, *RGB* color space is a device dependent color space that will have different coordinates for the same color for various output media (Pascale, 2003).

There are various *RGB* color spaces proposed in the last decades. One of the *RGB* color spaces that is practical and commonly used is the standard Red Green Blue (*sRGB*) color space. *sRGB* was created cooperatively by HP and Microsoft in 1996 for use on monitors, printers and the Internet, and subsequently standardized by the International Electrotechnical Commission (IEC) as IEC 61966-2-1:1999 (Pascale, 2003). Since then, it has often been used as the default color space for images in the digital world.

CIE XYZ color space can be transformed to and from any *RGB* color spaces by a 3×3 transformation matrix. Transformation from *CIE XYZ* into *RGB* can be performed using the transformation matrix as below.

$$\begin{bmatrix} R \\ G \\ B \end{bmatrix} = \begin{bmatrix} \alpha_{11} & \alpha_{12} & \alpha_{13} \\ \alpha_{21} & \alpha_{22} & \alpha_{23} \\ \alpha_{31} & \alpha_{32} & \alpha_{33} \end{bmatrix} \begin{bmatrix} X \\ Y \\ Z \end{bmatrix} \tag{2.13}$$

Meanwhile, the value of *RGB* can be transformed back to *CIE XYZ* using the inverse transformation matrix of Eq. (2.13) as below.

$$\begin{bmatrix} X \\ Y \\ Z \end{bmatrix} = \begin{bmatrix} \alpha_{11} & \alpha_{12} & \alpha_{13} \\ \alpha_{21} & \alpha_{22} & \alpha_{23} \\ \alpha_{31} & \alpha_{32} & \alpha_{33} \end{bmatrix}^{-1} \begin{bmatrix} R \\ G \\ B \end{bmatrix} = \begin{bmatrix} \beta_{11} & \beta_{12} & \beta_{13} \\ \beta_{21} & \beta_{22} & \beta_{23} \\ \beta_{31} & \beta_{32} & \beta_{33} \end{bmatrix} \begin{bmatrix} R \\ G \\ B \end{bmatrix} \tag{2.14}$$

2.5 Color Vision Deficiency

Color vision deficiency arises from the differences in the pigmentation of the cones in the human eye (Wandell, 1995). The vision of trichromats is characterized by three types of cones which collectively allow the reception of long (L), medium (M), and short (S) wavelengths of the visible spectrum. These long (L), medium (M), and short (S) wavelengths exhibits bluish, greenish, and reddish sensitivities respectively (Hunt, 2004; Pascale, 2003). However, people with color vision deficiency are unable to process the three wavelengths and thus, they cannot distinguish certain shades of colors.

Color vision deficiency can be categorized as either acquired or inherited color vision deficiencies (Verriest, 1963; Simunovic, 2016). In acquired color vision deficiency, color perception loss is due to medication, aging, disease or accidents. Meanwhile, in inherited color vision deficiency, color loss occurs due to changes in the cones in the human eye. Inherited color vision deficiency can be further classified into three types: dichromacy, monochromacy, and anamolous trichromacy.

Dichromacy occurs when one of the cones is absent or not functioning, and colors are reduced to two dimensions. The rarest type of inherited color vision deficiency is monochromacy. It occurs when two or three cones are absent or not functioning. Thus, people with monochromacy (monochromats) can only see shades of gray ranging from black to white. Anamolous trichromacy occurs in people with altered cones. Although all three cones exist, one of the cones is slightly out of alignment. This misalignment affects the way they perceive colors depending on which cone is misaligned.

2.6 Summary

In the chapter, a theoretical overview of the human visual system and color perception have been given. Research developments in color matching functions are also described in this chapter. The formulation and relationship between *XYZ* and *RGB* color spaces are described as well. Both color spaces are utilized in the formulation of the proposed methods to improve the color perception of people with color vision deficiency in this thesis.

CHAPTER 3: COLOR PERCEPTION OF THE ELDERLY

This chapter provides an overview of the color perception of the elderly. Fundamental theorems for color perception of the elderly are also described. The earlier works considered a non-uniform yellowing pigmentation model to mimic the color perception of the elderly. Recently, two clinical studies have shown that uniform yellowing pigmentation occurs on the human crystalline lens. Thus, a mathematical model of the uniform yellowing pigmentation is proposed in this chapter.

3.1 Introduction

Color images used by highly visual applications and services on websites and smartphone applications play an important role in distributing information to users of various ages (Soundararajan & Bovik, 2013; Yamazaki & Eto, 2015). As humans age, the functional ability of the eyes wane (Lerman, 1983; Salvi, Akhtar, & Currie, 2006; Weale, 1961a, 1961b; Werner et al., 1990) especially the ability to discriminate colors (Ball & Pollack, 1989; Fiorentini, Porciatti, Morrone, & Burr, 1996; Roy, Podgor, Collier, & Gunkel, 1991; Ruddock, 1965a, 1965b; Shinomori, 2005; Verriest, 1963; Werner et al., 1990). Color perception ability is the ability to recognize the set of signals that are produced when the three cones that are sensitive in the red, green, and blue spectral range in the human eye react with the incoming wavelength light (Hunt, 2004). The red, green, and blue spectral range are generally represented by the long (L), medium (M), and short (S) wavelengths respectively.

Throughout human life, the lens thickness continues to grow, and the accumulation of yellow pigmentation occurs (Artigas et al., 2012; Norren & Vos, 1974; Pokorny et al., 1986; Romano et al., 2011; Ruddock, 1965a; Said & Weale, 1959; Weale, 1961a). Norren and Vos (1974) state that the yellowing pigmentation process occurs after the age of 30. The yellow pigmentation contributes to a gradual reduction in the transparency of the human crystalline lens (Alio et al., 2005). Due to the yellowing pigmentation, the lens absorbs more short wavelength which reduces the amount of blue light entering the eyes (Fiorentini et al., 1996; K. Ishihara et al., 2001; Ruddock, 1965a; Salvi et al., 2006; Shinomori, 2005; Tanaka et al., 2011; Verriest, 1963; Xu et al., 1997). In addition, light scattering in the human lens of the elderly is much higher compared to the young (Boettner & Wolter, 1962). To describe the effect of the yellowing pigmentation to the human lens-density spectrum, several models were introduced: the two-factor model (Pokorny et al., 1986), the exponential model (Weale, 1988), and the linear model (Savage et al., 1993). A comparative experiment between the three models shows that the two-factor model produces better results (Xu et al., 1997).

In addition to yellowing, the size of the human pupil also reduces with age (Applegate et al., 2007; Birren et al., 1950; Bitsios et al., 1996; Kadlecova et al., 1958; Ortiz et al., 2013; Said & Sawires, 1972; Winn et al., 1994). Birren et al. (1950) investigated pupil size measurements and formulated a parabola relation between the pupil diameter and human age. Measurements performed by Said and Sawires show that pupil size reduces linearly with age (Said & Sawires, 1972). The concept of a linear relation between pupil size and human age is further strengthen by Winn et al. (1994) when they formulated mathematical linear relations between pupil size and human age. The reduced pupil size causes the effective light reaching the retina to reduce proportionally (Sloan, 1939; Weale, 1961a, 1961b; Werner et al., 1990). Moreover, the pupil's reflexive response also reduces with age (Bitsios et al., 1996) which in turn increases the reaction time of the elderly (T. Suzuki et al., 2012, 2005).

In Malaysia, the number of people aged 65 and above is expected to increase from 4.5% in 2009 to 7% by 2020 (Chua et al., 2015). The increase in the number of elderly people is also reflected globally (Hegde & Bishop, 2018). One of the areas of concern that needs to be addressed in order to eliminate barriers in terms of physical capabilities for the elderly is their color perception (Hassan et al., 2015; Hegde & Bishop, 2018). To understand the difficulties faced by the elderly due to the yellowing of the human crystalline lens, computerized simulation methods have been proposed in order to simulate the color perception of the elderly. Using the two-factor model (Pokorny et al., 1986), Okajima and Takase (2001) conducted computerized simulations using Munsell color chips to investigate the effect of yellowing on the color perception of the elderly. Meanwhile, (Tanaka et al., 2011) proposed a non-uniform yellowing pigmentation method to simulate the color perception of the elderly by implementing the two-factor model and taking into consideration the effect of retinal illuminance (Winn et al., 1994).

In the non-uniform yellowing pigmentation method, at a particular age, the different colors in the image are multiplied by the different levels of yellowing pigmentation. On the other hand, in the uniform yellowing pigmentation method, the colors in the image are multiplied by the same level of yellowing pigmentation. Figure 3.1 shows two examples of the yellowing pigmentation methods for people aged 80 years old and the simulated images as perceived by an 80-year-old.

(a) (b) (c) (d) (e)

Figure 3.1: Difference between non-uniform yellowing pigmentation and uniform yellowing pigmentation methods (a) Original image formed using color patches from Macbeth ColorCheckers; (b) Non-uniform yellowing pigmentation for people aged 80 years old from Tanaka's method; (c) Simulated image as perceived by an 80-year-old using Tanaka's method; (d) Proposed uniform yellowing pigmentation for people aged 80 years old; (e) Simulated image as perceived by an 80-year-old using the proposed method

The idea of uniform yellowing pigmentation on human crystalline lens was first initiated and implemented in Weale (1961a). Using this idea, Weale calculated the effective pathlength of the human crystalline lens. Said and Weale (1959) found that the white point in the chromaticity diagram moves nearer to the spectrum locus as humans age. It was stated in Werner and Steele (1988) that all three types of cones lose overall sensitivity at a similar rate; this is further supported in experiments performed by Nguyen, Overbury, and Faubert (2003).

Several experiments using artificial uniform yellowing filters that mimic the color vision of the elderly have been conducted (K. Ishihara, Ishihara, Nagamachi, & Osaki, 1997; K. Ishihara et al., 2001; Schneck et al., 1993; Yoshida & Sakuraba, 1996). Schneck et al. designed a three-layer filter that consists of a neutral density filter, a spectral filter and a scratched plastic sheet (Schneck et al., 1993). This 'sandwich' filter reduces the blue-yellow chromatic perception and mimics the color vision loss of the elderly. Yoshida et al. (Yoshida & Sakuraba, 1996) and Ishihara et al. (K. Ishihara et al., 1997, 2001), on the other hand, designed a yellowing filter using yellow films to study the effect of yellowing on the color perception of the elderly. When young observers wore the yellowing filter, they had difficulty differentiating colors due to the confusion that occurred when looking at multiple colored objects. Recently, clinical studies using enucleated human eyes performed by Artigas et al. (Artigas et al., 2012) and Romano et al. (Romano et al., 2011) showed that as human age increases, the chromaticity of the human crystalline lens shifts towards the yellow region of the chromaticity diagram.

Results from recent clinical studies (Artigas et al., 2012; Romano et al., 2011) have shown that uniform yellowing pigmentation occurs on the human crystalline lens. However, the uniform yellowing pigmentation is not represented mathematically. Hence, this has become the main motivation for developing a mathematical model of the uniform yellowing pigmentation and assessing the color perception experienced by the elderly. By understanding the process of color perception of the elderly, website designers and smartphone application developers can factor this consideration when choosing suitable color schemes to represent their information and avoid misinterpretation by the elderly. Moreover, it is also important for designers and architects to consider a good visual color presentation in order to enable the elderly to experience the built environment safely and with confidence. The chapter is therefore organized as follows. Section 3.2 describes the fundamental theorems used in the color perception of the elderly. Section 3.3 shows the proposed uniform yellowing pigmentation method. The performance of the proposed method and comparisons with the non-uniform yellowing pigmentation are shown and discussed in Section 3.4. Section 3.5 concludes this chapter.

3.2 Fundamental Theorems in Color Perception of the Elderly

This section describes the two fundamental theorems that are used in the study of the color perception of the elderly. The two fundamental theorems are the two-factor model and the retinal illuminance model.

3.2.1 Two-factor model

One of the fundamental models used in elderly color perception methods is the two-factor model proposed by Pokorny et al. (1986). This model describes the optical density of humans lens as a function of wavelength, λ and age, A and expresses it using the age-dependent TL_1 and age-independent components, TL_2 as below:

$$L(\lambda, A) = \begin{cases} [1.00 + 0.02(A - 32)]TL_1 + TL_2 & \text{for } 20 \leq A \leq 60 \\ [1.56 + 0.0667(A - 60)]TL_1 + TL_2 & \text{for } A > 60 \end{cases} \tag{3.1}$$

where TL_1 is the portion changed by aging after age 20 and TL_2 is the portion independent of age.

The optical density $L(\lambda, A)$ can also be expressed in terms of the spectral intensities as below:

$$L(\lambda, A) = log_{10}\left(\frac{I_i(\lambda)}{I_t(\lambda)}\right) \tag{3.2}$$

where $I_i(\lambda)$ and $I_t(\lambda)$ are the intensity of incident light and transmitted light respectively. Thus, the spectral transmittance of the human lens can be described as

$$\tau(\lambda, A) = \frac{I_i(\lambda)}{I_t(\lambda)} = 10^{-L(\lambda,A)} \tag{3.3}$$

Spectral transmittance of the human lens for several ages are illustrated in Figure 3.2.

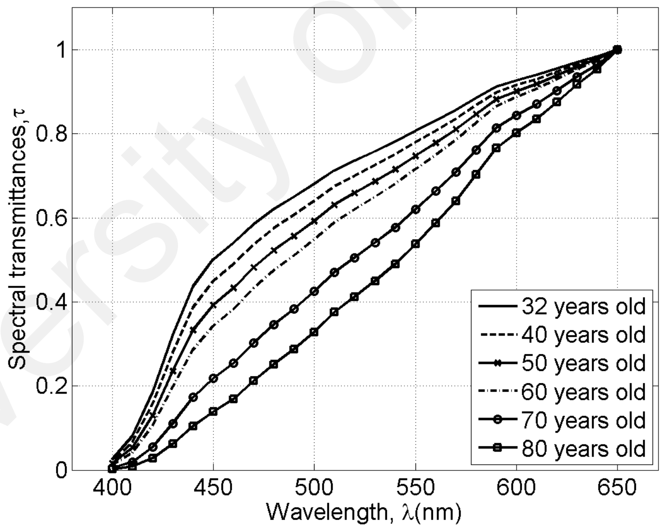

Figure 3.2: Spectral transmittances of human lens for several ages

In order to simulate the lens transmittance of an elderly person of aged A as seen by a young observer of age 32, the spectral transmission factor of the human lens can be derived from Eq. (3.3) as below:

$$F(\lambda, A, 32) = \frac{\tau(\lambda, A)}{\tau(\lambda, 32)} = \frac{10^{-L(\lambda,A)}}{10^{-L(\lambda,32)}} \tag{3.4}$$

Age 32 years old is chosen as a standard age for young people because it was the mean age used in the color matching experiment by Stiles and Burch (Stiles & Burch, 1955b).

3.2.2 Retinal Illuminance Model

Another model that is considered in elderly color perception methods is the retinal illuminance model. The model is based on the relation between pupil size and human age proposed in Winn et al. (1994). According to Winn et al., pupil size decreases linearly with age at all illuminance levels as shown in Figure 3.3. Thus, pupil size can be expressed in terms of age, A as below:

$$d(A) = -0.011A + 1.557 \tag{3.5}$$

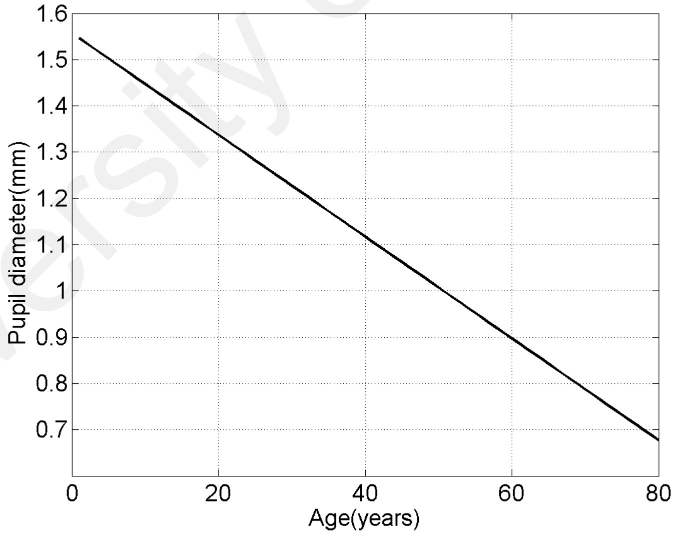

Figure 3.3: Pupil size decreases by aging

As in Tanaka et al. (2011), the rate of retinal illuminance of the elderly aged A as compared to the young observer aged 32 years old can be computed as below:

$$S(A, 32) = \frac{d(A)}{d(32)} = \frac{-0.011A + 1.557}{1.205} \tag{3.6}$$

3.3 Proposed Method - Uniform Yellowing Pigmentation Method

This section proposes a new method that utilizes the uniform yellowing pigmentation of the human crystalline lens to simulate the color perception of the elderly. The proposed method implements the same basic mathematical framework related to elderly color perception as applied in Tanaka et al. (2011). In Tanaka's method, 9 components called effective components were formulated to compute the non-uniform yellowing pigmentation (Hassan et al., 2015; Tanaka et al., 2011). Using this approach, at a particular age, the *RGB* components of the original image lose their overall sensitivity at a different rate. Thus, the non-uniform yellowing pigmentation formulated varies depending on the colors in the original image as shown in Figure 3.1(b).

Meanwhile, in the proposed method, the uniform yellowing pigmentation is formed using 3 components called the effective tristimulus ratios. In this approach, at a particular age, the *RGB* components in the original image lose their overall sensitivity at a similar rate which is in agreement with the results found in Nguyen et al. (2003) and Werner and Steele (1988). Figure 3.1(d) shows the uniform yellowing pigmentation in a person aged 80 years old. The simulated images as perceived by an elderly person of 80 years old using both methods are also illustrated in Figure 3.1.

In the proposed method, the original image is converted to *CIE XYZ* color space. *CIE XYZ* color space encompasses all the color sensations that a human perceives and is formulated based on the *RGB* version of the human eyes (Fairchild, 2005). Meanwhile, the measured transmittance functions and the spectral transmission factor (Pokorny et al., 1986) are utilized to compute the total tristimulus values at a particular age. Based on these values, the effective tristimulus ratios are computed. The uniform yellowing pigmentation is simulated using the effective tristimulus ratios. To simulate the color perception of the elderly, the *XYZ* tristimulus values of the original image are multiplied with the effective tristimulus ratios of the uniform yellowing pigmentation and the rate of retinal illuminance (Tanaka et al., 2011; Winn et al., 1994). The overall process of the proposed method is summarized in Figure 3.4.

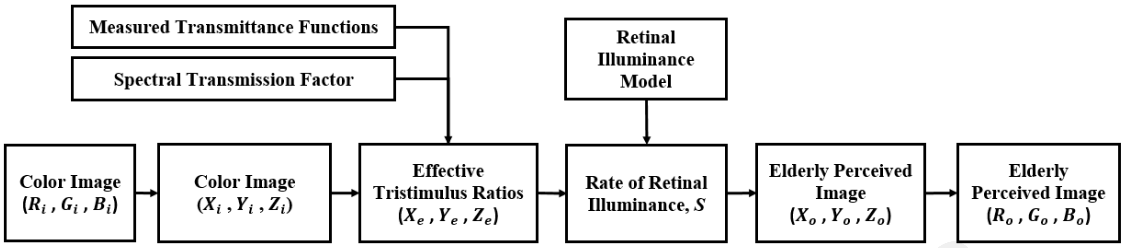

Figure 3.4: Overall process flow of the proposed method

Generally, the tristimulus values of reflected light can be represented as

$$X = k \sum_{\lambda=400}^{650} E(\lambda)\bar{x}(\lambda)\rho(\lambda) \tag{3.7}$$

$$Y = k \sum_{\lambda=400}^{650} E(\lambda)\bar{y}(\lambda)\rho(\lambda) \tag{3.8}$$

$$Z = k \sum_{\lambda=400}^{650} E(\lambda)\bar{z}(\lambda)\rho(\lambda) \tag{3.9}$$

where $E(\lambda)$ is the spectral energy for wavelength, $\bar{x}(\lambda)$, $\bar{y}(\lambda)$ and $\bar{z}(\lambda)$ are the standard CIE color matching functions, $\rho(\lambda)$ is the spectral reflectance, k is the normalization factor and the wavelength interval of 10nm.

However, since the image is presented on the Liquid Crystal Display (LCD), and the backlight of the LCD is observed through red, green, and blue filters, the proposed method utilizes the transmittance functions for red f_r, green f_g, and blue f_b filters of the LCD. The transmittance functions of the LCD are measured using a spectral luminance radiometer in a darkroom environment.

In the proposed method, the spectral reflectance $\rho(\lambda)$ in Eq. (3.7) to Eq. (3.9) are replaced with the respective transmittance functions and the spectral transmission factor

$F(\lambda, A, 32)$ as given in Eq. (3.4) (Pokorny et al., 1986).

Thus, the tristimulus values through the red, green, and blue filters for any given age A can be expressed as

$$X_m(A) = k \sum_{\lambda=400}^{650} E(\lambda)\bar{x}(\lambda) f_m(\lambda) F(\lambda, A, 32) \tag{3.10}$$

$$Y_m(A) = k \sum_{\lambda=400}^{650} E(\lambda)\bar{y}(\lambda) f_m(\lambda) F(\lambda, A, 32) \tag{3.11}$$

$$Z_m(A) = k \sum_{\lambda=400}^{650} E(\lambda)\bar{z}(\lambda) f_m(\lambda) F(\lambda, A, 32) \tag{3.12}$$

where $f_m(\lambda)$ is the transmittance functions of the LCD and $m = r, g, b$. Then, the total tristimulus values X, Y, Z for any given age, A can be computed using the summation of tristimulus value of each light component represented in Eq. (3.10) to (3.12).

$$X(A) = X_r(A) + X_g(A) + X_b(A) \tag{3.13}$$

$$Y(A) = Y_r(A) + Y_g(A) + Y_b(A) \tag{3.14}$$

$$Z(A) = Z_r(A) + Z_g(A) + Z_b(A) \tag{3.15}$$

The effective tristimulus ratios X_e, Y_e, and Z_e for the elderly aged A as compared to the young observer aged 32 years old can be expressed as

$$X_e = \frac{X(A)}{X(32)} \tag{3.16}$$

$$Y_e = \frac{Y(A)}{Y(32)} \tag{3.17}$$

$$Z_e = \frac{Z(A)}{Z(32)} \tag{3.18}$$

Finally, the tristimulus values of the elderly aged A are computed as

$$X_o(A) = X_e S X_i \tag{3.19}$$

$$Y_o(A) = Y_e S Y_i \tag{3.20}$$

$$Z_o(A) = Z_e S Z_i \tag{3.21}$$

where S is the rate of retinal illuminance as given in Eq. (3.6), X_e, Y_e, Z_e are the effective tristimulus ratios, and X_i, Y_i, Z_i are the tristimulus values of the color image converted using the *sRGB* to *CIE XYZ* transformation matrix as shown below.

$$\begin{bmatrix} X_i \\ Y_i \\ Z_i \end{bmatrix} = \begin{bmatrix} 0.4124 & 0.3576 & 0.1805 \\ 0.2126 & 0.7152 & 0.0722 \\ 0.0193 & 0.1192 & 0.9505 \end{bmatrix} \begin{bmatrix} R_i \\ G_i \\ B_i \end{bmatrix} \tag{3.22}$$

To simulate the image perceived by the elderly, $X_o(A)$, $Y_o(A)$, and $Z_o(A)$ are transformed to *RGB* values using the inverse of Eq. (3.22).

3.4 Experimental Studies

A number of experimental studies were performed to evaluate the proposed method. The transmittance functions of the LCD were measured to model the uniform yellowing pigmentation and then verified with the results from previous works. Using several type of images, the transition of the color perception of the elderly from different age groups were also observed. Lastly, an artificial SPP3 color perception test was conducted to young subjects and comparisons were made with the results from the clinical color perception test provided by eye doctors (Tanaka et al., 2011).

Prior to the experimental studies, the LCD was calibrated using X-Rite i1Display 2 based on sRGB color space and white point of D65. The gamma correction parameter, γ was set to 2.2. The calibration process ensures that the preciseness of color reproduction on the LCD is within a very small range of error (Tanaka et al., 2011).

3.4.1 Simulation of Uniform Yellowing Pigmentation

In this experiment, firstly, the transmittance functions of the LCD DELL S2440L were measured using a Konica Minolta CS-2000 spectral luminance radiometer in a darkroom environment. It should be noted here, the transmittance functions may vary slightly depending on the LCDs (Gibson & Fairchild, 2000). The normalized transmittance functions of the LCD are shown in Figure 3.5.

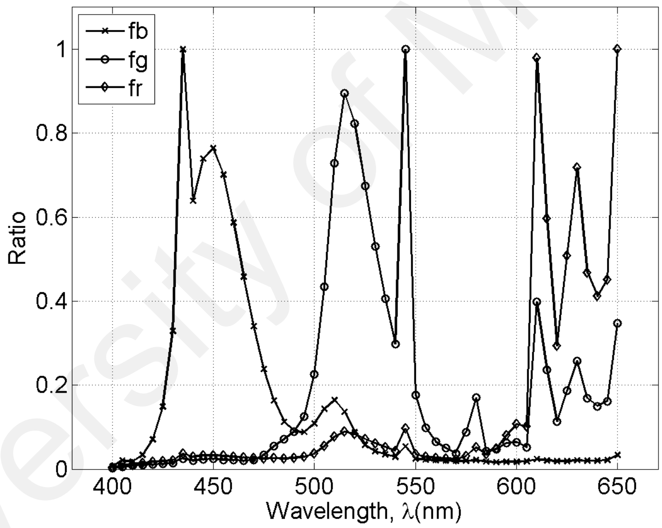

Figure 3.5: Normalized transmittance functions of LCD used in the experiment

Utilizing the values of the transmittance functions, the D65 spectral energy distribution, and the *CIE1931* color matching functions, the effective tristimulus ratios were computed. Then, the effective tristimulus ratios were converted into the effective *RGB* values. The effective *RGB* values computed represent the simulated image of the proposed uniform yellowing pigmentation. The simulated images of the uniform yellowing pigmentation are illustrated in Figure 3.6. It can be observed that as age increases, the simulated uniform yellowing pigmentation becomes yellower, which is consistent with the results found in Artigas et al. (2012) and Romano et al. (2011).

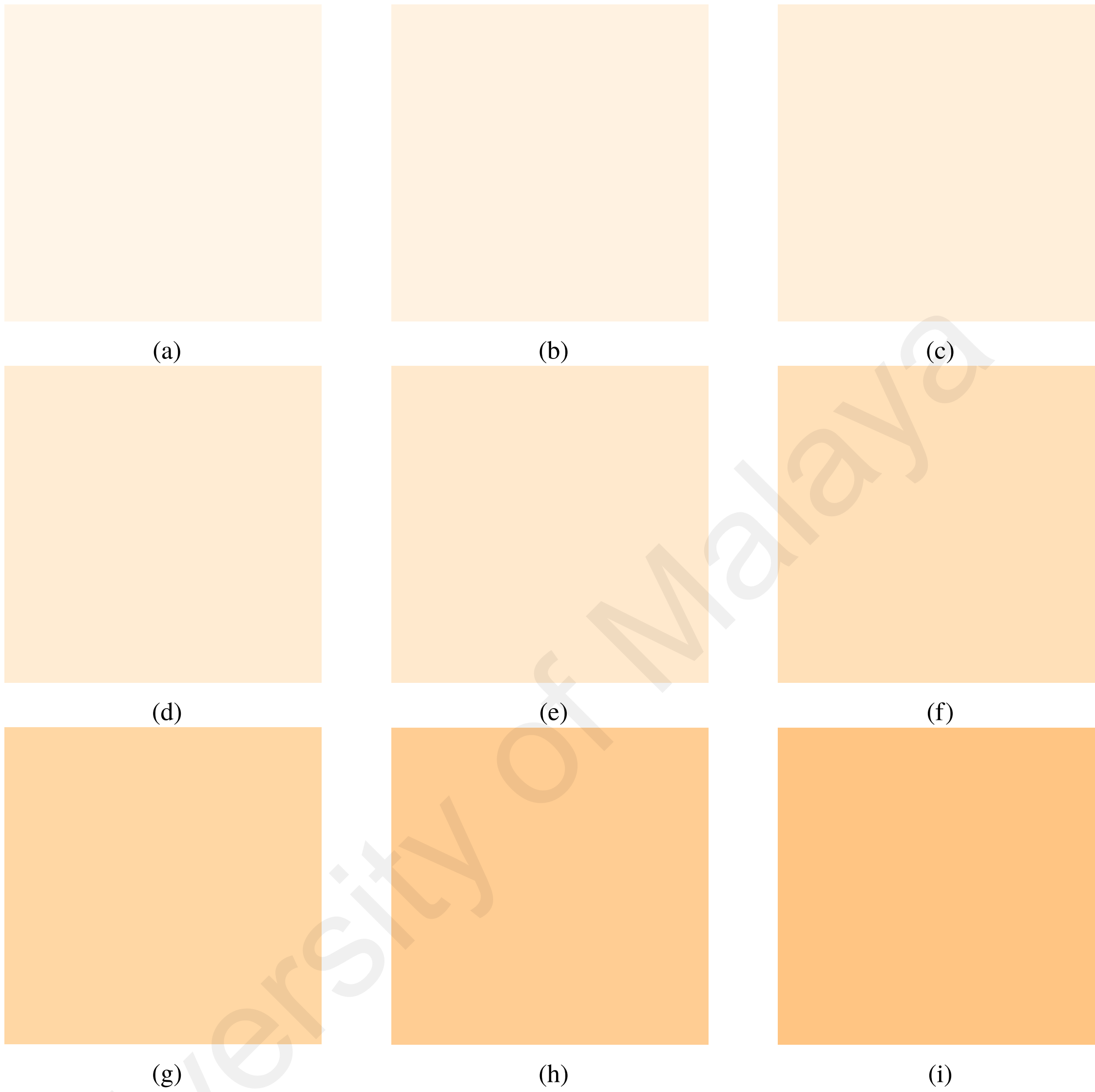

Figure 3.6: The simulated uniform yellowing pigmentation for age (a) 40 years old; (b) 45 years old; (c) 50 years old; (d) 55 years old; (e) 60 years old; (f) 65 years old; (g) 70 years old; (h) 75 years old; (i) 80 years old

Two tests were then conducted in order to verify that the proposed method has similar characteristics with the yellowing of the human crystalline lens found in previous works. As mentioned in Artigas et al. (2012), Pokorny et al. (1986), and Said and Weale (1959), the amount of blue light penetrating into human eyes decreases significantly after the age of 60. Thus, to compare their results with the proposed method, the effective *RGB* values as shown in Figure 3.7 were plotted. It can be seen that the effective value for blue, B_e

decreases significantly after the age of 60, which is in agreement with the results in Artigas et al. (2012), Pokorny et al. (1986), and Said and Weale (1959).

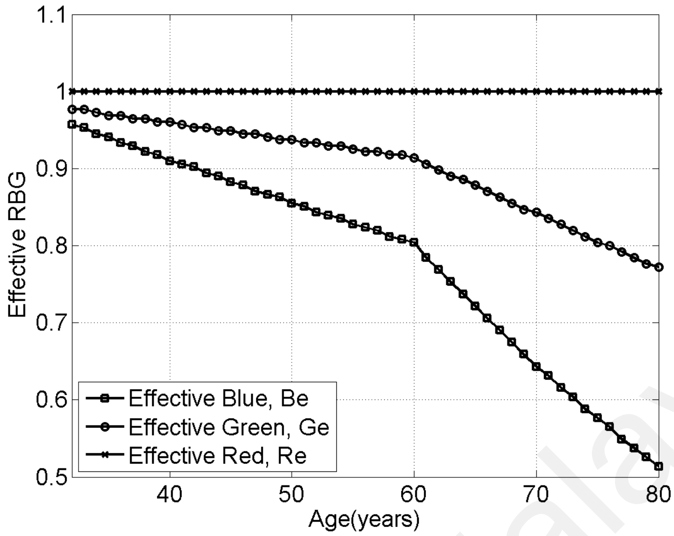

Figure 3.7: Age-related change of the effective *RGB* values for the simulated uniform yellowing pigmentation

The D65 white point was simulated using the proposed method, and the chromaticity points were plotted together with the results from the clinical studies (Artigas et al., 2012; Romano et al., 2011) as shown in Figure 3.8. The results in Artigas et al. (2012) were

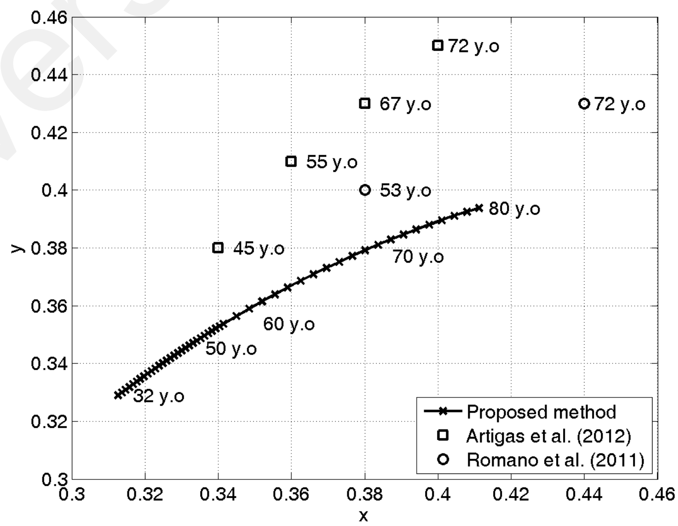

Figure 3.8: Comparison of the chromaticity points of the D65 white point between the proposed method and the results from the clinical studies

obtained from human eyes used for corneal transplants while the results in Romano et al.

(2011) were obtained from freshly enucleated human eyes.

It can be observed that as age increases, the chromaticity of the simulated D65 white point shifts to the yellow region of the chromaticity diagram. This is consistent with the results obtained in Artigas et al. (2012) and Romano et al. (2011). Based on the results of both tests, it can be deduced that the uniform yellowing pigmentation simulated by the proposed method has similar characteristics with the yellowing of the human crystalline lens.

3.4.2 Simulation of the Color Perception of the Elderly

To observe the transition of the color perception of the elderly from different age groups, three Macbeth ColorCheckers color patches (blue sky, green, and moderate red), three synthesized images created using Munsell colors, and three real images from LIVE database (Sheikh, Sabir, & Bovik, 2006) as perceived by the elderly aged 60, 70 and 80 years old were simulated using the proposed method. The original and simulated images are shown in Tables 3.1 to 3.3.

As shown in Table 3.1, as age increases, the blue sky color patch loses its bluish element. This is because the uniform yellowing pigmentation absorbs more blue stimulation than the red and green stimulations of the image. This is similar to the results in Norren and Vos (1974), Pokorny et al. (1986), Ruddock (1965b), and Said and Weale (1959). Their work shows that as human age increases, the amount of blue light that arrives into human eyes is less than green and red light. Moreover, all three color patches become darker as age increases. Other than the uniform yellowing pigmentation, this is also due to the retinal illuminance model in which the reduced pupil size causes the effective light reaching the retina to reduce proportionally (Weale, 1961a, 1961b; Werner et al., 1990).

It can also be observed from Table 3.2 that as age increases, the purple and light blue color blocks from the first synthesized image look like brown and beige respectively. In

Table 3.1: MacBeth ColorCheckers color patches and its simulated images as perceived by 60, 70, and 80-year old elderly using the proposed method

Original image	60 years old	70 years old	80 years old

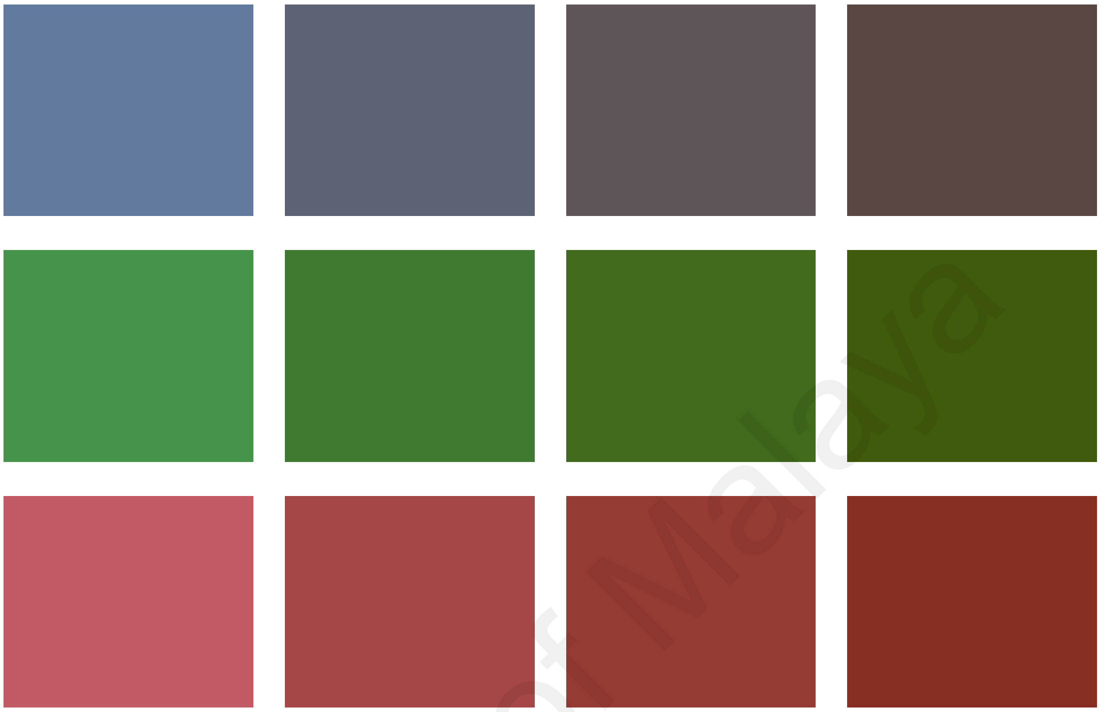

addition, yellow and cream color blocks in the second synthesized image look almost the same in the simulated image of the 80-year-old. Furthermore, the two blue color blocks in the second and third synthesized images lose their blueness and look more greyish as age increases. Thus, these may create confusion in the elderly. As reported in K. Ishihara et al. (2001), elderly may have difficulty finding goods in stores because of the confusion that occurs when looking at the color displays. Moreover, these confusions increase their response time and reduce their response speed in making decisions (T. Suzuki et al., 2005; T. Suzuki, Qiang, Sakuragawa, Tamura, & Okajima, 2006).

For real images, change in color perception can be observed in the first real image as the blue cap looks darker in the simulated image of the 80-year-old. This is illustrated in Table 3.3. The same applies to the red parrot in the second real image. Originally, the wing of the red parrot consists of blue and green colors. However, in the simulated image

Table 3.2: Synthesized images and its simulated images as perceived by 60, 70, and 80-year old elderly using the proposed method

Original image	60 years old	70 years old	80 years old
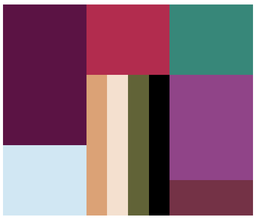	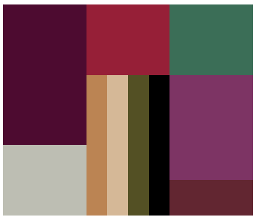	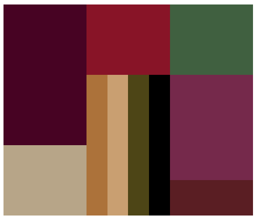	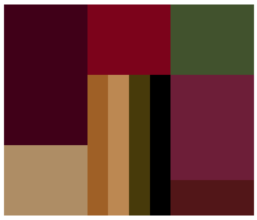
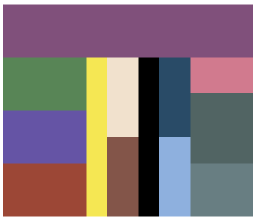	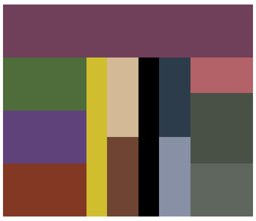	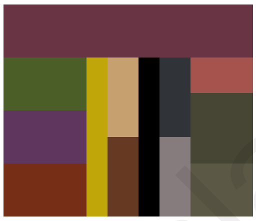	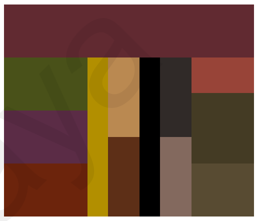
			

of the 80-year-old, the wing loses its blueness. In addition, as age increases, the images become yellowish and darker than the original images. These results may cause the elderly to experience color perception loss, and they may face difficulties in differentiating colors in their daily activities, which is also stated in K. Ishihara et al. (2001), Schneck et al. (1993), T. Suzuki et al. (2005), T. Suzuki et al. (2006), and Yoshida and Sakuraba (1996).

Based on these results, the transition of the color perception of the elderly can be simulated using the proposed method. Furthermore, the images produced from the proposed methods have similar effects as shown in previous works (Norren & Vos, 1974; Pokorny et al., 1986; Ruddock, 1965b; Said & Weale, 1959; Weale, 1961a, 1961b; Werner et al., 1990). To further evaluate the effectiveness of the proposed method, further evaluation tests were conducted in the next experiment.

Table 3.3: Real images and its simulated images as perceived by 60, 70, and 80-year old elderly using the proposed method

Original image	60 years old	70 years old	80 years old
			
			
			

3.4.3 Artificial SPP3 Color Perception Tests

The Standard Pseudoisochromatic Plates (SPP) color perception test is an effective screening test to assess the color perception of humans (Haskett & Hovis, 1987). Thus, in order to observe the similarity between the simulated elderly color perception with the actual elderly color perception, an artificial SPP3 color perception test was conducted. The SPP3 color perception test is a combination of the congenital (SPP1) and acquired (SPP2) color blindness test (Haskett & Hovis, 1987). Ten test images from SPP3 color perception test were utilized in the artificial SPP3 color perception test. These images were simulated as perceived by the 80-year old using the proposed method and Tanaka's method (Tanaka et al., 2011). The SPP3 test images and their simulated images are shown in Figures 3.9 to 3.11.

The subjects who attended this experiment were 22 undergraduate students between the

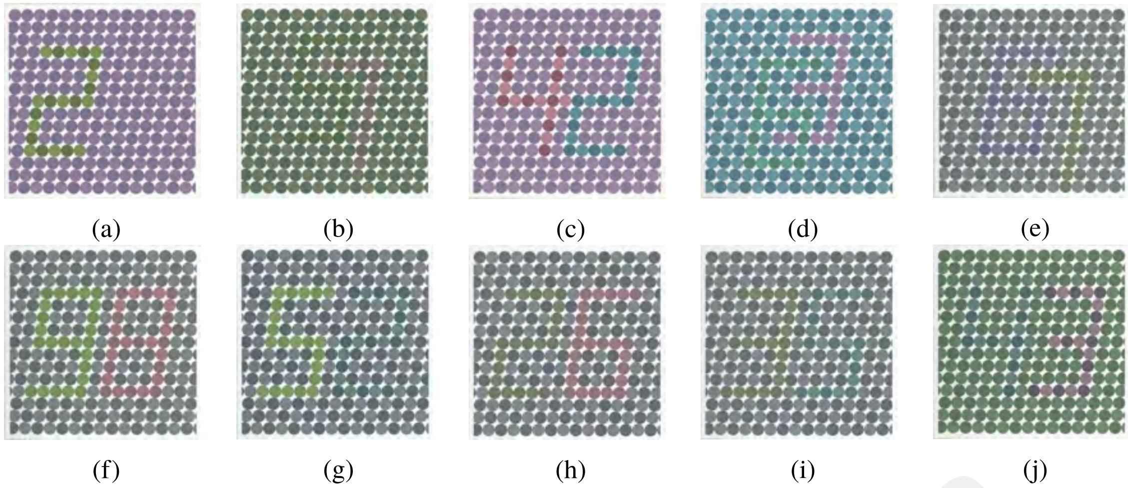

Figure 3.9: The Standard Pseudoisochromatic Plates 3 (SPP3) test images (a) no.1(2); (b) no.2(57); (c) no.3(42); (d) no.4(63); (e) no.5(67); (f) no.6(98); (g) no.7(52); (h) no.8(26); (i) no.9(35); (j) no.10(43)

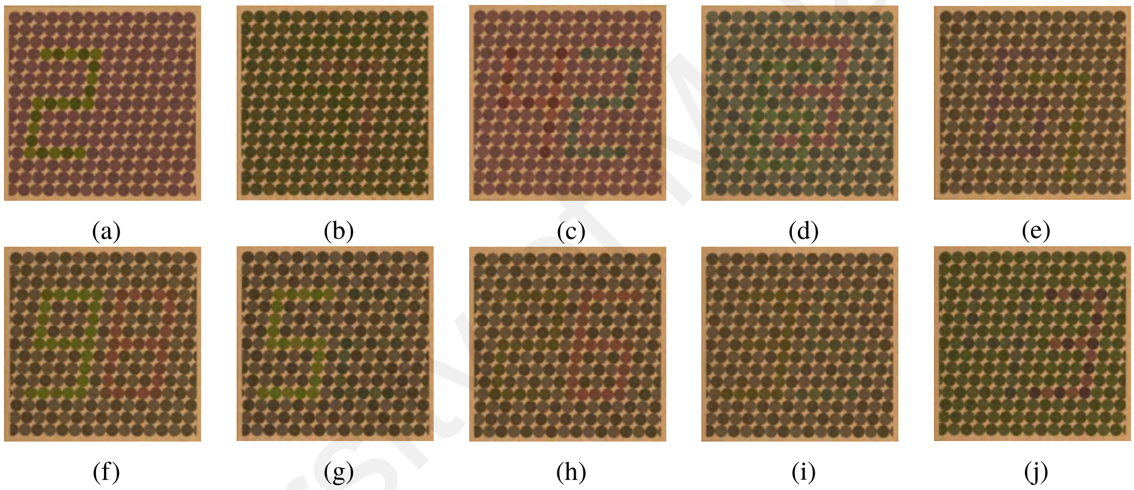

Figure 3.10: The Standard Pseudoisochromatic Plates 3 (SPP3) test images simulated as perceived by the 80-year old using the proposed method (a) no.1(2); (b) no.2(57); (c) no.3(42); (d) no.4(63); (e) no.5(67); (f) no.6(98); (g) no.7(52); (h) no.8(26); (i) no.9(35); (j) no.10(43)

age of 18 and 20 years with a mean age of 18.77. Experiments using young subjects to study the color perception of the elderly have been conducted in previous works (K. Ishihara et al., 2001; Okajima & Takase, 2001; T. Suzuki et al., 2006; Tanaka et al., 2011). As adopted in Tanaka et al. (2011), the color constancy hypothesis was not taken into consideration during the artificial color perception test. By adopting this, the yellowing pigmentation from Tanaka's method and the proposed method change the luminosity and the chromaticity of the color perception of the elderly.

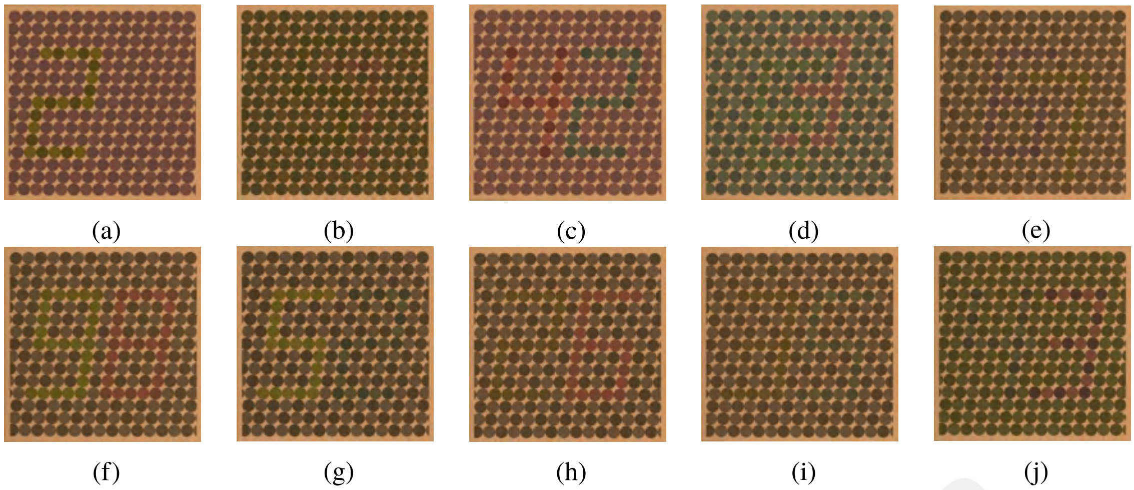

Figure 3.11: The Standard Pseudoisochromatic Plates 3 (SPP3) test images simulated as perceived by the 80-year old using Tanaka's method (a) no.1(2); (b) no.2(57); (c) no.3(42); (d) no.4(63); (e) no.5(67); (f) no.6(98); (g) no.7(52); (h) no.8(26); (i) no.9(35); (j) no.10(43)

The artificial color perception test was conducted in a darkroom environment. The distance between the subject and the LCD was approximately 60 cm. Each test image was displayed for 2 seconds and the interval between test images was 2 seconds. The conditions of the artificial color perception test are summarized in Table 3.4.

Table 3.4: Conditions of artificial color perception test

Item	Condition
Distance between LCD and subject	60 cm
Display time for each test image	2 seconds
Interval time between test images	2 seconds
Location of test image on LCD	Center
Size of test image	512×512 pixel (0.27 mm/pixel)
Background surrounding test image	Gray
Environmental condition	Darkroom

During the artificial color perception test, the test images were shown one at a time to each subject. Moreover, for each method, the test was conducted over two rounds. In the first round, the 10 images shown had the same numbers and background of SPP3 test images. In the second round, the 10 images shown had different numbers, and were presented in a different order from the previous round. This was to avoid habituation by the subjects.

Subjects had to recognize the numbers shown on the images whose colors had been simulated as perceived by the 80-year old. Each time a subject failed to recognize a number shown on a test image, it was considered as one error for that particular number. The average error ratio obtained from the experiment for both methods are shown in Figure 3.12 and compared with the results from the clinical color perception test obtained from eye doctors (Tanaka et al., 2011).

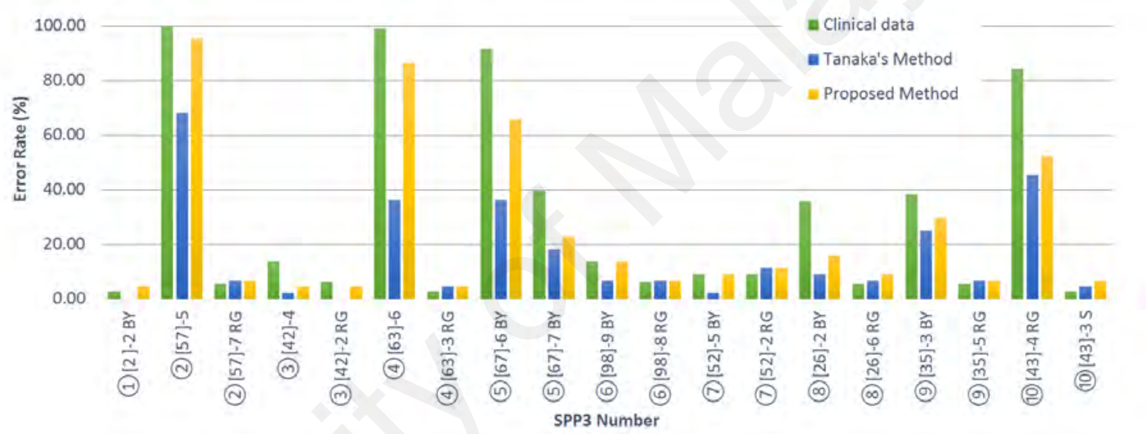

Figure 3.12: Average error ratio of the SPP3 color perception test

From Figure 3.12, it can be observed that the results from the proposed method are closer to the results of the clinical color perception test than the results from the Tanaka's method (Tanaka et al., 2011). This shows that the accuracy of mimicking the color perception of the elderly is fairly improved using the proposed method.

Based on Figure 3.12, results from the clinical data show that the elderly had difficulty recognizing the first number on test image no.2(57). The same thing happened to the subjects of the SPP3 artificial color perception test. Subjects had difficulty recognizing number 5 on the simulated images since the color looks similar to the background as shown in Figures 3.10 and 3.11. The error rates for the first number in the test images no.4(63), no.5(67), and no.10(43) were also high due to this reason.

On the other hand, for the test image no.6(98), the error rate was low because the colors of the numbers on the simulated images are slightly different from the background and could still be recognized by the subjects. As shown in Figures 3.10 and 3.11, both numbers 9 and 8 can still be differentiated from the background. Due to the same reason, the error rates for the test images no.1(2), no.3(42), no.6(98), and no.7(52) were also low.

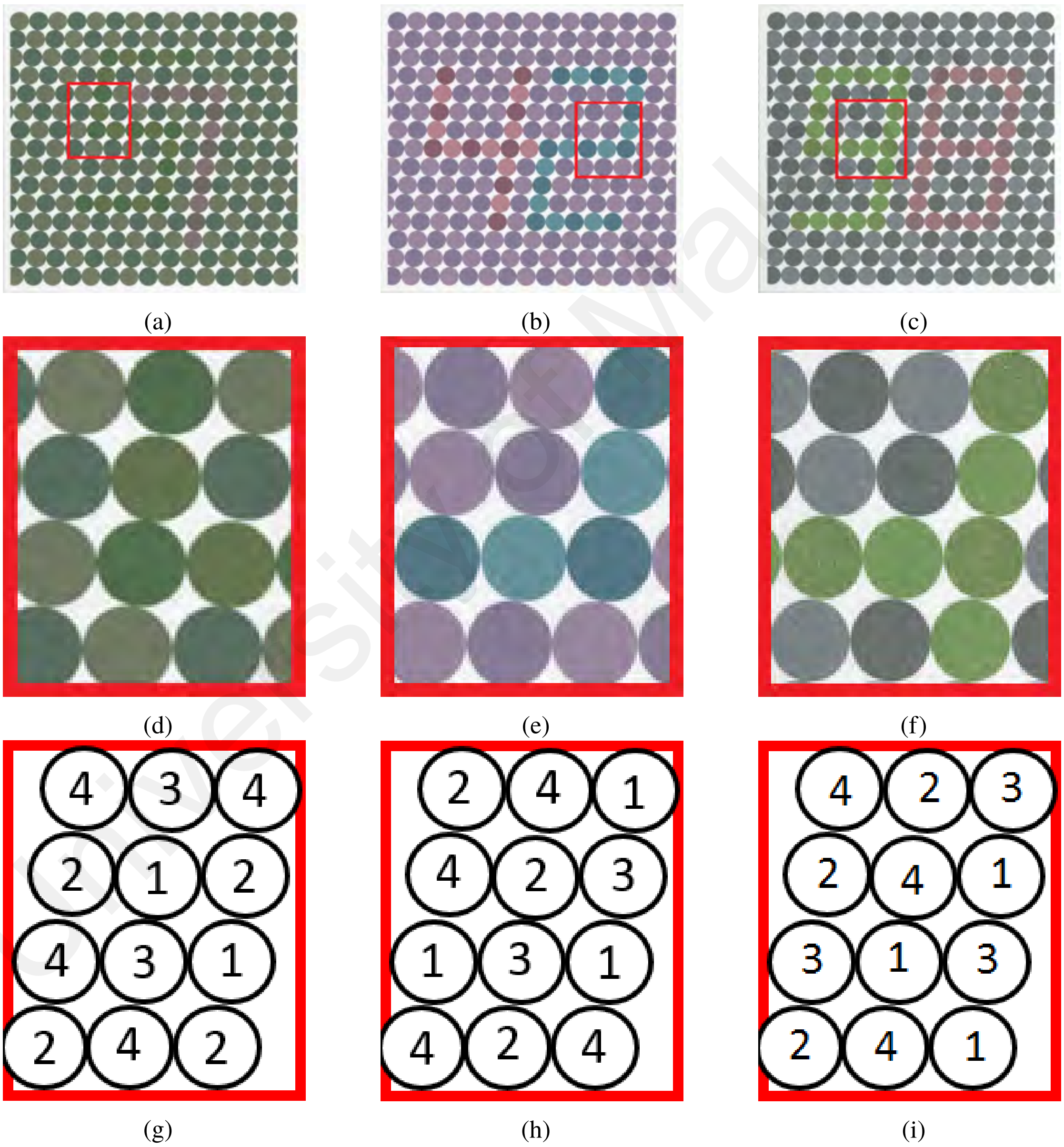

Figure 3.13: (a)-(c) Test images no.2(57), no.3(42), and no.6(98) showing the rectangular section; (d)-(f) Rectangular sections of the respective test images; (g)-(i) Rectangular sections of the respective test images with numbering

A further experiment was conducted to investigate the difference between the simulated images from the proposed method and Tanaka's method (Tanaka et al., 2011). As shown in Figure 3.13, a rectangular section from number 5 on the test image no.2(57), number 2 on the test image no.3(42), and number 9 on the test image no.6(98) were cut and the circles were numbered according to their color. Circles 1 and 3 represent the colors of the number on the test images while circles 2 and 4 represent the background colors.

The rectangular sections were simulated as perceived by the 80-year-old using both methods and the CIEDE2000 color difference, ΔE_{00} (Sharma, Wu, & Dalal, 2005) of the adjacent circles were computed. Tables 3.5 to 3.7 show the color difference values between the adjacent circles for both simulated images.

Table 3.5: Color difference ΔE_{00} of the adjacent circles of the rectangular section from test image no.2(57)

Circles	Proposed method	Tanaka's method
1 and 2	**3.8443**	5.2762
1 and 3	**2.2282**	3.8877
1 and 4	5.1708	**4.7688**
2 and 3	4.9888	**4.3213**
2 and 4	**5.8732**	6.9330
3 and 4	**7.0896**	8.1193

Table 3.6: Color difference ΔE_{00} of the adjacent circles of the rectangular section from test image no.3(42)

Circles	Proposed method	Tanaka's method
1 and 2	**12.9225**	15.7776
1 and 3	4.4172	**4.0841**
1 and 4	**19.9488**	20.8867
2 and 3	**15.4046**	16.0424
2 and 4	**3.6512**	4.9521
3 and 4	19.7509	**17.7028**

Table 3.7: Color difference ΔE_{00} of the adjacent circles of the rectangular section from test image no.6(98)

Circles	Proposed method	Tanaka's method
1 and 2	**16.5334**	16.7848
1 and 3	**2.0988**	3.6148
1 and 4	**4.4597**	18.1432
2 and 3	**10.1937**	10.6438
2 and 4	4.0640	**3.3931**
3 and 4	18.9405	**15.6612**

It can be seen from the tables that most of the color differences ΔE_{00} between horizontal adjacent circles of the proposed method are smaller than those of Tanaka's method. This means that the colors of circles 1 and 3 are almost similar to the colors of circles 2 and 4. It is more difficult for the subjects to recognize number 5, number 2, and number 9 on the simulated test images from the proposed method than the simulated test images from Tanaka's method. Therefore, the error rate of the proposed method is higher than the error rate of Tanaka's method. Moreover, the results from the proposed method are closer to the results of the clinical color perception test.

3.5 Summary

Currently, color images are extensively used to showcase information via websites and smartphone applications. Due to the yellowing on the human crystalline lens, the ability of humans to differentiate colors reduces as age increases, and this may cause confusion and misinterpretation of information by the elderly. Hence, understanding color perception of the elderly is essential in order to minimize this problem. Previous works on color perception of the elderly utilized the non-uniform yellowing pigmentation method. However, recent clinical studies have shown that a uniform yellowing pigmentation occurs on the human crystalline lens. Therefore, in this chapter, we have proposed a mathematical model of the uniform yellowing pigmentation to mimic the color perception experienced by the elderly.

Results obtained from the experimental studies conducted are in agreement with the results obtained from previous works on color perception of the elderly. In the artificial color perception test, the proposed method performed better than the non-uniform yellowing pigmentation method. Moreover, the results from the proposed method are also closer to the results of the clinical color perception test. Based on these results, the effect of the uniform yellowing pigmentation on the color perception of the elderly has been identified. Therefore, implementing the inverse computation of the proposed method, website designers and smartphone application developers can choose better color schemes to represent their information. Thus, misinterpretation of information by the elderly can be avoided. Moreover, designers and architects can produce better visual color representations for the elderly to experience the built environment safely and with confidence.

CHAPTER 4: COLOR PERCEPTION OF RED-GREEN DEFICIENTS

This chapter presents an overview of the color perception of red-green deficients. Mathematical algorithms that model their color perception are also described. Some of the image recoloring methods for red-green deficients are briefly discussed. However, each method has its own disadvantages, especially in preserving the naturalness of the recolored images. Therefore, this chapter proposes a simple and efficient recoloring method that enhances color perception and also maintains the naturalness of the images perceived by red-green deficients.

4.1 Introduction

Color vision, which interprets information from the visible light to form the visual color perception of the surrounding world, is one of the process carried out by the human central nervous system. People with normal color vision, or trichromats, have three independent channels to convey information of colors (Vienot, Brettel, Ott, M'Brek, & Mollon, 1995). These three independent channels are cone photoreceptors which are sensitive in the red, green, and blue spectral range in human eyes, and they are generally represented by the long (L), medium (M), and short (S) cone respectively (Hassan et al., 2015; Hunt, 2004; Vienot et al., 1995). About eight percent of the male population have some kind of inherited color vision deficiencies (Ching & Sabudin, 2010; Semary & Marey, 2014). These are caused by alterations in the opsin gene array in the X chromosome (Sharpe, Stockman, Jagle, & Nathans, 1999). Dichromacy is one of the inherited color vision deficiencies, and it occurs when one of the cones is absent or not functioning. Thus, individuals with dichromacy, or dichromats, experience color perception in a two-dimensional color space (Judd, 1949; Vienot et al., 1995).

Dichromacy can be further classified into three categories depending on which cone carries the defect (Neitz & Neitz, 2011). Protanopia, also known as red-deficiency, occurs when the defect is on the L-cone that carries red sensitivities. Deuteranopia also known as green-deficiency, occurs when the M-cone that carries green sensitivities is deficient. People with red-deficiency and green-deficiency are called protanopes and deuteranopes respectively. Both these categories are also called red-green deficiency (Alvaro, Linhares, Moreira, Lillo, & Nascimento, 2017; Moreira et al., 2018). People with red-green deficiency have difficulty in distinguishing between these two colors (Judd, 1949; Ching & Sabudin, 2010); they view red and green as yellow, orange, and beige (Alvaro, Moreira, Lillo, & Franklin, 2015; Alvaro et al., 2017). This creates confusion and may cause misinterpretation of information (Suetake et al., 2012). Another type of dichromacy is called tritanopia, in which the S cone that carries blue sensitivities is deficient. Tritanopia is also known as blue-yellow deficiency where people with tritanopia have difficulty to distinguish shades of blue and yellow. However, people with tritanopia, or tritanopes, comprise less than one percent of the male population (Moreira et al., 2018).

People with dichromacy or any other type of color vision deficiency experience great difficulty with color discrimination that not only affects their social life but may also affect their careers (Cole, 2007; Tagarelli et al., 2004). In order to understand color experience of dichromats, several methods to simulate their color perception have been proposed. Although it seemed impossible at first to know their color perception, a few individuals have been discovered to have one protanopia, deuteranopia, or tritanopia eye and one normal eye. These individuals are known to have unilateral protanopia, unilateral deuteranopia, and unilateral tritanopia respectively. Research on these individuals shows that a stimulus of 575 nm is perceived as the same yellow, and a stimulus of 475 nm as the same blue, by trichromats, protanopes, and deuteranopes (Judd, 1949). In the case of unilateral tritanopia, the corresponding two hues that are viewed similarly by trichromats and tritanopes are a red with a dominant wavelength of 660 nm and a blue-green with a dominant wavelength of approximately 485 nm (Alpern, Kitahara, & Krantz, 1983).

Based on this information, dichromats confusion lines or dichromatic isochromatic lines, exist and converge at a single point for each type of color vision deficiency (Birch, 1972). The confusion line for protanopia, deuteranopia and tritanopia are shown in Figures 4.1(a) to 4.1(c). Colors represented along such a line are perceived as identical if no luminance contrast is present.

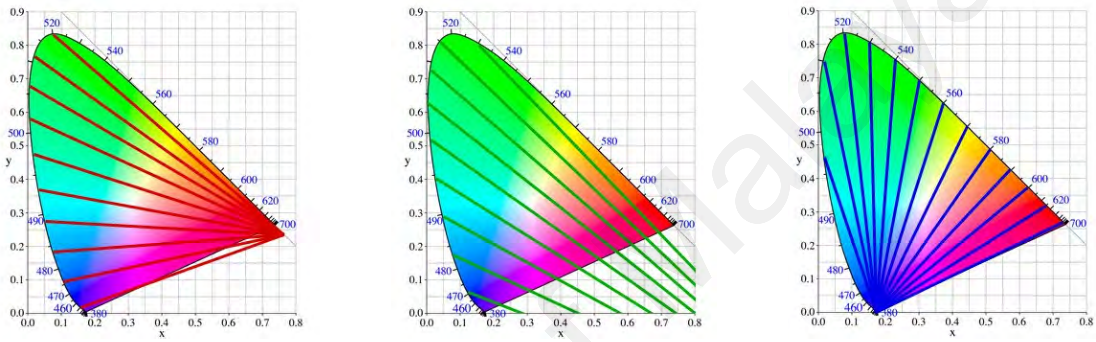

(a) (b) (c)

Figure 4.1: Confusion lines in the CIE 1931 color space for (a) protanopia; (b) deuteranopia; (c) tritanopia (Daniel, 2010)

Based on these findings, Meyer and Greenberg (1988) proposed a color reproduction method by utilizing the CIE color matching functions to produce an image that approximates the image seen by dichromats. Their work is considered a pioneer work in using color television displays and digitally controlling it to identify dichromatic color perception. Brettel et al. proposed a computerized simulation of dichromatic vision (Brettel et al., 1997). Their aims are to reproduce dichromatic color perception and also offer a plausible dichromatic color appearance to trichromats. Moreover, protanopes and deuteranopes confirmed that the colors produced by Brettel's algorithm are accurate. Further experiments on Brettel's algorithm by Vienot et al. produced the linear transformations from trichromatic color perception to dichromatic color perception (Vienot et al., 1999).

Another model to simulate the color perception of dichromats was proposed by Wachtler et al. (2004). The key feature of their model is the processing of the photoreceptor signals in parallel channels with different gains and nonlinearities. Meanwhile, Capilla, Diez-Ajenjo, et al. (2004) introduced an alternative algorithm called the corresponding-pair procedure . However, this procedure can only be applied to color models that fulfill certain conditions. Furthermore, Capilla, Luque, and Diez-Ajenjo (2004) utilized different color vision models to represent dichromatic color perception. In this method, they implemented either a cone-loss model, setting the appropriate cone responses to zero, or a cone-replacement model, in which the L cone becomes an M cone for protanopia and the M cone becomes an L cone for deuteranopia.

A more recent work conducted by Machado et al. (2009) presents a physiologically based model to simulate dichromatic color perception. Their model is based on the stage theory of human color vision and is derived from the data obtained in electrophysiological studies. Their work not only simulates dichromatic color perception, but it can also be utilized to represent anomalous trichromacy. Meanwhile, Lee and dos Santos (2011) modified Brettel's algorithm (Brettel et al., 1997) using an adaptive fuzzy-based system to represent the linear transformation of anamolous trichromacy. Furthermore, a two stage model of dichromatic color perception is introduced by Rodriquez-Pardo and Sharma (2011). Their model consists of a first sensor stage with per-channel gain control and a second opponent encoding stage. However, although their model is in agreement with the perceptual data, they have not performed any psychophysical validation to verify their model. Of all the models discussed above, Brettel's algorithm (Brettel et al., 1997; Vienot et al., 1999) is the most accepted method due to its mathematical simplicity and its usability in expressing dichromatic color perception.

Utilizing Brettel's algorithm to simulate dichromatic color perception, several methods using different strategies have been proposed to enhance the visual details missed by dichromats. Most of the recoloring methods proposed for dichromacy focus on protanopia and deuteranopia. This is due to the fact that protanopia and deuteranopia are from the red-green deficiency group that corresponds to over 99.9 percent of all color vision deficiency cases worldwide (Sharpe et al., 1999). Rigden (1999) created color palette for protanopia and deuteranopia based on the standard 216-color web-safe palette. Another method for website color modification was proposed by Ichikawa et al. (2003). They proposed an automatic color arrangement optimization process using a genetic algorithm known as the robust optimization method. Wakita and Shimamura (2005) proposed a repainting system called SmartColor which replaces the set of colors used in the original documents with another set of colors. However, although these methods help designers plan a proper color scheme for their designs, these methods are not suitable for natural images since they consist of limited colors. Moreover, the use of a limited number of colors may harm a designer's creativity.

To overcome this issue, Yang and Ro (2003) proposed an adaptive recoloring method that allows color adaptation at anytime and anywhere according to the type and severity of the color vision deficiency. Their color adaptation method consists of two stages; hue adaptation and saturation adaptation. Meanwhile, Jefferson and Harvey proposed a recoloring method that selects key colors from the difference between the original image and dichromat perceived image histograms (Jefferson & Harvey, 2006). They utilize four objective functions to preserve brightness, color contrast, colors in available gamut, and color naturalness.

Another recoloring process was proposed in Anagnostopoulos et al. (2007). Their method implemented logical image masking in order to modify the colors that are confused, and to preserved colors that are perceived correctly. To improve the efficiency of this method, Doliotis et al. (2009) added a color clustering process to automatically differentiate between colors that need to be recolored and colors that need to be preserved. However, this method implemented a complex computational algorithm that may not be suitable for practical applications.

Rasche et al. (2005a) proposed an automatic recoloring method that implemented an optimization process using an affine transformation in order to preserve the perceptual color differences between all pairs of colors. However, this method does not capture the color variation along many directions and does not ensure that the mapped colors are all within the available color gamut. To address this limitation, they implemented a constrained multivariate optimization procedure applied to a reduced set of quantized color, which are then used to optimize the entire set of colors (Rasche et al., 2005b). Even though they improved their previous method, they did not take into consideration the problem of naturalness preservation, and the method can arbitrarily change all the colors of the original images.

One of the concerns in the recoloring method for dichromats is to preserve the naturalness of the recolored images. Kuhn et al. (2008) proposed a naturalness-preserving recoloring method by implementing a mass-spring system to optimize the colors in the input image and enhance the color contrast for dichromats. However, this method did not preserve the temporal coherence of the images. Thus, Machado and Oliveira (2010) proposed an automatic image-recoloring technique for enhancing color contrast for dichromats while maintaining the temporal coherence of the images. Moreover, due to this characteristic, it is also suitable for video recoloring. Although this technique is better than Kuhn's method, this method is more suitable to recolor scientific visualization images.

In natural images, the number of colors may be less than the whole range of the color spectrum. Hence, there are a lot of color redundancies that can be utilized. By exploiting the color redundancies, Ma et al. (2006) proposed a nonlinear transformation method.

Their method uses the self-organizing map to change the colors. This method has two advantages: global nonlinearity, which is more effective that linearity or local nonlinearity and adaptability, which makes the practical implementation more viable.

Huang et al. (2007) developed a recoloring process that can automatically construct a transformation process which maintains the visual details for dichromats and preserves the naturalness for trichromats. Their method utilized a rotational process in CIELAB color space to transform the colors in the image while maintaining the luminance of the original image. However, the results from this method may not be depictive enough. In Huang et al. (2009), they proposed another recoloring method that implemented a more depictive strategy: the Gaussian Mixture Model (GMM) together with the Expectation-Maximization (EM) algorithm to represent the colors in the images. Using the optimization process, they determined the optimal mapping to maintain the color contrast between a pair of colors. The optimal mapping functions are then used in the recoloring process.

Recently, Ribeiro and Gomes (2013) proposed a simpler recoloring method by implementing the Hue-Saturation-Value (HSV) color model. Their main objective is to avoid confusion between red and green colors. To achieve that, they remapped the confused colors using trivariate recoloring and hue remapping functions. These functions ensure that any two different colors are mapped into two distinct colors.

Although all the aforementioned recoloring methods enhance the visual details and improve the color perception of the red-green deficients, the recolored images may look nonpleasing to trichromats (Huang et al., 2007; Jeong et al., 2011). Moreover, the recoloring methods may potentially change all the colors of the original images and thus, may make the recolored images look unnatural to the red-green deficients as well (Kuhn et al., 2008). If the recoloring method focuses only on the needs of red-green deficients, these recolored images may appear awkward to trichromats. On the other hand, if the needs of the red-green deficients are not taken into consideration, they may face difficulties when looking at the images. This may happen in public places such as in airports, shopping malls, and train stations where color images used in advertisements and maps are observed by both trichromats and red-green deficients. Thus, it is important to have a recoloring method that takes into consideration the needs of both parties.

Therefore, this chapter proposes a simple and efficient recoloring method that improves visual details and color perception of the red-green deficients and also preserves the naturalness of the recolored images for both trichromats and red-green deficients. The main advantage of the proposed method is that it recolors the colors confused by the red-green deficients with colors that have the same hue as the original. Moreover, the recolored images have the same luminance as the original images. The proposed method consists of two main parameters: error parameters and a rotation parameter. These parameters are used to compute the modified error parameters that will be distributed back into the original colors. The rest of the chapter is organized as follows. Section 4.2 describes the fundamental algorithm of the color perception of dichromats. The proposed recoloring method is described in Section 4.3. The performance of the proposed recoloring method and comparison with other recoloring methods are discussed in Section 4.4. Lastly, the chapter conclusion is presented in Section 4.5.

4.2 Dichromatic Color Perception Model

Of all the models that represent the dichromatic color perception, Brettel's algorithm (Brettel et al., 1997; Vienot et al., 1999) is the most accepted model due to its mathematical simplicity and its usability in expressing the color discrimination of dichromats. Hence, this section describes Brettel's algorithm.

4.2.1 Brettel's Algorithm

Brettel's algorithm (Brettel et al., 1997; Vienot et al., 1999) represents color stimuli as a vector in a three-dimensional LMS color space. The LMS color space is specified by the peak responses of the three types of cones for the human eye, which are named after the human eyes cone photoreceptors which are long (L), medium (M), and short (S).

Thus, to implement Brettel's algorithm, color images need to be transformed to the LMS color space. This is done first by transforming the RGB color space to the XYZ color space using the transformation matrix obtained via Judd-Vos colorimetric modification (Travis, 1991; Vienot et al., 1999)

$$\begin{bmatrix} X \\ Y \\ Z \end{bmatrix} = \begin{bmatrix} 40.9568 & 35.5041 & 17.9167 \\ 21.3389 & 70.6743 & 7.98680 \\ 1.86297 & 11.4620 & 91.2367 \end{bmatrix} \begin{bmatrix} R \\ G \\ B \end{bmatrix} \tag{4.1}$$

Then, the XYZ color space is transformed to LMS color space according to Smith and Pokorny (1995)

$$\begin{bmatrix} L \\ M \\ S \end{bmatrix} = \begin{bmatrix} 0.15514 & 0.54312 & -0.03286 \\ -0.15514 & 0.45684 & 0.03286 \\ 0 & 0 & 0.01608 \end{bmatrix} \begin{bmatrix} X \\ Y \\ Z \end{bmatrix} \tag{4.2}$$

For simplification, these computations can be combined as shown below:

$$\begin{bmatrix} L \\ M \\ S \end{bmatrix} = \begin{bmatrix} 17.8824 & 43.5161 & 4.11935 \\ 3.45565 & 27.1554 & 3.86714 \\ 0.0299566 & 0.184309 & 1.46709 \end{bmatrix} \begin{bmatrix} R \\ G \\ B \end{bmatrix} \tag{4.3}$$

To understand the algorithm more clearly, a geometric representation of the algorithm is shown in Figures 4.2 and 4.3. As shown in Figures 4.2 and 4.3, in dichromatic vision, the

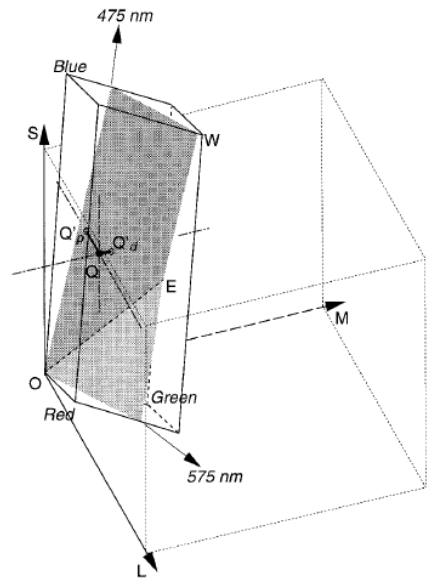

Figure 4.2: Geometric representation of the reduced stimuli surface for protanopia and deuteranopia (Brettel et al., 1997; Vienot et al., 1999)

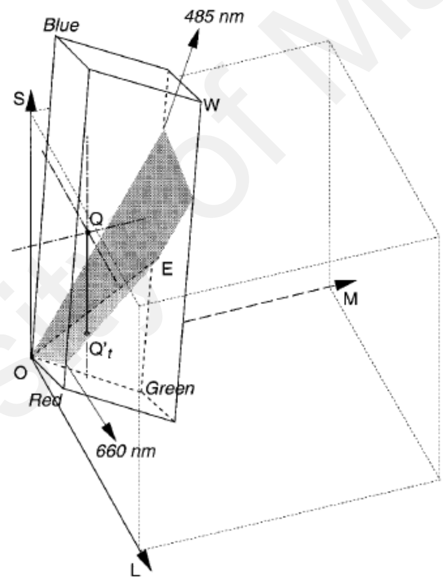

Figure 4.3: Geometric representation of the reduced stimuli surface for tritanopia (Brettel et al., 1997; Vienot et al., 1999)

LMS color space is reduced to two color domains which include the origin **O**, the nominal white stimulus **W**, and the neutral color stimulus **E**. In these figures, OE represents the neutral stimuli for dichromats as well as for trichromats. The neutral axis OE divides the surface of the reduced stimuli into two half-planes, each of which is anchored on a point specifying an invariant hue for a given type of dichromat.

The wings from OE toward the 475 nm and 575 nm locations represent the reduced stimuli surface for protanopia and deuteranopia stimulation as shown in Figure 4.2. Meanwhile, the wings from OE toward the 485 nm and 660 nm locations represent the reduced stimuli surface for tritanopia as shown in Figure 4.3. For any given stimulus **Q** located on the LMS color space, Brettel's algorithm replaces the undetermined component of a dichromat by the value corresponding to the projection of **Q** onto the wing, parallel to the direction of the missing fundamental axis.

Using vector algebra, the equation for any given stimulus **Q'** on a plane defined by the origin **O**, the monochromatic anchor stimulus **A** with coordinates of (L_A, M_A, S_A) and stimuli **E** with coordinates of (L_E, M_E, S_E) is given as

$$(\mathbf{E} \times \mathbf{A})\mathbf{Q'} = 0 \tag{4.4}$$

since **Q'** is always orthogonal to the normal vector $\mathbf{E} \times \mathbf{A}$ of the plane. Solving the plane relation gives the linear equation of the stimulus **Q'** with coordinates (L_Q, M_Q, S_Q) as

$$\alpha L_Q + \beta M_Q + \gamma S_Q = 0 \tag{4.5}$$

with

$$\alpha = M_E S_A - S_E M_A \tag{4.6}$$

$$\beta = S_E L_A - L_E S_A \tag{4.7}$$

$$\gamma = L_E M_A - M_E L_A \tag{4.8}$$

From these relations, the reduction of the normal color domain to the dichromatic color domain maintains the unaffected values that correspond to the existing photoreceptors.

Thus, the replacement tristimulus values corresponding to the missing photoreceptor is, for the protanopia

$$L_p = \frac{-(\beta M + \gamma S)}{\alpha} \tag{4.9}$$

for the deuteranopia,

$$M_d = \frac{-(\alpha L + \gamma S)}{\beta} \tag{4.10}$$

and for the tritanopia

$$S_t = \frac{-(\alpha L + \beta M)}{\gamma} \tag{4.11}$$

where L, M, S are the values obtained in Eq. (4.3).

Further experiments by Vienot et al. produced the linear transformation from trichromatic vision to the red-green deficiency using the following transformation matrices (Vienot et al., 1999). For protanopia,

$$\begin{bmatrix} L_p \\ M_p \\ S_p \end{bmatrix} = \begin{bmatrix} 0 & 2.02344 & -2.52581 \\ 0 & 1 & 0 \\ 0 & 0 & 1 \end{bmatrix} \begin{bmatrix} L \\ M \\ S \end{bmatrix} \tag{4.12}$$

and for deuteranopia,

$$\begin{bmatrix} L_d \\ M_d \\ S_d \end{bmatrix} = \begin{bmatrix} 1 & 0 & 0 \\ 0.494207 & 0 & 1.24827 \\ 0 & 0 & 1 \end{bmatrix} \begin{bmatrix} L \\ M \\ S \end{bmatrix} \tag{4.13}$$

Finally, to form the image viewed by protanopes and deuteranopes, the LMS values obtained from Eq. (4.12) and Eq. (4.13) are transformed back to the RGB color space using the inverse of Eq. (4.3).

Table 4.1 illustrates the color perception of protanopes and deuteranopes using Brettel's algorithm for natural images taken from Kuhn et al. (2008), Martin, Fowlkes, Tal, and Malik (2001), and Rasche et al. (2005b).

Table 4.1: Color perception of the red-green deficiency

Original image	Protanopia	Deuteranopia
		
		
		
	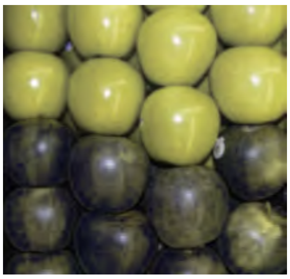	

4.3 Proposed method - Naturalness Preservation Recoloring Method

This section proposes a simple and efficient recoloring method that enhances visual details and improves the color perception of the red-green deficients. The proposed method also maintains the naturalness of the recolored image for both trichromats and red-green deficients. To achieve these objectives, the proposed method adopts two premises. First, the luminance of the recolored image is the same as the luminance of the original image. Second, the recolored image has the same hue as the original image.

In the proposed method, the original image and the image perceived by the red-green deficients are converted into the XYZ color space. The XYZ color space is chosen as the working domain because it encompasses all color sensations that a human can perceive and is formulated based on the RGB version of the human eye (Fairchild, 2005). Moreover, the XYZ color space can be easily mapped to many alternative RGB color spaces by simply choosing any point of the chromaticity diagram.

To maintain the same luminance, the XYZ tristimulus values for both images are normalized. The error parameters and rotation parameter are then computed. These parameters are used to compute the modified error parameters. To obtain the recolored image, the modified error parameters are distributed back to the original image but in such a way that it increases the blue stimulation of the recolored image while maintaining the same hue as the original image. The overall process of the proposed method is summarized in Figure 4.4.

To start the recoloring process, the original image, R_o, G_o, B_o and the image perceived by red-green deficients R_s, G_s, B_s are converted to X_o, Y_o, Z_o and X_s, Y_s, Z_s respectively using Eq. (4.1). Next, both sets of tristimulus values are normalized so that the value of the luminance Y_o and Y_s are set to 100. This is so that the luminance of the recolored image can be maintained as similar to the original one. Thus, the normalized tristimulus

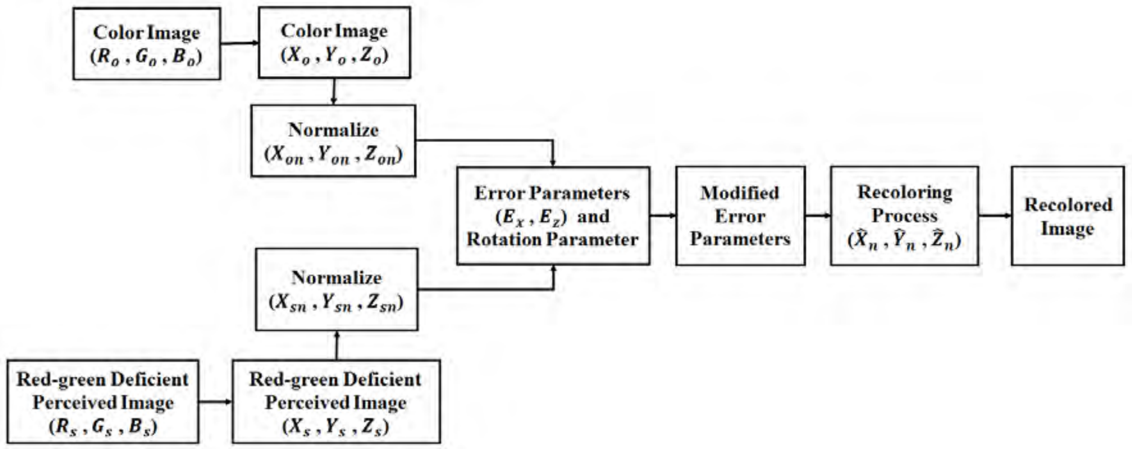

Figure 4.4: Overall process flow of the proposed image recoloring method

values of the original image and the image perceived by red-green deficients are given as X_{on}, Y_{on}, Z_{on} and X_{sn}, Y_{sn}, Z_{sn} respectively.

Based on Brettel's algorithm (Brettel et al., 1997; Vienot et al., 1999), it is evident that the red-green deficients have difficulty discriminating colors and thus changing their color perception. Hence, the error parameters are defined as the absolute difference between the normalized tristimulus values of the original image and the image perceived by the red-green deficients. Since Y_{on} and Y_{sn} have the same value, there are only two error parameters that need to be computed, E_x and E_z.

$$E_x = |X_{on} - X_{sn}| \tag{4.14}$$

$$E_z = |Z_{on} - Z_{sn}| \tag{4.15}$$

In the proposed method, we modified the error parameters by adopting a rotation operation in the XZ plane in order to transform the information of X onto the Z-axis. The rotation operation is performed according to the value of the rotation parameter, ϕ. In order to compute the rotation parameter, ϕ, the normalized X and Z values of both the original image and the image perceived by red-green deficients are plotted on the XZ plane as illustrated in Figure 4.5.

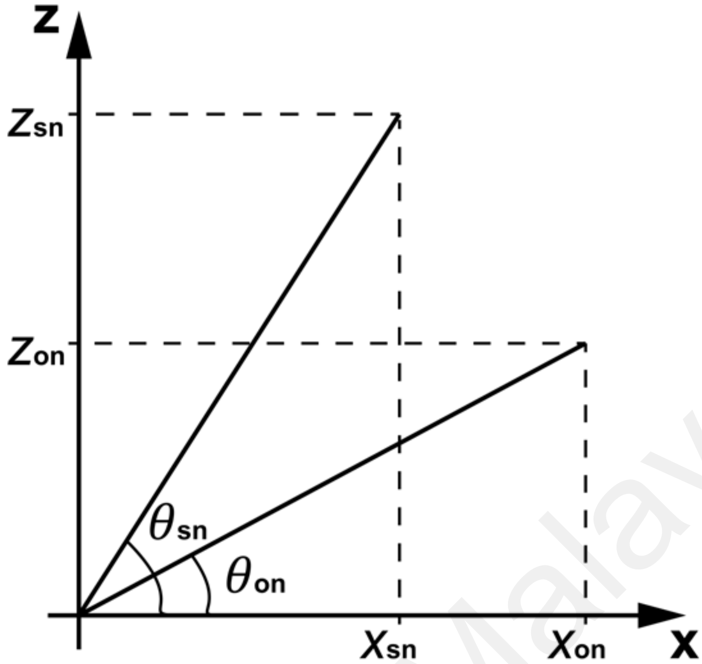

Figure 4.5: Angles of elevation of the normalized X and Z values

Based on Figure 4.5, the angles of elevation from the X-axis are computed for both points and they are defined as

$$\theta_{on} = tan^{-1}\left(\frac{Z_{on}}{X_{on}}\right) \tag{4.16}$$

$$\theta_{sn} = tan^{-1}\left(\frac{Z_{sn}}{X_{sn}}\right) \tag{4.17}$$

Hence, the rotation parameter, ϕ, is defined as the absolute difference between the angles of elevation, θ_{on} and θ_{sn}.

$$\phi = |\theta_{on} - \theta_{sn}| \tag{4.18}$$

As illustrated in Figure 4.6, the error parameters are plotted on the XZ plane and the point is rotated according to the rotation parameter, ϕ. The rotation operation increases the value of E_z which is related to the error of the blue stimulation and simultaneously decreases the value of E_x. From the rotation operation, the value of E_x and E_z are

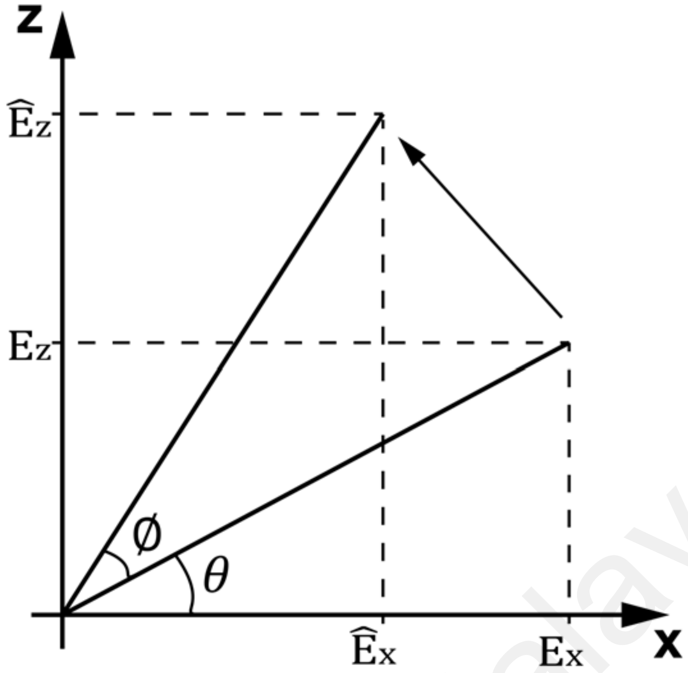

Figure 4.6: Rotation operation of the error parameters

modified to $\widehat{E}_x$ and $\widehat{E}_z$ respectively. Mathematically, $\widehat{E}_x$ and $\widehat{E}_z$ can be formulated as matrix multiplication.

$$\begin{bmatrix} \widehat{E}_x \\ \widehat{E}_z \end{bmatrix} = \begin{bmatrix} cos\phi & -sin\phi \\ sin\phi & cos\phi \end{bmatrix} \begin{bmatrix} E_x \\ E_z \end{bmatrix} \tag{4.19}$$

The modified error parameters $\widehat{E}_x$ and $\widehat{E}_z$ are distributed back to the normalized tristimulus values of the original image X_{on}, Y_{on}, Z_{on} as shown below.

$$\widehat{X}_n = X_{on} + \widehat{E}_x \tag{4.20}$$

$$\widehat{Y}_n = Y_{on} \tag{4.21}$$

$$\widehat{Z}_n = Z_{on} + \left(\widehat{E}_x + \widehat{E}_z\right) \tag{4.22}$$

The $\widehat{E}_x$ and $\widehat{E}_z$ are both added into Z_{on} in order to increase the blue stimulation of the recolored image so as to enhance the color perception of the red-green deficients. Moreover, the distribution process recolored the original image with the colors of the same hue so as to preserve the naturalness of the original image from a trichromat's point of view.

Finally, the recolored tristimulus values $\widehat{X}_n, \widehat{Y}_n, \widehat{Z}_n$ are un-normalized and converted back to the *RGB* values using the inverse relation of Eq. (4.1). The recolored image perceived by red-green deficients can be observed using Brettel's algorithm (Brettel et al., 1997; Vienot et al., 1999).

4.4 Experimental Studies

In this section, two experimental studies were performed to evaluate the proposed method. The naturalness error, E_{nat} (Huang et al., 2007; Jeong et al., 2011) and the Feature Similarity chrominance (FSIMc) index (Zhang, Zhang, Mou, & Zhang, 2011) were computed to objectively evaluate the effectiveness of the proposed method and other recoloring methods in preserving the naturalness of the recolored images. Moreover, a visual comparison of the protanopic and deuteranopic views of the recolored images was also performed.

Lastly, paired comparison tests (Thurstone, 1927) were conducted with trichromats and red-green deficients in order to evaluate the performance of the proposed method in terms of the naturalness preservation of the recolored images and the overall preference.

Prior to the studies, the LCD was calibrated using X-Rite i1Display 2 based on sRGB color space and white point of D65. The gamma correction parameter, γ was set to 2.2. The calibration process ensures that the preciseness of color reproduction on LCD display is within a very small range of error (Tanaka et al., 2011).

4.4.1 Objective Evaluations

In this experiment, 6 natural images taken from Kuhn et al. (2008), Martin et al. (2001), and Rasche et al. (2005b) were utilized. The proposed method was compared with two recoloring methods: Huang's (Huang et al., 2009) and Ribeiro's methods (Ribeiro & Gomes, 2013). These two methods were chosen for comparison because they implemented a similar recoloring framework as the proposed method in which the original images are recolored instead of the images perceived by the red-green deficients.

The images were recolored using the proposed method, Huang's method (Huang et al., 2009), and Ribeiro's method (Ribeiro & Gomes, 2013). Then, to observe how protanopes and deuteranopes view the recolored images, the recolored images were simulated using Brettel's algorithm (Brettel et al., 1997; Vienot et al., 1999). To objectively evaluate the performance of these three recoloring methods, the naturalness error, E_{nat} (Huang et al., 2007; Jeong et al., 2011) of the recolored images was computed. The naturalness error is defined as

$$E_{nat} = \sum_{i} \left\| C_i - \hat{C}_i \right\|^2 \tag{4.23}$$

where i ranges over the colors contained in the images, C is the original image and $\hat{C}$ is the recolored image. Table 4.2 shows that the proposed method produced recolored images that have the smallest naturalness errors. This means that the proposed method produces recolored images that have a better degree of correspondence with the original images than the other two recoloring methods.

Table 4.2: Naturalness error, E_{nat} of the recolored images

Original image	Proposed method	Huang's method	Ribeiro's method
Red Berries	**1,817**	2,772	3,093
Apples	**4,138**	4,180	6,746
Red Flowers	**3,051**	9,915	4,049
Orange Flower	**2,275**	7,024	2,374
Peppers	**2,408**	3,702	3,761
Flowers	**4,259**	8,198	7,129

In addition, the chrominance information of the recolored images with respect to the original images was computed using Feature Similarity chrominance (FSIMc) index (Zhang et al., 2011). Higher FSIMc index shows that the chrominance information of the recolored images is closer to the chrominance information of the original images. Hence, the recolored images with a higher FSIMc index look almost similar to the original images from a trichromat's point of view. As shown in Table 4.3, the recolored images from the proposed method obtained the highest FSIMc index as compared to the other two recoloring methods.

Table 4.3: Feature Similarity (FSIMc) index of the recolored images

Original image	Proposed method	Huang's method	Ribeiro's method
Red Berries	**0.986**	0.974	0.965
Apples	**0.974**	0.889	0.920
Red Flowers	**0.961**	0.949	0.944
Orange Flower	**0.988**	0.928	0.973
Peppers	**0.990**	0.987	0.932
Flowers	**0.967**	0.953	0.917

Next, a visual comparison was conducted between the recolored images of the proposed method and the other two recoloring methods. As shown in Tables 4.4 and 4.5, the recolored images from the proposed method look more similar to the original images than the recolored images from the other two recoloring methods. This is in agreement with the results obtained in Tables 4.2 and 4.3. Since the proposed method recolors the red-green deficients confused colors with colors that have the same hue as the original, the recolored images maintain the naturalness of the original images as much as possible.

On the other hand, in Huang's and Ribeiro's methods, the recolored images lose their naturalness as the red-green deficients' confused colors are recolored with colors that have different hues. Moreover, Huang's method has the tendency to recolor colors

Table 4.4: Recolored images and images perceived by the red-green deficients

Original image	Perceived by protanopes	Perceived by deuteranopes
		
	Proposed method	
Recolored image	Perceived by protanopes	Perceived by deuteranopes
	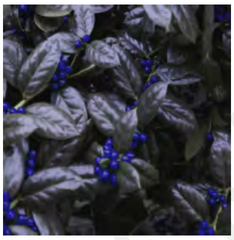	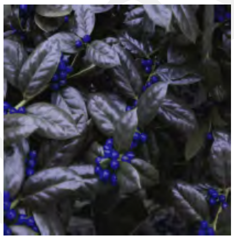
	Huang's method	
Recolored image	Perceived by protanopes	Perceived by deuteranopes
	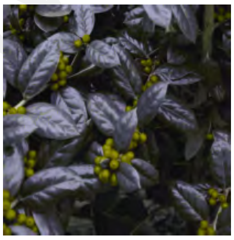	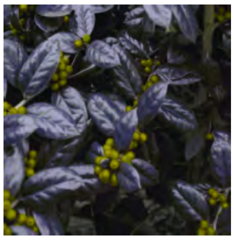
	Ribeiro's method	
Recolored image	Perceived by protanopes	Perceived by deuteranopes
		

whose differences are perfectly visible to trichromats to colors that look identical to them (Simon-Liedtke & Farup, 2016). Therefore, their recolored images may look weird and

Table 4.5: Recolored images and images perceived by the red-green deficients

Original image	Perceived by protanopes	Perceived by deuteranopes
		
	Proposed method	
Recolored image	Perceived by protanopes	Perceived by deuteranopes
	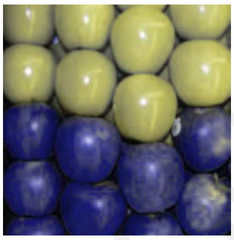	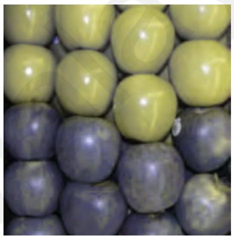
	Huang's method	
Recolored image	Perceived by protanopes	Perceived by deuteranopes
		
	Ribeiro's method	
Recolored image	Perceived by protanopes	Perceived by deuteranopes
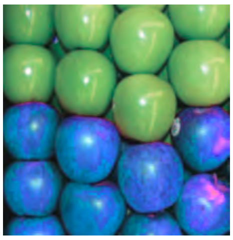	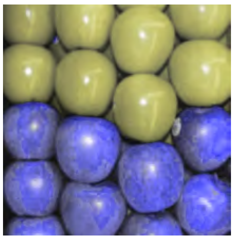	

unnatural. This can be observed from Table 4.4 where the color of the red berries are recolored to orange and light blue by Huang's and Ribeiro's methods respectively. The same happened to the color of the red apples in Table 4.5 where Huang's and Ribeiro's methods recolored the red apples with purple and blue respectively.

Images perceived by red-green deficients can also be observed in Tables 4.4 and 4.5. From the results, it can be observed that all three methods enhance the visual details of the original images. Moreover, compared to the original images perceived by red-green deficients, all the recolored images improve the color perception of the red-green deficients. As shown in Table 4.4, the red berries of the recolored images perceived by red-green deficients are more visible as compared to the original image perceived by them. In addition, the recolored images perceived by red-green deficients in Table 4.5 show the difference between the green and red apples more clearly than the original image perceived by them. However, in order to further evaluate the effectiveness of the proposed method and other recoloring methods, subjective evaluations were conducted in the next experiment.

4.4.2 Paired Comparison Tests

In this experiment, paired comparison tests (Thurstone, 1927) were conducted with trichromats and red-green deficients. The main objective of this experiment is to evaluate the performance of the proposed method with Huang's (Huang et al., 2009) and Ribeiro's methods (Ribeiro & Gomes, 2013) in terms of the naturalness preservation of the recolored images and the overall preference by the trichromats and red-green deficients. Twenty-four test images were utilized for protanopia and deuteranopia paired comparison tests and these images are shown in Table 4.6.

There were a total of 36 pairs of test images for each paired comparison test and these images were arranged side-by-side; *(Or, P), (Or, H), (Or, R), (P, H), (P, R),* and *(H, R)* where *Or* stands for original image, *P* for the image recolored by the proposed method, *H* for Huang's method, and *R* for Ribeiro's method. To avoid habituation, the order of the images in each pair, as well as the order of each pair were defined randomly. These images

Table 4.6: Images used in the paired comparison test

Original image	Recolored images for protanopia test			Recolored images for deuteranopia test		
	Proposed method	Huang's method	Ribeiro's method	Proposed method	Huang's method	Ribeiro's method

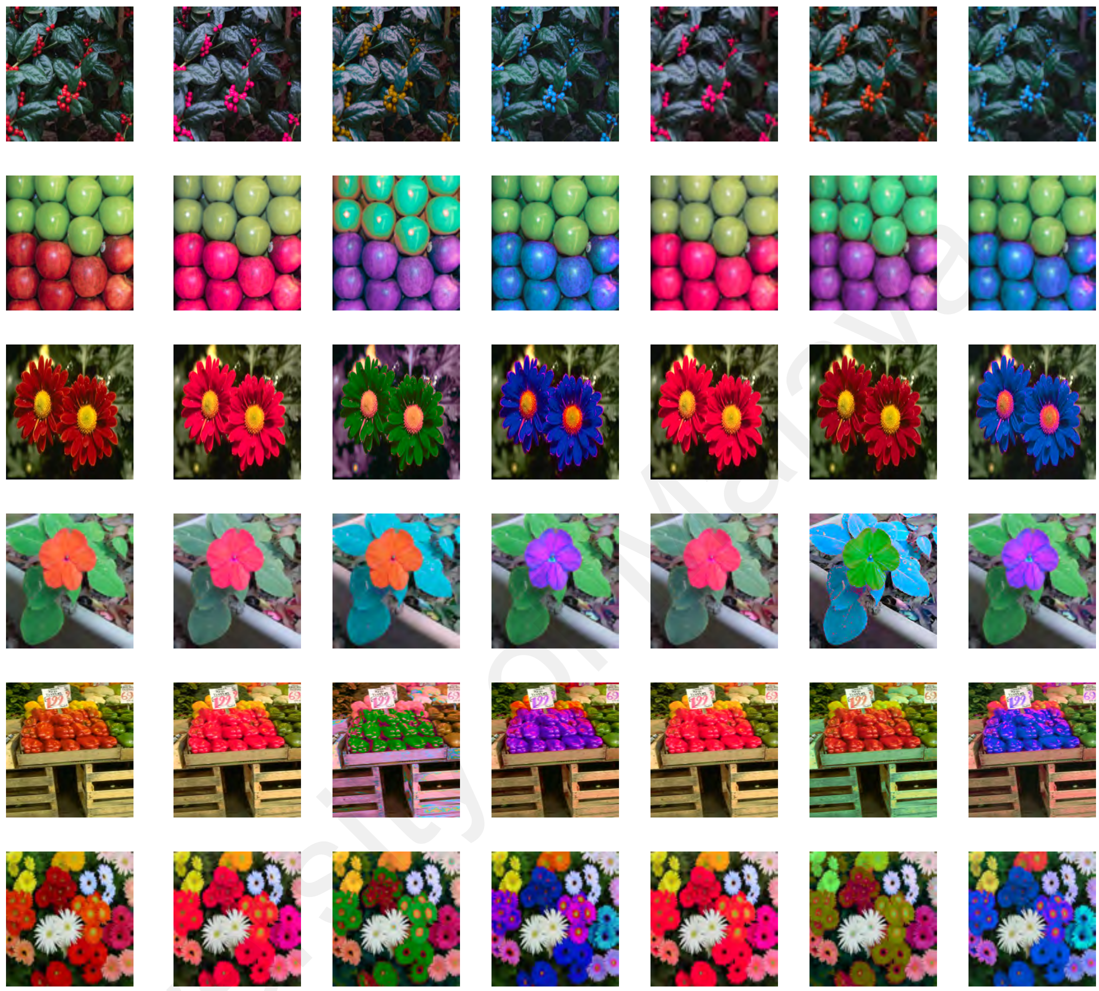

were displayed on a DELL S2440L LCD display at approximately 60 cm from the subject.

The trichromat subjects consisted of 15 volunteers between the ages of 20 and 34 years with a mean age of 26.33. Meanwhile, for red-green deficients, the subjects consisted of 11 male volunteers who declared themselves as color vision deficient. Their age ranged between 11 and 37 years with a mean age of 27.64. The color vision deficient volunteers were subjected to the Ishihara test (S. Ishihara, 1979) to confirm their color vision deficiency. Based on the outcome of the Ishihara test, the 11 male volunteers were classified as deuteranopes. It should be noted here that the Ishihara test cannot achieve a precise diagnosis of protanopia and deuteranopia. In order to obtain precise results, they would have been required to submit to an anomaloscope test.

The subjects were then grouped into two groups; trichromats and deuteranopes. Each subject is the trichromats group underwent two paired comparison tests. The first paired comparison test was to evaluate the protanopia recolored images and the second one was to evaluate the deuteranopia recolored images. Each subject in the deuteranopes group underwent the paired comparison test for deuteranopia recolored images. During the paired comparison test, each subject was asked to indicate their binary preference in terms of the naturalness and their overall preference for the images.

The results obtained for the paired comparison tests were analyzed using Thurstone's Law of Comparative Judgment (Thurstone, 1927). Case V Law of Comparative Judgment is a classical tool that ranks items based on subjective choices, which allows one to measure individuals' preference orderings for some stimuli from a set of discrete binary choices (Kuhn et al., 2008). Moreover, we used the maximum a posteriori estimation method in our analysis. The maximum a posteriori estimation method was chosen because it is an optimal approach to estimation and can be solved efficiently as a convex optimization problem (Tsukida & Gupta, 2011). We also computed the corresponding 95% confidence intervals using the formulation in Montag (2006). The 95% confidence intervals are shown as vertical bars in Figures 4.7 to 4.9.

The preference scores of protanopia paired comparison test by trichromats are shown in Figure 4.7(a) for naturalness and Figure 4.7(b) for overall preference. Since the original images are recolored to match the reduced color gamut of protanopia, it can be observed that trichromats preferred the original images more than the recolored images in terms of naturalness and overall preference. However, between the recolored images, the results show that trichromats preferred images recolored using the proposed method.

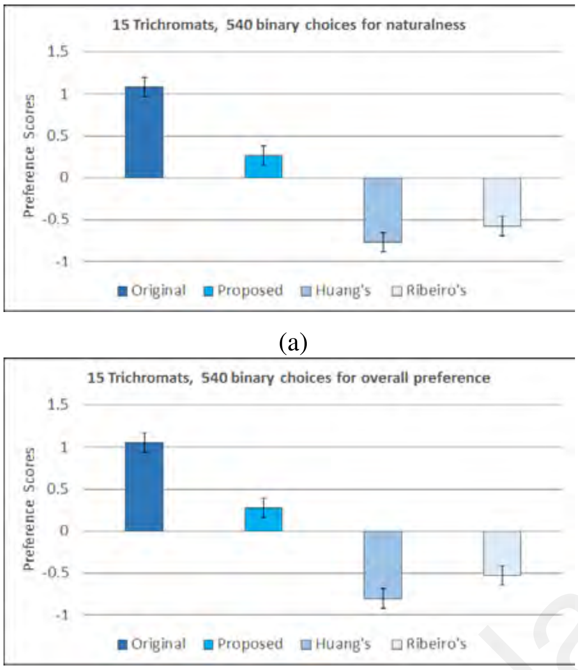

(a)

(b)

Figure 4.7: Preference scores of protanopia paired comparison test by trichromats, (a) Naturalness, (b) Overall preference

The same thing was observed from the results of the deuteranopia paired comparison test by trichromats. They preferred the original images more than the recolored images in terms of naturalness and overall preference. Images recolored using the proposed method achieved slightly higher preference scores than images recolored using Huang's method and significantly higher preference scores than images recolored using Ribeiro's method. Figure 4.8(a) shows preference for naturalness and Figure 4.8(b) for overall preference. Thus, these results show that the proposed method maintained the naturalness of the original images, and enhanced the visual details better than the two other recoloring methods for both protanopia and deuteranopia recolored images.

The preference scores for the deuteranopia paired comparison test by deuteranopes are shown in Figure 4.9(a) for naturalness and Figure 4.9(b) for overall preference. It can be deduced that most of the deuteranopes preferred the original images in terms of naturalness and overall preference. This is because they are used to their color perception when looking at natural images such as flowers and fruits (Oliveira, 2013). Moreover, deuteranopes

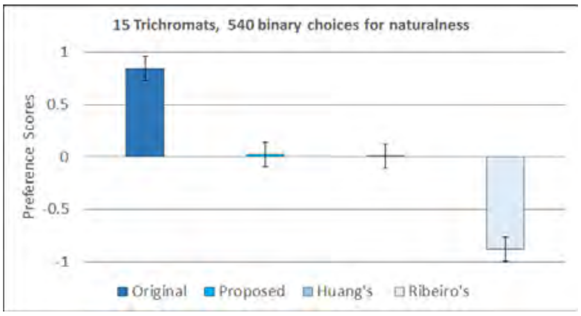

(a)

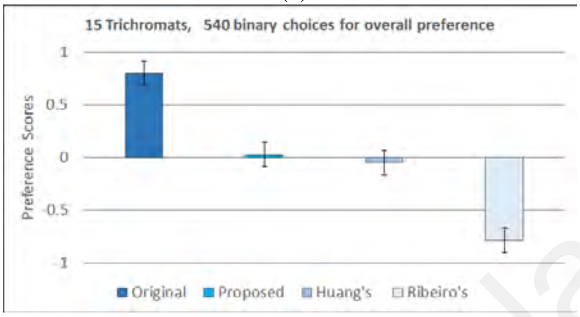

(b)

Figure 4.8: Preference scores of deuteranopia paired comparison test by trichromats, (a) Naturalness, (b) Overall preference

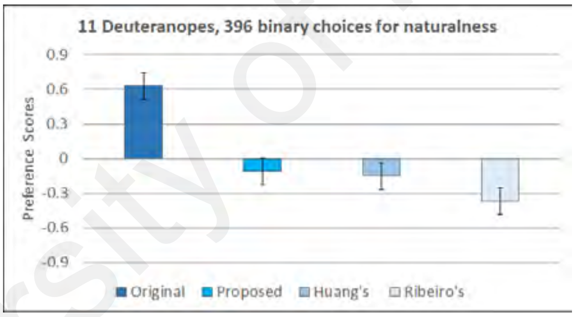

(a)

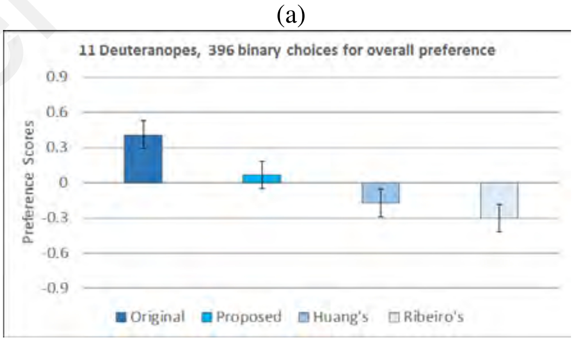

(b)

Figure 4.9: Preference scores of deuteranopia paired comparison test by deuteranopes, (a) Naturalness, (b) Overall preference

prefer saturated yellow compared to other colors (Alvaro et al., 2015). As such, most of the recolored images used in this test did not look natural to them. However, among the three recoloring methods, in terms of naturalness and overall preference, deuteranopes preferred the recolored images from the proposed method more than the other two recoloring methods. Hence, these results show that the proposed method produced images that look natural to deuteranopes and also enhanced their visual details better than Huang's and Ribeiro's methods.

In addition, a second paired comparison test was conducted to evaluate the proposed method with the recoloring method that recolored the images perceived by the red-green deficients instead of the original images. Applying the same setup as the previous paired comparison test, we compared the effectiveness of the proposed method with Kuhn's method (Kuhn et al., 2008) in terms of the naturalness preservation of the recolored images and the overall preference. Since in Kuhn's method the recolored images remained in the reduced color space of red-green deficients, the second paired comparison test was only conducted to the deuteranopes.

Here, the same set of the original and recolored images from the proposed method used in the previous deuteranopia paired comparison test and the recolored images from Kuhn et al. (2008) as shown in Figure 4.10 were utilized. Hence, there were a total of 18 pairs of test images for the second deuteranopia paired comparison test and these images were arranged side-by-side; *(Or, P), (Or, K),* and *(P, K)* where *Or, P,* and *K* stand for original image, image recolored by the proposed method and Kuhn's method respectively.

Applying Thurstone's Law of Comparative Judgment (Thurstone, 1927) with the maximum a posteriori estimation method and the corresponding 95% confidence intervals (Montag, 2006), the preference scores for naturalness and overall preference are shown in Figure 4.11. The 95% confidence intervals are shown as vertical bars.

Similar to the previous deuteranopia paired comparison test, most of the deuteranopes preferred the original images more than the recolored images from both methods due to their previous color experiences. However, the proposed method has slightly higher

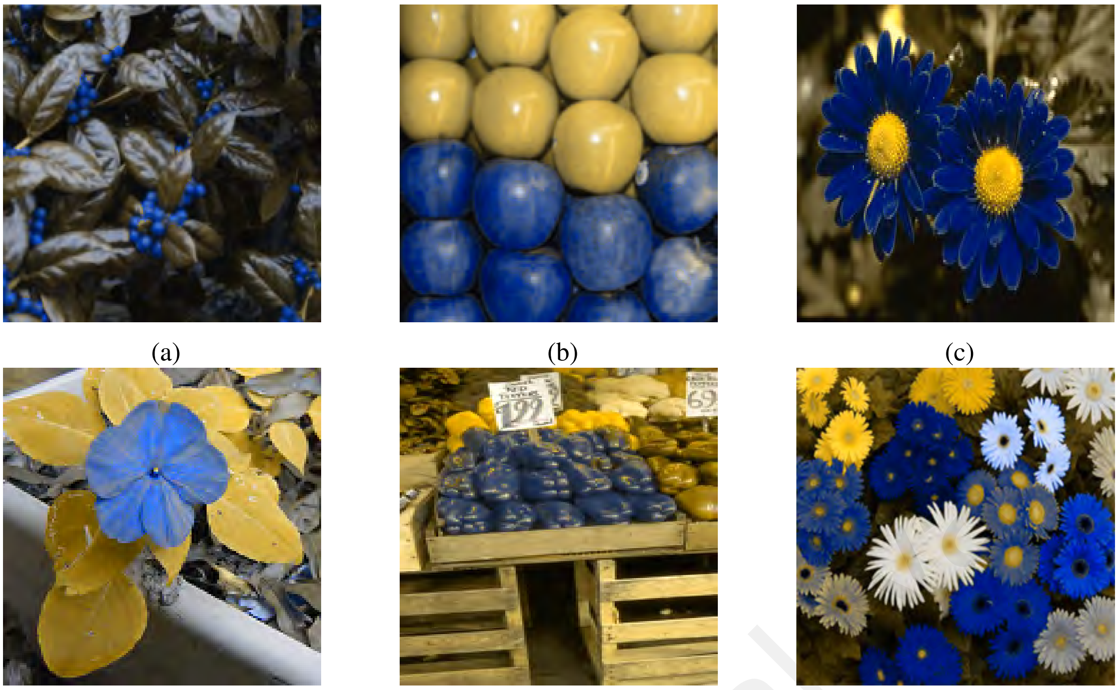

(a) (b) (c)

(d) (e) (f)

Figure 4.10: Images recolored using Kuhn's method

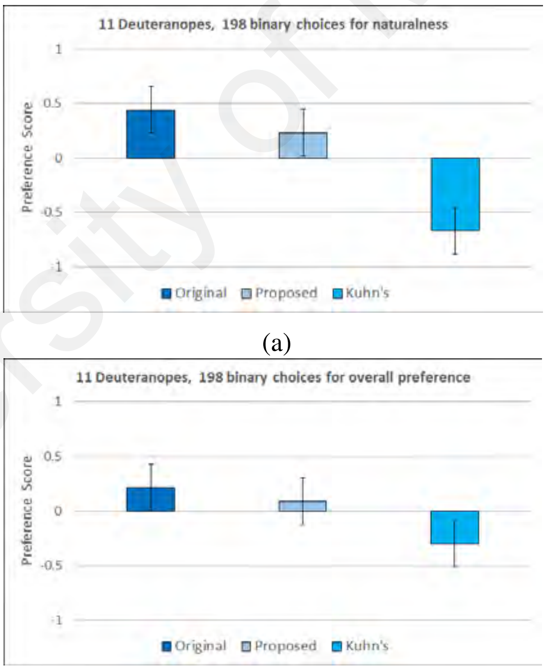

(a)

(b)

Figure 4.11: Preference scores of the second deuteranopia paired comparison test by deuteranopes, (a) Naturalness, (b) Overall preference

preference scores than Kuhn's method for both naturalness and overall preference.

4.5 Summary

Color images in public places such as in airports, shopping malls, and train stations are observed by everyone. However, loss of information may occur when the images are viewed by red-green deficients. Various recoloring methods have been proposed to overcome this problem. However, the recolored images may look non-pleasing to trichromats. Moreover, the recoloring methods may change all the colors of the images, and as a result, the recolored images may look unnatural to the red-green deficients as well. Therefore, it is essential that recoloring methods take into consideration the needs of both trichromats and red-green deficients.

Thus, in this chapter, a simple and efficient recoloring method that considers the needs of both trichromats and red-green deficients is proposed. The proposed method improves visual details and enhances the color perception of the red-green deficients while preserving the naturalness of the recolored images for both trichomats and red-green deficients. The main advantage of the proposed method is that it recolors the colors confused by the red-green deficients with the colors that have the same hue as the original ones. Moreover, the recolored images have the same luminance as the original images.

Results obtained from the experimental studies show that the proposed method performed better than three other existing methods. The proposed method not only improves visual details and enhances the color perception of the red–green deficients, but it also preserves the naturalness of the recolored images for both trichromats and red–green deficients.

CHAPTER 5: CONCLUSIONS

Color vision deficiency is the inability to discriminate certain shades of colors. This inability arises from the differences in the pigmentation of the cones in the human eye. Color vision deficiency can be categorized as acquired or inherited color vision deficiencies. In acquired color vision deficiency, elderly people suffer from certain degrees of color perception loss while some people with inherited color vision deficiency have difficulty in distinguishing between red and green colors. Thus, people with color vision deficiency may experience some difficulty in performing their daily activities. In order to improve their quality of life and ease their physical limitations, this thesis describes research on human color perception that has been conducted. The main objectives of this thesis are to propose a mathematical formulation of the uniform yellowing pigmentation to model the color perception of the elderly, and to introduce an image recoloring method for red-green deficients that enhances the visual details and preserves the naturalness of the original image.

Previous studies in color perception of the elderly utilized the non-uniform yellowing pigmentation model. However, recent clinical studies indicate that uniform yellowing pigmentation occurs on the human lens as human age increases. Therefore, to understand the effect of the uniform yellowing pigmentation on the color perception of the elderly, a mathematical formulation of the uniform yellowing pigmentation is proposed in Chapter 3. It uses three effective tristimulus ratios to form the uniform yellowing pigmentation. Experimental studies verified that the uniform yellowing pigmentation is in agreement with the results from clinical studies. In the experiments, the color perception of the elderly is simulated using the uniform yellowing pigmentation. The artificial SPP3 color perception test was conducted to compare the proposed method with the non-uniform yellowing pigmentation method and the clinical data. Results from the artificial SPP3 color perception test show that the proposed method performed better than the non-uniform yellowing pigmentation method. In addition, the results from the proposed method are closer to the clinical data.

In Chapter 4, a naturalness preserving recoloring method for the red-green deficients is proposed. The proposed method considers the needs of both trichromats and red-green deficients. The main advantages of the proposed method are that it recolors the confused colors with the colors that have the same hue as the original ones, and the recolored images have the same luminance as the original ones. Therefore, the proposed method improves the visual details of the recolored image and also preserves the naturalness from both trichromats' and red-green deficients' points of view. In objective evaluations, recolored images from the proposed method obtained better scores in term of naturalness preservation and chrominance similarity index than the other two recoloring methods that implemented similar recoloring framework. Moreover, in the paired comparison tests, the proposed method achieved higher preference scores than three other recoloring methods.

5.1 Future Research Directions

There are still many possibilities for extensions of the proposed methods and improvement for the applications discussed in this thesis. In the study of the color perception of the elderly, one possible future research direction is to formulate an image enhancement method to mitigate the effect of the uniform yellowing pigmentation on color perception of the elderly. Moreover, non-natural color images such as scientific visualization (SciVis) and information visualization (InfoVis) require contrast enhancement for the red-green deficients. In future research, the proposed naturalness preservation recoloring method can be extended to cater to this requirement of color contrast enhancement. In addition, both of the methods proposed in this thesis can also be extended to video recoloring.

REFERENCES

Alio, J. L., Schimchak, P., Negri, H. P., & Montes-Mico, R. (2005). Crystalline lens optical dysfunction through aging. *Ophthalmology*, *112*(11), 2022 - 2029.

Alpern, M., Kitahara, K., & Krantz, D. H. (1983). Perception of colour in unilateral tritanopia. *The Journal of Physiology*, *335*(1), 683 - 697.

Alvaro, L., Linhares, J., Moreira, H., Lillo, J., & Nascimento, S. (2017). Robust colour constancy in red-green dichromats. *PLos ONE*, *12*(6).

Alvaro, L., Moreira, H., Lillo, J., & Franklin, A. (2015). Color preference in red-green dichromats. *Proceedings of the National Academy of Sciences*, 9316 - 9321.

Anagnostopoulos, C. N., Tsekouras, G., Anagnostopoulos, I., & Kalloniatis, C. (2007). Intelligent modification for the daltonization process of digitized paintings. *International Conference on Computer Vision Systems*.

Applegate, R. A., Donnelly, W. J., Marsack, J. D., & Koenig, D. E. (2007). Three-dimensional relationship between high-order root-mean-square wavefront error, pupil diameter, and aging. *Journal of the Optical Society of America*, *24*(3), 578 - 587.

Artigas, J. M., Felipe, A., Navea, A., Fandino, A., & Artigas, C. (2012). Spectral transmission of the human crystalline lens in adult and elderly persons: color and total transmission of visible light. *Investigative Ophthalmology & Visual Science*, *53*(7), 4076 - 4084.

Ball, L. J., & Pollack, R. H. (1989). The effects of color and preretinal aging on embedded figures test performance: a failure to replicate. *Experimental Aging Research*, *15*(4), 177 - 180.

Birch, J. (1972). Dichromatic convergence points obtained by subtractive colour matching. *Vision Research*, *13*, 1755 - 1765.

Birren, J. E., Casperson, R. C., & Botwinick, J. (1950). Age changes in pupil size. *Journal of Gerontology*, *5*(3), 216 - 221.

Bitsios, P., Prettyman, R., & Szabadi, E. (1996). Changes in autonomics function with age: a study of pupipupil kinetics in healthy young and old people. *Age and Ageing*, *25*, 432 - 438.

Boettner, E. A., & Wolter, J. (1962). Transmission of the ocular media. *Investigative Ophthalmology & Visual Science*, *1*(6), 776 - 783.

Brettel, H., Vienot, F., & Mollon, J. D. (1997). Computerized simulation of color appearance for dichromats. *Journal of the Optical Society of America*, *14*(10), 2647 - 2655.

Bright, K., & Egger, V. (2008). Using visual contrast for effective, inclusive environments. *Information Design Journal*, *16*(3), 178 - 189.

Broadbent, A. D. (2017). Colorimetry, methods. *Encyclopedia of Spectroscopy and Spectrometry (Third Edition)*, 321 - 327.

Capilla, P., Diez-Ajenjo, M. A., Luque, M. J., & Malo, J. (2004). Corresponding-pair procedure: a new approach to simulation of dichromatic color perception. *Journal of the Optical Society of America A*, *21*(2), 176 - 186.

Capilla, P., Luque, M. J., & Diez-Ajenjo, M. A. (2004). Looking for the dichromatic version of a colour vision model. *Journal of Optics A Pure and Applied Optics*, *6*, 906 - 919.

Ching, S. L., & Sabudin, M. (2010). A study of color transformation on website images for the color blind. *World of Academy of Science, Engineering and Technology*, *4*(2), 684 - 687.

Chua, J.-L., Chang, Y. C., & Lim, W. K. (2015). A simple vision-based fall detection technique for indoor video surveillance. *Signal, Image and Video Processing*, *9*(3), 623 - 633.

Colantoni, P. (2004). *Color space transformations.* Retrieved from `http://faculty.kfupm.edu.sa/ics/lahouari/Teaching/colorspacetransform-1.0.pdf`

Cole, B. L. (2007). Assessment of inherited colour vision defects in clinical practice. *Clinical and Experimental Optometry*, *90*(3), 157 - 175.

Daniel. (2010). *There is not one color blindness.* Retrieved from http://www.daltonize.org/2010/05/there-is-not-just-one-color-blindness.html

DesMarais, C. (2013). *Facebook's instagram says it has 90 million monthly active users.* Retrieved from https://www.pcworld.com/article/2025801/facebooks-instagram-says-it-has90-million-monthly-active-users.html

Doliotis, P., Tsekouras, G., Anagnostopoulos, C. N., & Athitsos, V. (2009). Intelligent modification of color in digitized paintings for enhancing the visual perception of color-blind viewers. *Artificial Intelligence Applications and Innovations III*, *296*, 292 - 301.

Fairchild, M. D. (2005). *Color appearance models*. John Wiley & Sons, Ltd.

Fiorentini, A., Porciatti, V., Morrone, M. C., & Burr, D. C. (1996). Visual ageing: unspecific decline of the responses to luminance and colour. *Vision Research*, *36*(21), 3557 - 3566.

Gibson, J. E., & Fairchild, M. D. (2000). Colorimetric characterization of three computer displays (lcd and crt). *Munsell Color Science Laboratory Technical Report*.

Guild, J. (1932). The colorimetric properties of the spectrum. *Philosophical Transactions of the Royal Society of London. Series A, Containing Papers of a Mathematical or Physical Character*, *230*, 149 - 187.

Haskett, M. K., & Hovis, J. K. (1987). Comparison of the standard pseudoisochromatic plates to the ishihara color vision test. *American Journal of Optometry and Physiological Optics*, *46*(3), 211 - 216.

Hassan, M. F., Kugimiya, T., Tanaka, Y., Tanaka, K., & Paramesran, R. (2015). Comparative analysis of the color perception loss for elderly people. *Asia-Pacific Signal and Information Processing Association (APSIPA) Annual Summit and Conference*, 1176 - 1181.

Hassan, M. F., & Paramesran, R. (2017). Naturalness preserving image recoloring method for people with red-green deficiency. *Signal Processing: Image Communication*, *57*, 126 - 133.

Hassan, M. F., Paramesran, R., Tanaka, Y., & Tanaka, K. (2018). A method using uniform yellowing pigmentation to model the color perception of the elderly people. *Signal, Image and Video Processing*, *12(6)*, 1019 - 1026.

Hegde, A. L., & Bishop, N. (2018). Saturation based color appearance of objects: a comparison between healthy elderly, young adults, and young adults wearing goggles simulating cataract. *Building and Environment*, *127*, 148 - 156.

Huang, J. B., Chen, C. S., Jen, T. C., & Wang, S. J. (2009). Image recolorization for the colorblind. *IEEE International Conference on Acoustics, Speech and Signal Processing*, 1161 - 1164.

Huang, J. B., Tseng, Y. C., Wu, S. I., & Wang, S. J. (2007). Information preserving color transformation for protanopia and deuteranopia. *IEEE Signal Processing Letters*, *14*(10), 711 - 714.

Hunt, R. W. G. (2004). *The reproduction of colour*. John Wiley & Sons.

Ichikawa, M., Tanaka, K., Kondo, S., Hiroshima, K., Ichikawa, K., Tanabe, S., & Fukami, K. (2003). Web-page color modification for barrier-free color vision with genetic algorithm. *Genetic and Evolutionary Computation - GECCO*, *2724*, 2134 - 2146.

Ishihara, K., Ishihara, S., Nagamachi, M., Hiramatsu, S., & Osaki, H. (2001). Age-related decline in color perception and difficulties with daily activities-measurement, questionnaire, optical and computer-graphics simulation studies. *International Journal of Industrial Ergonomics*, *28*, 153 - 163.

Ishihara, K., Ishihara, S., Nagamachi, M., & Osaki, H. (1997). Difficulties for elderly people caused by age-related yellowing vision. *Proceedings of Trienniel Congress of the International Ergonomics Association*, *5*, 579 - 581.

Ishihara, S. (1979). *Tests for colour-blindness*. Tokio: Kanehara Shuppan Co. Ltd.

Jefferson, L., & Harvey, R. (2006). Accomodating color blind computer users. *Proceedings of the 8th international ACM SIGACCESS Conference on Computers and Accessibility*, 40 - 47.

Jeong, J. Y., Kim, H. J., Wang, T. S., & Yoon, Y. J. (2011). An efficient re-coloring method with information preserving for the color-blind. *IEEE Transactions on Consumer Electronics*, *57*(4), 1953 - 1960.

Judd, D. B. (1949). The color perceptions of deuteranopic and protanopic observers. *Journal of the Optical Society of America*, *39*(3), 252 - 256.

Kadlecova, V., Peleska, M., & Vasko, A. (1958). Dependance on age of the diameter of the pupil in the dark. *Nature*, *182*, 1520 - 1521.

Kuhn, G. R., Oliviera, M. M., & Fernandes, L. A. F. (2008). An efficient naturalness-preserving image-recoloring method for dichromats. *IEEE Transactions on Visualization and Computer Graphics*, *14*(6), 1747 - 1754.

Lee, J., & dos Santos, W. P. (2011). An adaptive fuzzy-based system to simulate, quantify and compensate color blindness. *Integrated Computer-Aided Engineering*, *18*, 29 - 40.

Lerman, S. (1983). An experimental and clinical evaluation of lens transparency and aging. *Journal of Gerontology*, *38*(3), 293 - 301.

Ma, Y., Gu, X. D., & Wang, Y. Y. (2006). A new color blindness cure model based on bp neural network. *Advances in Neural Networks - ISNN 2006*, *3973*, 740 - 745.

Machado, G. M., & Oliveira, M. M. (2010). Real-time temporal-coherent color constrast enhancement for dichromats. *Proceedings of the 12th Eurographics / IEEE - VGTC conference on Visualization*, 933 - 942.

Machado, G. M., Oliveira, M. M., & Fernandes, L. A. F. (2009). A physiologically-based model for simulation of color vision deficiency. *IEEE Transactions on Visualization and Computer Graphics*, *15*(6), 1291 - 1298.

Malacara, D. (2011). *Color vision and colorimetry: Theory and applications*. SPIE Press.

Martin, D., Fowlkes, C., Tal, D., & Malik, J. (2001). A database of human segmented natural images and its application to evaluating segmentation algorithms and measuring ecological statistics. *IEEE International Conference on Computer Vision*, *2*, 416 - 423.

Meyer, G. W., & Greenberg, D. P. (1988). Color-defective vision and computer graphics displays. *IEEE Computer Graphics and Applications*, *8*(5), 28 - 40.

Montag, E. D. (2006). Empirical formula for creating error bars for the method of paired comparison. *Journal of Electronic Imaging*, *15*(1).

Moreira, H., Alvaro, L., Melnikova, A., & Lillo, J. (2018). Colorimetry and dichromatic vision, colorimetry and image processing carlos travieso-gonzalez. In (p. 1 - 21). IntechOpen.

Neitz, J., & Neitz, M. (2011). The genetics of normal and defective color vision. *Vision Research*, *51*, 633 - 651.

Nguyen, D. T., Overbury, O., & Faubert, J. (2003). The role of lenticular senescence in age-related color vision changes. *Investigative Ophthalmology and Visual Science*, *44*(8), 3698 - 3704.

Norren, D. V., & Vos, J. J. (1974). Spectral transmission of the human ocular media. *Vision Research*, *14*, 1237 - 1244.

Okajima, K., & Takase, M. (2001). Computerized simulation and chromatic adaptation experiments based on a model of aged human lens. *Optical Review*, *8*(1), 64 - 70.

Oliveira, M. M. (2013). Towards more accessible visualizations for color-vision-deficient individuals. *Computing in Science and Engineering*, *15*(5), 80 - 87.

Ortiz, E., Bowyer, K. W., & Flynn, P. J. (2013). A linear regression analysis of the effects of age related pupil dilation change in iris biometrics. *IEEE International Conference on Biometrics: Theory, Applications and Systems (BTAS)*, 1 - 6.

Pascale, D. (2003). *A review of rgb color spaces ... from xyy to r'g'b'.* The BabelColor Company.

Pokorny, J., Smith, V. C., & Lutze, M. (1986). Aging of the human lens. *Applied Optics*, *26*(8), 1437 - 1440.

Poynton, C. A. (1995). A guided tour of colour space. *New Foundation for Video Technology: The SMPTE Advanced Television and Electronic Imaging Conference*.

Rasche, K., Geist, R., & Westall, J. (2005a). Detail preserving reproduction of color images for monochromats and dichromats. *IEEE Computer Graphics and Applications*, *25*(3), 22 - 30.

Rasche, K., Geist, R., & Westall, J. (2005b). Re-coloring images for gamuts of lower dimension. *Computer Graphics Forum*, *24*(3), 423 - 432.

Ribeiro, M. G., & Gomes, A. J. P. (2013). A skillet-based recoloring algorithm for dichromats. *International Conference on e-Health Networking, Applications and Services*, 702 - 706.

Rigden, C. (1999). The eye of the beholder - designing for colour-blind users. *British Telecommunications Engineering*, *17*, 2 - 6.

Rodriquez-Pardo, C. E., & Sharma, G. (2011). Dichromatic color perception in a two stage model: testing for cone replacement and cone loss models. *IEEE IVMSP Workshop*, 12 - 17.

Romano, G., Mercatelli, L., Fusi, F., Guasti, A., Favuzza, E., Monici, M., & Mencucci, R. (2011). Colorimetric comparison of light-filtering intraocular lelens and human crystalline lenses at various ages. *Journal of Cataract and Refractive Surgery*, *37*(4), 758 - 762.

Roy, M. S., Podgor, M. J., Collier, B., & Gunkel, R. D. (1991). Color vision and age in a normal north american population. *Graefe's Archive for Clinical and Experimental Ophthalmology*, *229*, 139 - 144.

Ruddock, K. H. (1965a). The effect of age upon colour vision - ii. changes with age in light transmission of the ocular media. *Vision Research*, *5*, 47 - 58.

Ruddock, K. H. (1965b). The effect of age upon colour vision - i. response in the receptoral system of the human eye. *Vision Research*, *5*, 37 - 45.

Said, F. S., & Sawires, W. S. (1972). Age dependance of changes in pupil diameter in the dark. *Optica Acta*, *19*(5), 359 - 361.

Said, F. S., & Weale, R. A. (1959). The variation with age of the spectral transmissivity of the living human crystalline lens. *Gerontologia*, *3*(37), 213 - 231.

Salvi, S. M., Akhtar, S., & Currie, Z. (2006). Ageing changes in the eye. *Postgraduate*

Medical Journal, *82*(971), 581 - 587.

Savage, G. L., Haegerstrom-Portnoy, G., Adams, A. J., & Hewlett, S. E. (1993). Age changes in the optical density of human ocular media. *Clinical Vision Science*, *8*, 97 - 108.

Schneck, M. E., Adams, A. J., Huie, K., & Lee, E. (1993). A filter for simulating color and spatial vision of the elderly. *Colour Vision Deficiencies XI*, 357 - 364.

Schubert, E. F. (1996). *Light-emitting diodes*. Cambridge University Press.

Semary, N. A., & Marey, H. M. (2014). An evaluation of computer based color vision deficiency test: Egypt as a study case. *International Conference on Engineering and Technology (ICET)*, 1 - 7.

Sharma, G., Wu, W., & Dalal, E. N. (2005). The ciede2000 color-difference formula: Implementation notes, supplementary test data and mathematical observations. *COLOR Research and Application*, *30*(1), 21 - 30.

Sharpe, L. T., Stockman, A., Jagle, H., & Nathans, J. (1999). *Color vision: From genes to perception*. Cambrigde University Press.

Sheikh, H. R., Sabir, M. F., & Bovik, A. C. (2006). A statistical evaluation of recent full reference quality assessment algorithms. *IEEE Transactions on Image Processing*, *15*(11), 3440 - 3451.

Shinomori, K. (2005). Ageing effects on colour vision changed and unchanged perception . *Congress of the International Colour Association*, 7 - 12.

Simon-Liedtke, J. T., & Farup, I. (2016). Evaluating color vision deficiency daltonization method using a behavorial visual-search method. *Journal of Visual Communication and Image Representation*, *35*, 236 - 247.

Simunovic, M. P. (2016). Acquired color vision deficiency. *Survey of Ophthalmology*, *61*, 132 - 155.

Sloan, L. L. (1939). Instruments and techniques for the clinical testing of light sense. *Archives of Ophthalmology*, 258 - 270.

Smith, V., & Pokorny, J. (1995). Spectral sensitivity of the foveal cone photopigments between 400 and 500 nm. *Vision Research*, *15*, 161 - 171.

Soundararajan, R., & Bovik, A. C. (2013). Survey of information theory in visual quality assessment. *Signal, Image and Video Processing*, *7*(3), 391 - 401.

Stiles, W. S., & Burch, J. M. (1955a). Interium report to the cie, zurich, 1955, on the national physical laboratory's investigation of colour-matching. *Optica Acta*, *2*, 168 - 181.

Stiles, W. S., & Burch, J. M. (1955b). Interium report to the cie, zurich, 1955, on the national physical laboratory's investigation of colour-matching. *Optica Acta*, *2*, 168 - 181.

Stiles, W. S., & Burch, J. M. (1959). N.p.l. colour-matching investigation: final report (1958). *Optica Acta*, *6*(1).

Suetake, N., Tanaka, G., Hashii, H., & Uchino, E. (2012). Simple lightness modification for color vision impaired based on craik-o'brien effect. *Journal of Franklin Institute*, *349*, 2093 - 2107.

Suzuki, R., Tanaka, Y., Aguirre, H., Tanaka, K., Yokoyama, S., Nakamura, H., . . . Tanabe, S. (2012). Color compensation method to display images looking similar to their original ones for elderly people. *Proceedings of the IIEEJ Image Electronics and Visual Computing Workshop*.

Suzuki, T., Okajima, K., & Funai, T. (2012). Optical simulation of reduced retinal illuminance caused by senile miosis. *Optical Review*, *19*(3), 174 - 181.

Suzuki, T., Qiang, Y., Sakuragawa, S., Tamura, H., & Okajima, K. (2006). Age-related changes of reaction time and p300 for low-contrast color stimuli: effects of yellowing of the aging human lens. *Journal of Physiological Anthropology*, *25*(2), 179 - 187.

Suzuki, T., Yi, Q., Sakuragawa, S., Tamura, H., & Okajima, K. (2005). Comparing the visibility of low-contrast color landolt-cs: Effect of aging human lens. *Color Research and Application*, *30*, 5 - 12.

Tagarelli, A., Piro, A., Tagarelli, G., Lantieri, P. B., Risso, D., & Olivieri, R. L. (2004). Colour blindness in everyday life and car driving. *Acta Ophthalmologica Scandinavica*, *82*(4), 436 - 442.

Tanaka, Y., Tanaka, K., Yokoyama, S., Nakamura, H., Ichikawa, K., & Tanabe, S. (2011). An improved simulation method of color perception by elderly people based on measured luminescence spectrum and color constancy relaxation. *Journal of the Institute of Image Electronics Engineers of Japan*, *40*(1), 86 - 95.

Thomas, O. (2012). *Facebook: Users upload 300 million images a day (so please let us buy instagram).* Retrieved from `http://www.businessinsider.com/facebook-images-a-day-instagram-acquisition-2012-7/?IR=T`

Thurstone, L. L. (1927). A law of comparative judgment. *Psychological Review*, *34*(4), 273 - 286.

Travis, D. (1991). *Effective color display, theory and practice*. Academic Press.

Tsukida, K., & Gupta, M. R. (2011). How to analyze paired comparison data. *UWEE Technical Report*.

Ueda, C., Azetsu, T., Suetake, N., & Uchino, E. (2015a). Gamma correction-based image enhancement for elderly vision. *International Symposium on Communications and Information Technologies*, 141 - 144.

Ueda, C., Azetsu, T., Suetake, N., & Uchino, E. (2015b). Light transform method considering visual feature of elderly vision. *International Symposium on Intelligent Signal Processing and Communication Systems*, 62 - 65.

Ueda, C., Azetsu, T., Suetake, N., & Uchino, E. (2016). Improvement in appearance of colors for elderly persons using lightness transform. *The Optical Society of Japan*, *23*, 917 - 925.

Verriest, G. (1963). Further studies on acquired deficiency of color discrimination. *Journal of the Optical Society of America*, *53*(1), 185 - 195.

Vienot, F., Brettel, H., & Mollon, J. D. (1999). Digital video colourmaps for checking the legibility of displays by dichromats. *COLOR Research and Application*, *24*(4), 243 - 252.

Vienot, F., Brettel, H., Ott, L., M'Brek, A. B., & Mollon, J. D. (1995). What do colour-blind people see? *Nature*, *376*, 127 - 128.

Wachtler, T., Dohrmann, U., & Hertel, R. (2004). Modeling color percepts of dichromats. *Vision Research*, *44*, 2843 - 2855.

Wakita, K., & Shimamura, K. (2005). Smartcolor: disambiguation framework for the colorblind. *Proceedings of the 7th International ACM SIGACCESS Conference on Computers and Accessibility*, 158 - 165.

Wandell, B. A. (1995). *Foundations of vision*. Sinauer Associates.

Weale, R. A. (1961a). Notes on the photometric significance of the human crystalline lens. *Vision Research*, *1*, 183 - 191.

Weale, R. A. (1961b). Retinal illumination and age. *Lighting Research and Technology*, *26*(2), 95 - 100.

Weale, R. A. (1988). Age and the transmittance of the human crystalline lens. *Journal of Physiology*, *395*, 577 - 587.

Werner, J. S., Peterzell, D. H., & Scheetz, A. J. (1990). Light, vision, and aging. *Optometry and Vision Science*, *67*(3), 214 - 229.

Werner, J. S., & Steele, V. G. (1988). Sensitivity of the human foveal color mechanisms throughout the life span. *Journal of the Optical Society of America*, *5*, 2122 - 2130.

Winn, B., Whitaker, D., Elliott, D. B., & Phillips, N. J. (1994). Factors affecting light-adapted pupil size in normal human subjects. *Investigative Ophthalmology & Visual Science*, *35*(3), 1132 - 1137.

Wright, W. D. (1928). A re-determination of the trichromatic coefficients of the spectral colours. *Transactions of the Optical Society*, *30*(4), 141 - 161.

Xu, J., Pokorny, J., & Smith, V. C. (1997). Optical density of the human lens. *Journal of the Optical Society of America*, *14*(5), 953 - 960.

Yamazaki, A. K., & Eto, K. (2015). A preliminary experiment to investigate the effects of blue backgrounds on a tablet screen for elderly people. *International Conference in Knowledge Based and Intelligent Information and Engineering Systems*, *60*, 1490 - 1496.

Yang, S., & Ro, Y. M. (2003). Visual contents adaptation for color vision deficiency. *International Conference on Image Processing*, *1*, 453 - 456.

Yoshida, C. A., & Sakuraba, S. (1996). The use of films to simulate age-related decline in yellow vision. *Journal of Occupational Rehabilitation*, *6*(2), 119 - 134.

Zhang, L., Zhang, L., Mou, X., & Zhang, D. (2011). Fsim: a feature similarity index for image quality assessment. *IEEE Transactions in Image Processing*, *20*(8), 2378 - 2386.

LIST OF PUBLICATIONS AND PAPERS PRESENTED

Hassan, M. F., Kugimiya, T., Tanaka, Y., Tanaka, K., & Paramesran, R. (2015). Comparative analysis of the color perception loss for elderly people. *Asia-Pacific Signal and Information Processing Association (APSIPA) Annual Summit and Conference*, 1176 - 1181.

Hassan, M. F., & Paramesran, R. (2017). Naturalness preserving image recoloring method for people with red-green deficiency. *Signal Processing: Image Communication*, *57*, 126 - 133.

Hassan, M. F., Paramesran, R., Tanaka, Y., & Tanaka, K. (2018). A method using uniform yellowing pigmentation to model the color perception of the elderly people. *Signal, Image and Video Processing*, *12(6)*, 1019 - 1026.

APPENDIX A: TRANSMITTANCE FUNCTIONS OF THE LCD

Table A.1: Transmittance Functions of the LCD

Wavelength, λ (nm)	Red filter, f_r ($\times 10^{-4}$)	Green filter, f_g ($\times 10^{-4}$)	Blue filter, f_b ($\times 10^{-4}$)
400	0.103	0.085	0.184
410	0.295	0.285	0.514
420	0.423	0.405	2.050
430	0.519	0.530	9.470
440	0.744	0.750	18.400
450	0.818	0.871	22.000
460	0.730	0.774	16.900
470	0.638	0.782	9.800
480	0.639	1.970	4.700
490	0.654	3.240	2.590
500	0.914	8.160	3.120
510	1.910	26.400	4.740
520	2.050	29.800	2.510
530	1.520	19.200	1.230
540	1.070	10.800	0.841
550	0.875	6.390	0.717
560	0.662	2.380	0.601
570	0.581	1.350	0.552
580	1.270	6.150	0.616
590	1.210	1.720	0.467
600	2.650	2.310	0.500
610	24.300	14.400	0.680
620	07.270	4.100	0.547
630	17.800	9.340	0.594
640	10.200	5.430	0.577
650	24.800	12.600	0.955

APPENDIX B: SPECTRAL ENERGY DISTRIBUTION OF THE CIE STANDARD ILLUMINANT D65

Table B.1: D65 Spectral Energy Distribution

Wavelength, λ (nm)	Spectral Energy, $E(\lambda)$
400	82.755
410	91.486
420	93.432
430	86.682
440	104.865
450	117.008
460	117.812
470	114.861
480	115.923
490	108.811
500	109.354
510	107.802
520	104.790
530	107.689
540	104.405
550	104.046
560	100.000
570	96.334
580	95.788
590	88.686
600	90.006
610	89.599
620	87.699
630	83.289
640	83.699
650	80.027

APPENDIX C: CIE1931 COLOR MATCHING FUNCTIONS

Table C.1: CIE1931 Color Matching Functions

Wavelength, λ (nm)	$\bar{x}(\lambda)$	$\bar{y}(\lambda)$	$\bar{z}(\lambda)$
400	0.014	0.000	0.068
410	0.044	0.001	0.207
420	0.134	0.004	0.646
430	0.284	0.012	1.386
440	0.348	0.023	1.747
450	0.336	0.038	1.772
460	0.291	0.060	1.669
470	0.195	0.091	1.288
480	0.096	0.139	0.813
490	0.032	0.208	0.465
500	0.005	0.323	0.272
510	0.009	0.503	0.158
520	0.063	0.710	0.078
530	0.166	0.862	0.042
540	0.290	0.954	0.020
550	0.434	0.995	0.009
560	0.595	0.995	0.004
570	0.762	0.952	0.002
580	0.916	0.870	0.002
590	1.026	0.757	0.001
600	1.062	0.631	0.000
610	1.003	0.503	0.000
620	0.854	0.381	0.000
630	0.642	0.265	0.000
640	0.448	0.175	0.000
650	0.284	0.107	0.000

APPENDIX D: SOURCE CODE FOR THE UNIFORM YELLOWING PIGMENTATION METHOD

```
\% ========================================================================================
\% Uniform yellowing pigmentation method
\% ========================================================================================
\%
\%  se : Spectral energy of CIE standard illuminant (D65)
\%  x_hat, y_hat, z_hat : XYZ color matching values (CIE 1931)
\%  fr, fg, fb : Transmittance functions of LCD display
\%  F : Spectral transmission factor
\%  Xr, Yr, Zr : Tristimulus values through red filter for standard observer
\%  Xg, Yg, Zg : Tristimulus values through green filter for standard observer
\%  Xb, Yb, Zb : Tristimulus values through blue filter for standard observer
\%  Xr_e, Yr_e, Zr_e : Tristimulus values through red filter for elderly age A
\%  Xg_e, Yg_e, Zg_e : Tristimulus values through green filter for elderly age A
\%  Xb_e, Yb_e, Zb_e : Tristimulus values through blue filter for elderly age A
\%  X_2, Y_2, Z_2 : Total tristimulus values of standard observer
\%  X_e, Y_e, Z_e : Total tristimulus values of elderly age A
\%  X_ratio, Y_ratio, Z_ratio : Effective tristimulus ratios
\%  S : Rate of retinal illuminance
\%  X_o, Y_o, Z_o : Original image in XYZ color space
\%  elderly_X, elderly_Y, elderly_Z : Elderly perceived image in XYZ color space
\%
\% ========================================================================================

\& Tristimulus values through red, green, and blue filters of standard observer
last = 0;
for i = 1:1:26
    X_r = last + (se(i,1)*x_hat(i,1)*fr(i,1));
    last = X_r;
    Xr = last;
end

last = 0;
for i = 1:1:26
```

```
    X_g = last + (se(i,1)*x_hat(i,1)*fg(i,1));
    last = X_g;
    Xg = last;
end

last = 0;
for i = 1:1:26
    X_b = last + (se(i,1)*x_hat(i,1)*fb(i,1));
    last = X_b;
    Xb = last;
end

last = 0;
for i = 1:1:26
    Y_r = last + (se(i,1)*y_hat(i,1)*fr(i,1));
    last = Y_r;
    Yr = last;
end

last = 0;
for i = 1:1:26
    Y_g = last + (se(i,1)*y_hat(i,1)*fg(i,1));
    last = Y_g;
    Yg = last;
end

last = 0;
for i = 1:1:26
    Y_b = last + (se(i,1)*y_hat(i,1)*fb(i,1));
    last = Y_b;
    Yb = last;
end

last = 0;
for i = 1:1:26
    Z_r = last + (se(i,1)*z_hat(i,1)*fr(i,1));
```

```
    last = Z_r;
    Zr = last;
end

last = 0;
for i = 1:1:26
    Z_g = last + (se(i,1)*z_hat(i,1)*fg(i,1));
    last = Z_g;
    Zg = last;
end

last = 0;
for i = 1:1:26
    Z_b = last + (se(i,1)*z_hat(i,1)*fb(i,1));
    last = Z_b;
    Zb = last;
end

\& Tristimulus values through red, green, and blue filters of elderly people age A
last = 0;
for i = 1:1:26
    X_r_hat = last + (se(i,1)*x_hat(i,1)*fr(i,1)*F(i,1));
    last = X_r_hat;
    Xr_e = last;
end

last = 0;
for i = 1:1:26
    X_g_hat = last + (se(i,1)*x_hat(i,1)*fg(i,1)*F(i,1));
    last = X_g_hat;
    Xg_e = last;
end

last = 0;
for i = 1:1:26
    X_b_hat = last + (se(i,1)*x_hat(i,1)*fb(i,1)*F(i,1));
```

```
    last = X_b_hat;
    Xb_e = last;
end

last = 0;
for i = 1:1:26
    Y_r_hat = last + (se(i,1)*y_hat(i,1)*fr(i,1)*F(i,1));
    last = Y_r_hat;
    Yr_e = last;
end

last = 0;
for i = 1:1:26
    Y_g_hat = last + (se(i,1)*y_hat(i,1)*fg(i,1)*F(i,1));
    last = Y_g_hat;
    Yg_e = last;
end

last = 0;
for i = 1:1:26
    Y_b_hat = last + (se(i,1)*y_hat(i,1)*fb(i,1)*F(i,1));
    last = Y_b_hat;
    Yb_e = last;
end

last = 0;
for i = 1:1:26
    Z_r_hat = last + (se(i,1)*z_hat(i,1)*fr(i,1)*F(i,1));
    last = Z_r_hat;
    Zr_e = last;
end

last = 0;
for i = 1:1:26
    Z_g_hat = last + (se(i,1)*z_hat(i,1)*fg(i,1)*F(i,1));
    last = Z_g_hat;
```

```
    Zg_e = last;
end

last = 0;
for i = 1:1:26
    Z_b_hat = last + (se(i,1)*z_hat(i,1)*fb(i,1)*F(i,1));
    last = Z_b_hat;
    Zb_e = last;
end

\& Total tristimulus values of standard observer
X_2 = Xr + Xg + Xb;
Y_2 = Yr + Yg + Yb;
Z_2 = Zr + Zg + Zb;

\& Total tristimulus values of elderly people age A
X_e = Xr_e + Xg_e + Xb_e;
Y_e = Yr_e + Yg_e + Yb_e;
Z_e = Zr_e + Zg_e + Zb_e;

\% Effective tristimulus ratios
X_ratio = X_e/X_2;
Y_ratio = Y_e/Y_2;
Z_ratio = Z_e/Z_2;

\% Elderly color perception in XYZ color space
elderly_X = S*(X_ratio*X_o);
elderly_Y = S*(Y_ratio*Y_o);
elderly_Z = S*(Z_ratio*Z_o);

\% ==========================================================================================
```

APPENDIX E: SOURCE CODE FOR THE NATURALNESS PRESERVATION RECOLORING METHOD FOR THE RED-GREEN DEFICIENTS

```
\% ==========================================================================================
\% Naturalness preservation recoloring method for the red-green deficients
\% ==========================================================================================
\%
\%  X_o, Y_o, Z_o : Original image in XYZ color space
\%  X_s, Y_s, Z_s : Image perceived by the red-green deficients in XYZ color space
\%  X_on, Y_on, Z_on : Normalized values for original image
\%  X_sn, Y_sn, Z_sn : Normalized values for image perceived by the red-green deficients
\%  Theta_on, Theta_sn : Angles of elevation
\%  Ex, Ez : Error parameters
\%  phy : Rotation parameter
\%  Ex_bar, Ez_bar : Modified error parameters
\%  X_enhance, Y_enhance, Z_enhance : Recolored image in XYZ color space
\%
\% ==========================================================================================

\% Normalization
X_on = (X_o./Y_o)*100;
Y_on = (Y_o./Y_o)*100;
Z_on = (Z_o./Y_o)*100;

X_sn = (X_s./Y_s)*100;
Y_sn = (Y_s./Y_s)*100;
Z_sn = (Z_s./Y_s)*100;

\% Error Parameters
Ex = abs(X_on - X_sn);
Ez = abs(Z_on - Z_sn);

\% Angle of elevation, theta_on
Theta_on = atand (Z_on./X_on);
Theta_on(isnan(Theta_on)) = 0;
```

```
\% Angle of elevation, theta_sn
Theta_sn = atand (Z_sn./X_sn);
Theta_sn(isnan(Theta_sn)) = 0;

\% Rotation parameter
phy = abs(Theta_on - Theta_sn);

\% Rotation operation to get modified error parameters
Ex_bar = (Ex.*cosd(phy)) - (Ez.*sind(phy));
Ez_bar = (Ex.*sind(phy)) + (Ez.*cosd(phy));

Ex_bar(isnan(Ex_bar)) = 0;
Ez_bar(isnan(Ez_bar)) = 0;

\% Redistribution of error
X_enhance = X_on + Ex_bar;
Y_enhance = Y_on;
Z_enhance = Z_on + (Ez_bar + Ex_bar);

\% Recolored image in XYZ color space
X_enhance = (X_enhance./100).*Y_o;
Y_enhance = (Y_enhance./100).*Y_o;
Z_enhance = (Z_enhance./100).*Y_o;

\% =======================================================================================
```

UNIVERSITY OF MALAYA
DISSERTATION / THESIS CORRECTION REPORT

NAME : Mohd Fikree bin Hassan
MATRIC NO. : KHA 150003
PROGRAMME : Doctoral

TITLE OF DISSERTATION / THESIS *(as approved by Committee of Examiners)*: IMPROVED METHODS TO ENHANCE THE COLOR PERCEPTION FOR PEOPLE WITH COLOR VISION DEFICIENCY

DATE OF COMMITTEE OF EXAMINERS' MEETING / VIVA VOCE : 30 AUGUST 2018

COMMITTEE OF EXAMINERS' RECOMMENDATION : Minor corrections

Please list down ALL the required corrections as recommended by the Committee of Examiners (CoE).

Correction as Required by Examiners			Corrections made /Comments by Candidate	Comments/ Confirmation by Supervisor	Comments/ Confirmation by Internal Examiner *(if required by CoE)*
Section/ Chapter	Page	Comment			
		EXTERNAL EXAMINER 1 Small changes will make more unified. For example, the numbers in Tables 3.5 – 3.7 are necessary for 4 decimal places? Table 4.3 and Tables A.1 – C.1 are similar?	All the numbers in the Tables stated have been standardized to 3 decimal places. Tables 3.5 & 3.6 – page 45. Table 3.7 – page 46. Table 4.3 – page 67. Table A.1 – page 93. Table B.1 – page 94. Table C.1 – page 95.		

Correction as Required by Examiners			Corrections made /Comments by Candidate	Comments/ Confirmation by Supervisor	Comments/ Confirmation by Internal Examiner *(if required by CoE)*
Section/ Chapter	**Page**	**Comment**			
		Grammar is almost perfect. But p.18 Eq. (2.1) to (2.3) -> Eqs. (2.1) to (2.3) P.62 Zsn, respectively -> no comma p.61 Figure 4.4 all letters are too small compared with Figures 4.5 and 4.6. Figures 4.2 and 4.3 would make clear. p.49 L16 affect -> affects, L22 show -> shows	All the grammatical errors have been corrected. Page 18 – changed to Eqs. (2.1) to (2.3) Page 61 – changed the font to bigger size Page 57 – changed to clearer images for Figures 4.5 and 4.6. Page 49, Line 16 – changed to 'affects' Page 49, Line 22 – changed to 'shows'		
		EXTERNAL EXAMINER 2			
		INTERNAL EXAMINER During viva, the internal examiner commented that there is no corrective measure proposed to improve yellowing pigmentation seen by the elderly. During viva, the internal examiner commented about the images in Tables 4.4 and 4.5. In his comments, he suggested that the Tables should include images perceived by both groups of red-green deficients. During viva, the internal examiner commented that the function S(λ) is not defined in the thesis.	Corrective measure has been briefly proposed in Section 3.5: Summary in Chapter 3, Page 47, Line 9. The images for both groups of red-green deficients have been added into Tables 4.4 and 4.5. Chapter 4, Table 4.4, Page 68. Chapter 4, Table 4.5, Page 69. This is a typo error, S(λ) is actually E(λ). Corrected the error and the function is defined in Chapter 1, Page 17, Line 15.		

Correction as Required by Examiners			Corrections made /Comments by Candidate	Comments/ Confirmation by Supervisor	Comments/ Confirmation by Internal Examiner *(if required by CoE)*
Section/ Chapter	Page	Comment			
		COMMITTEE OF EXAMINERS (IF ANY)			
		Chapter 1: Add problem statement Add the main aim of this research	Section 1.2: Problem Statement is added in Chapter 1, Page 5. The main aim of this research is added under Section 1.3, Chapter 1, Page 6.		
		Sections 2.6 and 3.5 Change 'Conclusion' to 'Summary'	Changed to 'Summary'. Section 2.6, Page 22. Section 3.5. Page 46. Section 4.5, Page 77.		
		Remove doi number from reference list.	Removed all the doi numbers from reference list – Page 80 to 91.		
		Check the objectives. Should reflect the title of the thesis.	Edited the objectives to reflect the title of the thesis, Section 1.3, Chapter 1, Page 6.		
		For abstract, maximum keywords are 5.	Reduced the keywords in abstract to 5. Pages iv and vi.		
		Remove flow chart 1.1.	Removed flow chart in Figure 1.1.		

Correction prepared by:

Signature of Candidate

Name: Mohd Fikree bin Hassan

Date:

Verified by:

Signature of Supervisor (1)	Signature of Supervisor (2)	Signature of Supervisor (3)	Signature of Internal Examiner *(if required by the Committee of Examiners)*
Name: Prof. Dr. P. Raveendran	Name:	Name:	Name: Prof. Dr. Hamzah bin Arof
Date:	Date:	Date:	Date:

UNIVERSITY OF MALAYA

PENYERAHAN AKHIR TESIS/DISERTASI
FINAL SUBMISSION OF THESIS/DISSERTATION

BAHAGIAN A – BUTIR-BUTIR CALON (UNTUK DIISI OLEH CALON)
SECTION A – CANDIDATE'S DETAILS (TO BE COMPLETED BY THE CANDIDATE)

Nama Calon / *Name of Candidate* : MOHD FIKREE BIN HASSAN

No. Matrik / *Matric No.* : KHA 150003 Program / *Programme* : Ph.D

Mod Program / *Mode of Programme* : [X] Penyelidikan / *Research* [ ] Mod Campuran / *Mixed Mode*

Fakulti / *Faculty* : FACULTY OF ENGINEERING

Alamat Surat-Menyurat / *Mailing Address* : C-11-11, AMADESA CONDOMINIUM, JALAN 5/125,
DESA PETALING, 57100 KUALA LUMPUR.

No. Telefon Bimbit / *Mobile Phone No.* : 013-3999190 E-mel / *E-mail* : mfikree.hassan@gmail.com

Tajuk Tesis/Disertasi seperti yang diluluskan oleh Jawatankuasa Pemeriksa (dalam huruf besar):
**Sila lampirkan salinan surat/emel makluman keputusan Jawatankuasa Pemeriksa dan/atau pindaan tajuk (jika berkenaan)*

***Title of Thesis/Dissertation as approved by the Committee of Examiners** (in block letters):*
**Kindly provide a copy of the letter/email regarding the recommendation of the Committee of Examiners and/or revision of title (if applicable)*

IMPROVED METHODS TO ENHANCE THE COLOR PERCEPTION FOR PEOPLE
WITH COLOR VISION DEFICIENCY

Format Tesis/Disertasi / ***Format of Thesis/Dissertation*** :
- [ ] Biasa / *Conventional*
- [X] Gaya Artikel / *Article Style*
- [ ] *Kertas Kerja yang Diterbitkan / **Published Papers*

*Hanya untuk calon ijazah Kedoktoran
**Only applicable to Doctoral candidates*

Anggaran Patah Perkataan
*tidak termasuk nota kaki, rujukan, lampiran, jadual, gambar rajah dan prakata

Approximate Word Length
**excluding footnotes, references, appendices, tables, figures and preface*

: 20,000 Patah perkataan / *Words*

BAHAGIAN B – PERAKUAN CALON (UNTUK DIISI OLEH CALON)
SECTION B – DECLARATION OF CANDIDATE (TO BE COMPLETED BY CANDIDATE)

Tuan / Puan,

PENYERAHAN AKHIR TESIS/DISERTASI

Bersama-sama ini saya kemukakan tesis / disertasi dalam bentuk berikut:

(a) **DUA (2)** naskhah bercetak dijilid dengan kulit tebal jenis rexine (Merah Tua atau *Maroon* untuk tesis/disertasi); dan

(b) **Satu (1)** salinan elektronik (format PDF)

- yang telah disemak dan diberi perakuan oleh penyelia, melalui ***Ketua Jabatan / Timbalan Dekan Ijazah Tinggi / Timbalan Pengarah** saya untuk penyerahan akhir.

Saya juga mengesahkan bahawa saya telah mengikut format penulisan tesis/disertasi yang ditetapkan oleh Universiti dan mengisi senarai semak (*Bahagian C*) dan senarai tersebut telah disemak oleh penyelia sebelum penyerahan akhir tesis/disertasi.

Saya bersetuju sekiranya borang ini tidak lengkap, senarai semak tidak diisi dan maklumat yang diberikan tidak betul, Unit Tesis mempunyai hak untuk tidak menerima tesis saya.

Sekian, terima kasih.

*sila potong yang mana tidak berkenaan

Sir / Madam,

SUBMISSION OF FINAL THESIS/ DISSERTATION

I hereby submit my thesis / dissertation as follows:

*(a) **TWO (2)** printed hardbound copies in rexine (Dark Red or Maroon for thesis and dissertation); and*

*(b) **One (1)** electronic copy (PDF format)*

*- which have been checked and declared by my supervisor(s), through the ***Head of Department / Deputy Dean / Deputy Director** for final submission.*

I have also followed the format of thesis/dissertation set by the University and have completed the checklist (Section C) and verified by my supervisor(s) prior to the final submission of thesis/dissertation.

I hereby agree if this form and the checklist are incomplete, and information given is not accurate, the Institut has the right not to accept my thesis.

Thank you.

**please strike out whichever is not applicable*

Dokumen lain yang diperlukan:
Other required documents:

☐ Polisi Repositori (Borang Embargo Tesis/Disertasi)
Repository Policy (Thesis/Dissertation Embargo Form)

☐ Laporan Pembetulan Tesis/Disertasi
Thesis/Dissertation Correction Report

Tandatangan Calon
Signature of Candidate : ____________________
Nama Calon
Name of Candidate : ____________________
No. Matrik
Matric No. : ____________________
Tarikh
Date : ____________________

BAHAGIAN C – SENARAI SEMAK BAGI FORMAT TESIS/DISERTASI
SECTION C – CHECKLIST FOR FORMAT OF THESIS/DISSERTATION

Sila rujuk **Panduan Penyediaan Laporan Penyelidikan, Disertasi dan Tesis** untuk butir-butir terperinci (Panduan ini boleh dimuaturun dari http://ips.um.edu.my/).

*Please refer to **Guidelines for the Preparation of Research Reports, Dissertations and Theses** for further details (The guidelines is available on http://ips.um.edu.my/).*

SENARAI SEMAK	*CHECKLIST*	Semakan Calon *Verified by Candidate*	Semakan Penyelia *Verified by Supervisor*
1. TAJUK (a) Kulit hadapan dan halaman tajuk tesis/disertasi hendaklah seperti diluluskan oleh Fakulti. (b) Nama calon seperti yang didaftar dengan Universiti.	***1. TITLE*** *(a) Front cover and title page of the research/dissertation which has been approved by the Faculty.* *(b) The name of the candidate must be the name registered with the University.*		
2. ABSTRAK (a) Tidak melebihi 500 patah perkataan (b) Ditulis dalam Bahasa Malaysia dan Bahasa Inggeris (Termasuk abstrak dalam Bahasa Arab sekiranya tesis/disertasi ditulis dalam Bahasa Arab)	***2. ABSTRACT*** *(a) Not more than 500 words* *(b) Written in both Bahasa Malaysia and English (Include abstract in Arabic if the thesis/dissertation is written in Arabic)*		
3. PENJILIDAN (a) **DUA (2)** naskah bercetak dan dijilid dengan kulit keras jenis rexine (Merah Tua atau *Maroon* untuk tesis/disertasi, serta kulit berwarna biru laut untuk laporan penyelidikan); dan (b) **Satu (1)** salinan elektronik (PDF)	***3. BINDING*** *(a) **TWO (2)** printed hardbound copies in rexine (Dark Red or Maroon for thesis/dissertation, and navy blue for research report); and* *(b) **One (1)** electronic copy (PDF)*		
4. KUALITI PERCETAKAN (a) Ditaip dua jarak (double-spacing) bagi semua teks dan satu jarak (single-spacing) bagi catatan kaki, apendiks, jadual dan rajah. (b) Corak font yang digunakan iaitu **Times New Roman** dan **Latex** atau **Equation Editor** untuk teks matematik. (c) Font bersaiz 12 bagi keseluruhan teks dan font bersaiz 8 digunakan bagi catatan kaki. (d) Kualiti kertas A4 hendaklah tidak kurang dari 80 gm.	***4. PRINTING QUALITY*** *(a) Double-spacing for all sections. Single-spacing can be used for footnote, appendices, tables and diagrams.* *(b) Font type: **Times New Roman** and **Latex** or **Equation Editor** for mathematical text.* *(c) Font size 12 for all text and font size 8 for footnotes.* *(d) Must use high quality A4 paper 80 gm.*		

SENARAI SEMAK	*CHECKLIST*	Semakan Calon *Verified by Candidate*	Semakan Penyelia *Verified by Supervisor*
5. HAD MAKSIMUM PATAH PERKATAAN (a) Tesis (Ijazah Kedoktoran) • Secara Penyelidikan: 100,000 patah perkataan; • Secara Mod Campuran: 80,000 patah perkataan; (b) Disertasi (Ijazah Sarjana) • Secara Penyelidikan: 60,000 patah perkataan; • Secara Mod Campuran: 40,000 patah perkataan; (c) Laporan Penyelidikan (Ijazah Sarjana) • Secara Kursus: 30,000 patah perkataan; (Anggaran jumlah patah perkataan tidak termasuk nota kaki, rujukan, lampiran, jadual, gambar rajah dan prakata)	***5. MAKSIMUM WORD LIMIT*** *(a) Thesis (Doctoral Degree)* • *Research: 100,000 words;* • *By Mixed Mode: 80,000 words;* *(b) Dissertation (Master's Degree)* • *By Research: 60,000 words;* • *By Mixed Mode: 40,000 words;* *(c) Research Report (Master's Degree)* • *By Coursework: 30,000 words* *(Approximate word length excluding footnotes, references, appendices, tables, figures and preface)*		
6. BIRAI Birai yang ditetapkan bagi teks adalah seperti berikut: Atas : 2.0 cm Kanan : 2.0 cm Bawah : 2.0 cm Kiri : 4.0 cm	***6. INDENT*** *The indents of pages are as follows:* *Top : 2.0 cm Right : 2.0 cm* *Bottom : 2.0 cm Left : 4.0 cm*		
7. PENOMBORAN MUKA SURAT (a) Font bersaiz 10; (b) Nombor muka surat dicetak 1.0 cm dari bahagian kanan bawah muka surat; (c) Nombor Roman (i, ii, iii dan seterusnya) diletakkan di bahagian permulaan (Preface); (d) Muka surat tajuk (Title page) pada muka hadapan dianggap sebagai muka surat 'i', tetapi nombor 'i' tidak ditaip. Nombor muka surat bermula selepas muka surat tajuk (Title page) disambung terus dengan nombor Roman 'ii'.	***7. PAGE NUMBERING*** *(a) Font size 10;* *(b) All page numbers should be printed 1.0 cm from the bottom margin and placed on the right-hand side;* *(c) Roman numerals (i, ii, iii etc) should be used in the Preface section;* *(d) The Title Page and the first page of the Preface should not be numbered. Numbering begins on the second page with 'ii'.*		
8. PERAKUAN KEASLIAN PENULISAN Borang Perakuan Keaslian Penulisan boleh dimuatturun dari laman web http://ips.um.edu.my dan perlu ditandatangani oleh calon dan saksinya serta diletakkan dalam tesis/disertasi **SEBELUM** Abstrak. (Calon perlu menggunakan borang perakuan sama ada Bahasa Malaysia atau Bahasa Inggeris)	***8. ORIGINAL LITERARY WORK DECLARATION*** *Original Literary Work Declaration form can be downloaded from the website at http://ips.um.edu.my and must be signed by the candidate and witness. The form should be placed in the thesis/dissertation immediately **BEFORE** the abstract.* *(Candidate should use the declaration form either the Bahasa Malaysia or English version)*		

SENARAI SEMAK	*CHECKLIST*	Semakan Calon *Verified by Candidate*	Semakan Penyelia *Verified by Supervisor*
9. FORMAT SALINAN ELEKTRONIK Satu salinan elektronik dalam bentuk PDF mesti diserahkan bersama dengan label yang mengandungi maklumat berikut: (a) Nama; (b) No. Matrik; (c) Tajuk Tesis/Disertasi; (d) Fakulti; (e) Tahun penyerahan	***9. ELECTRONIC COPY FORMAT*** *The submitted electronic copy in the form of CD (in PDF format) must be labeled with the following details: (a) Name; (b) Matric No.; (c) Title of Thesis/Dissertation; (d) Faculty; (e) Year of submission*		
10. 'TURNITIN' Penggunaan perisian ini adalah bergantung kepada Fakulti. Sila rujuk dengan fakulti berkenaan mengenai peratus indeks pertindihan yang diterima dan lampirkan muka surat pertama laporan peratus pertindihan.	***10. 'TURNITIN'*** *The usage of this software is subject to the Faculty. Please refer to your faculty for the accepted similarity index percentage and attach the first page of the report upon the submission.*		
11. Penggunaan program ***Spellchecker*** atau **Dewan Eja** untuk menyemak kesalahan ejaan adalah digalakkan.	***11.*** *The use of **Spellchecker** or '**Dewan Eja'** programme to check for spelling errors is recommended.*		
12. Penggunaan program **'EndNote'** untuk menyelaraskan rujukan adalah digalakkan.	***12.*** The use *of **'EndNote'** programme for referencing is recommended.*		

Nama calon
Name of candidate :

Tandatangan Calon
Candidate's Signature

Tarikh :
Date

Cop dan Tandatangan Penyelia
Supervisor's Signature and Official Stamp

Tarikh :
Date:

Cop dan Tandatangan Penyelia
Supervisor's Signature and Official Stamp

Tarikh :
Date:

Cop dan Tandatangan Penyelia
Supervisor's Signature and Official Stamp

Tarikh :
Date:

BAHAGIAN D – PENGESAHAN PENYELIA/PEMERIKSA
(UNTUK DIISI OLEH PENYELIA DAN/ATAU PEMERIKSA)

SECTION D – DECLARATION OF SUPERVISOR(S) / EXAMINER(S)
(TO BE COMPLETED BY THE SUPERVISOR(S) AND/OR EXAMINER(S))

Calon perlu mendapatkan pengesahan daripada Penyelia dan/atau Pemeriksa (jika berkenaan) tertakluk kepada keputusan Jawatankuasa Pemeriksa.
Candidate is required to get the verification by the Supervisor(s) and/or Examiner(s) (if applicable) subject to the decision of the Committee of Examiners.

PENYELIA / *SUPERVISOR*

1. **Nama Penyelia**
Name of Supervisor : ______________________

Saya telah menyemak tesis/disertasi calon dan mengesahkan bahawa calon telah membuat pembetulan seperti yang disarankan oleh Jawatankuasa Pemeriksa.
I have checked the candidate's thesis/dissertation and hereby confirm that the candidate has done all corrections recommended by the Committee of Examiners.

Tandatangan dan Cop Rasmi
Official Stamp and Signature

Tarikh:
Date: ______________________

2. **Nama Penyelia**
Name of Supervisor : ______________________

Saya telah menyemak tesis/disertasi calon dan mengesahkan bahawa calon telah membuat pembetulan seperti yang disarankan oleh Jawatankuasa Pemeriksa.
I have checked the candidate's thesis/dissertation and hereby confirm that the candidate has done all corrections recommended by the Committee of Examiners

Tandatangan dan Cop Rasmi
Official Stamp and Signature

Tarikh:
Date: ______________________

3. **Nama Penyelia**
Name of Supervisor : ______________________

Saya telah menyemak tesis/disertasi calon dan mengesahkan bahawa calon telah membuat pembetulan seperti yang disarankan oleh Jawatankuasa Pemeriksa.
I have checked the candidate's thesis/dissertation and hereby confirm that the candidate has done all corrections recommended by the Committee of Examiners

Tandatangan dan Cop Rasmi
Official Stamp and Signature

Tarikh:
Date: ______________________

PEMERIKSA (tertakluk kepada keputusan Jawatankuasa Pemeriksa)
EXAMINER (subject to the decision of the Committee of Examiners)

1. **Nama Pemeriksa**
Name of Examiner : ______________________

Saya telah menyemak tesis/disertasi calon dan mengesahkan bahawa calon telah membuat pembetulan seperti yang disarankan oleh Jawatankuasa Pemeriksa.
I have checked the candidate's thesis/dissertation and hereby confirm that the candidate has done all corrections recommended by the Committee of Examiners

Tandatangan dan Cop Rasmi
Official Stamp and Signature

Tarikh:
Date: ______________________

2. **Nama Pemeriksa**
Name of Examiner : ______________________

Saya telah menyemak tesis/disertasi calon dan mengesahkan bahawa calon telah membuat pembetulan seperti yang disarankan oleh Jawatankuasa Pemeriksa.
I have checked the candidate's thesis/dissertation and hereby confirm that the candidate has done all corrections recommended by the Committee of Examiners

Tandatangan dan Cop Rasmi
Official Stamp and Signature

Tarikh:
Date: ______________________

BAHAGIAN E – PENGESAHAN OLEH FAKULTI
SECTION E – VERIFICATION BY FACULTY

Sila kemukakan borang ini bersama **senaskhah tesis/disertasi dan Laporan Pembetulan Tesis/Disertasi** ke Jabatan/Pejabat Ijazah Tinggi di fakulti berkenaan. Bahagian ini hendaklah dilengkapkan oleh Ketua Jabatan/Timbalan Dekan Ijazah Tinggi/Timbalan Pengarah (Akademik) sebelum penyerahan akhir tesis/disertasi

*Please submit this form together with **a copy of thesis/dissertation and Thesis/Dissertation Correction Report** to the Department/Postgraduate Office of your respective faculty. This section is completed by the Head of Department / Deputy Dean of Higher Degree / Deputy Director (Academic) prior to final submission of thesis/dissertation.*

Saya memperakukan penyerahan akhir tesis/disertasi calon ini.

I acknowledge the candidate's final submission of thesis/dissertation.

Tandatangan dan Cop Rasmi
Official Stamp and Signature

Ketua Jabatan/Timbalan Dekan Ijazah Tinggi/Timbalan Pengarah (Akademik)
Head of Department / Deputy Dean of Higher Degree / Deputy Director (Academic)

Tarikh
Date : ______________________

REPOSITORY POLICY FOR UNIVERSITY OF MALAYA POSTGRADUATE THESES/DISSERTATIONS/RESEARCH REPORTS

1. AIM

The aim of this policy is to establish the procedures to be followed for the setting-up of a repository for the University of Malaya postgraduate candidates' theses/dissertations/research reports.

2. POLICY

1) The University, via the Library, collects all the theses, dissertations and research reports produced in the University of Malaya in both the print and electronic format. It is the policy of the University that the public should be given access to the theses/dissertations/research reports resulting from postgraduate research work. Thus, all postgraduate candidates undertaking research work are required to submit ONE print copy and ONE electronic copy of their thesis/dissertation/research reports to be kept by the University of Malaya Library.

2) The University acknowledges that there are commercially viable research products. Public access to such theses and dissertations may be placed on hold to enable registration or intellectual property control such as patent registration and publication of articles.

3) The University of Malaya Library had established a EPrints-based theses/dissertations/research reports repository system (*http://studentsrepo.um.edu.my*) in 2010. The advantages of EPrints are as follows :
   a) Free access
   b) User friendly
   c) Open source where information can be shared with higher learning institutions all over the world
   d) Documents are controlled in terms of security
   e) The system has been customized to cater to the needs of the University of Malaya
   f) The system is controlled by the University of Malaya

3. IMPLEMENTATION

1) Candidate

Signs a thesis/dissertation/research report repository submission form as in **Appendix** when submitting the final copy of their thesis/dissertation/research report to IGS or to their respective faculty.

2) Institute of Graduate Studies/Faculties

IGS/Faculties will forward to the Library one copy in print and electronic format of the graduating candidate's thesis/dissertation/research report.

3) The University of Malaya Library (UML)

- Uploads the thesis/dissertation into the repository at the University of Malaya Library.
- Manages the repository.

Appendix

THE CANDIDATE'S AGREEMENT

The Faculty examination committee and I agree that the document described in this application should be placed in the University of Malaya Open Access repository. I will provide two hardbound copies as well as one electronic copy of the work in PDF format to the Faculty and agree to release the entire work immediately.
(Tick (√) whichever applicable)

(√) I **AGREE** to allow **Open Access (public view)** to my thesis/~~dissertation/research report~~#

(   ) I wish to **restrict access** to the public availability of both **the Library paper bound copy** and **the electronic copy** of my thesis/dissertation until ________________ for the following reason(s)*:
(*The library will block access to both **print** and **electronic copy** for up to **two (2) years***)

____

____

____

(   ) I wish to **restrict access** to the public availability of **the electronic copy** of my thesis/dissertation until ________________ for the following reason(s)*:
(*The library will only block access to the **electronic copy** for up **to two (2) years***)

____

____

____

#If none of the options are selected, the first option will be carried out by default
****Only the title, table of content and bibliography will be made available***

I hereby certify that, if appropriate, I have obtained and attached hereto a written permission statement from the owner(s) of each third-party copyrighted matter to be included in my thesis or selected project, and will allow inclusion in the Open Access repository. I certify that the version I am submitting is the same as that approved by the faculty examination committee.

I hereby grant to the University of Malaya and its agents the non-exclusive license to archive and make accessible my thesis or selected project in whole or in part in all forms of media, now or hereafter known. I retain all other ownership rights to the copyright of the theses or selected project. I also retain the right to use in future works (such as articles or books) all or part of this thesis or selected project.

Canddate's Signature : ____________________ Date : ____________________

Name of Candidate (*IN PRINTED LETTERS*) : MOHD FIKREE BIN HASSAN E-mail : mfikree.hassan@gmail.com

Verified by:

Name of Supervisor : PROF. DR. P. RAVEENDRAN Signature and Official Stamp : ____________________

Name of Supervisor : ____________________ Signature and Official Stamp : ____________________

Deputy Dean/Deputy Director (Higher Degree) Signature and Official Stamp : ____________________

* By 'open access' to this literature, we mean it is freely available on the public internet, permitting any users to read, download, copy, distribute, print, search, or link to the full texts of these articles, crawl them for indexing, pass them as data to software, or use them for any other lawful purpose, without financial, legal, or technical barriers other than those inseparable from gaining access to the internet itself. The only constraint on reproduction and distribution, and the only role for copyright in this domain, should be to give authors control over the integrity of their work and the right to be properly acknowledged and cited (Chan et al, 2002).
Chan, L. et al (2002) Budapest Open Access Initiative. New York: Open Society Institute. http://www.soros.org/openaccess/read.shtml (Retrieved 22 January 2007)

turnitin

Digital Receipt

This receipt acknowledges that Turnitin received your paper. Below you will find the receipt information regarding your submission.

The first page of your submissions is displayed below.

Submission author:	Mohd Fikree Hassan
Assignment title:	Postgraduate 2/2018
Submission title:	Thesis PhD
File name:	thesis_turnitin_final.pdf
File size:	29.28M
Page count:	92
Word count:	21,597
Character count:	114,544
Submission date:	02-Sep-2018 01:46PM (UTC+0800)
Submission ID:	995862755

Thesis PhD

by Mohd Fikree Hassan

Submission date: 02-Sep-2018 01:46PM (UTC+0800)
Submission ID: 995862755
File name: thesis_turnitin_final.pdf (29.28M)
Word count: 21597
Character count: 114544

CHAPTER 1: INTRODUCTION

1.1 Overview

An image is an object that portrays visual perception. It can be two-dimensional, such as a photograph and a map, and it can also be three-dimensional, such as a hologram. In the current world of digital information technology that we live in, two-dimensional color images play an important role in human lives. Color images not only embody information but are also used as a medium of communication among people. Hence, the usage of color images in distributing information via websites and smartphone applications has increased in the 21st century. Electronic devices such as laptops and smartphones have become essential items as millions of color images are shared on Facebook (Thomas, 2012) and Instagram (DesMarais, 2013) everyday. Moreover, color images are also utilized in advertisement boards, traffic maps, and signboards in public places such as airports, shopping malls, and train stations.

Color is an attribute of visual sensation and the color appearance of an object depends on the interaction between three main components; light sources, objects and the human visual system (Fairchild, 2005). The interaction between the light sources and the physical and chemical properties of an object creates a modulated energy that will be processed by the human visual system to produce the perceptions of color. The ability to distinguish the set of signals that are produced by the modulated energy is known as human color perception (Fairchild, 2005). The modulated energy reacts with the three types of cone photoreceptors in the human eye. Each of the cone photoreceptors is sensitive to either short (S), medium (M), and long (L) wavelength light, and each wavelength light exhibits bluish, greenish, and reddish sensitivity respectively (Hunt, 2004; Pascale, 2003).

However, a percentage of people have some kind of color vision deficiency that arise from differences in the pigmentation of the cone photoreceptors in their eyes (Wandell, 1995). Thus, they are unable to distinguish certain shades of colors. This inability may create barriers in terms of physical capabilities (Hassan & Paramesran, 2017). Some of them may have difficulty finding goods in stores, and some may even bump into a glass door due to the confusion that occurs to their color perception (K. Ishihara, Ishihara, Nagamachi, Hiramatsu, & Osaki, 2001). Moreover, the reaction time and cognitive time of the elderly are slower compared to younger people (T. Suzuki, Okajima, & Funai, 2012; T. Suzuki, Yi, Sakuragawa, Tamura, & Okajima, 2005). In addition, their social life and even their career may be affected due to their inability to discriminate colors (Cole, 2007; Tagarelli et al., 2004).

Color vision deficiency can be categorized as acquired and inherited (Simunovic, 2016; Verriest, 1963). In acquired color vision deficiency, color perception loss is due to medication, aging, disease, or accidents. As reported by the Department of Statistics, there are about 2.5 million people over the age of 60 in Malaysia (Hassan, Kugimiya, Tanaka, Tanaka, & Paramesran, 2015), and this number is expected to grow by 2020 (Chua, Chang, & Lim, 2015). This trend is also reflected globally (Hegde & Bishop, 2018). Hence, it is important to understand the difficulties experienced by the elderly in order to provide various support systems to assist them during their daily activities (Bright & Egger, 2008; Hegde & Bishop, 2018).

Thus, much has been conducted on acquired color vision deficiencies due to aging. Earlier studies have confirmed that as human age increases, the thickness of the lens continues to grow and the accumulation of yellow pigmentation occurs (Artigas, Felipe, Navea, Fandino, & Artigas, 2012; Norren & Vos, 1974; Pokorny, Smith, & Lutze, 1986; Romano et al., 2011; Ruddock, 1965a; Said & Weale, 1959; Weale, 1961a). This yellowing pigmentation effects the transparency of the human crystalline lens (Alio, Schimchak, Negri, & Montes-Mico, 2005). Apart from the yellowing pigmentation, the size of human pupil also reduces with age (Applegate, Donnelly, Marsack, & Koenig, 2007; Birren, Casperson, & Botwinick, 1950; Bitsios, Prettyman, & Szabadi, 1996; Kadlecova, Peleska, & Vasko, 1958; Ortiz, Bowyer, & Flynn, 2013; Said & Sawires, 1972; Winn, Whitaker, Elliott, & Phillips, 1994) which causes the reduction of the effective light reaching the retina (Sloan, 1939; Weale, 1961a, 1961b; Werner, Peterzell, & Scheetz, 1990). Due to these reasons, elderly people experience yellowish and darker color perception than younger people.

A lot of effort has been poured into research on the elderly color perception model. The effect of yellowing pigmentation to the human lens-density spectrum has been studied in Pokorny et al. (1986), Savage, Haegerstrom-Portnoy, Adams, and Hewlett (1993), Weale (1988), and Xu, Pokorny, and Smith (1997) while the investigation of pupil size has been studied in Birren et al. (1950), Said and Sawires (1972), and Winn et al. (1994). To replicate the experience of elderly color perception, experimental studies using artificial uniform yellowing filter have been conducted in K. Ishihara et al. (2001), Schneck, Adams, Huie, and Lee (1993), and Yoshida and Sakuraba (1996). Computerized simulations of elderly color perception have also been conducted in Okajima and Takase (2001) and Tanaka et al. (2011). Based on the non-uniform yellowing pigmentation method by Tanaka et al. (2011), several image enhancement methods to improve the elderly color perception have been proposed in R. Suzuki et al. (2012), Ueda, Azetsu, Suetake, and Uchino (2015a), Ueda, Azetsu, Suetake, and Uchino (2015b, 2016), and Ueda et al. (2016).

Meanwhile, for inherited color vision deficiency, color loss occurs due to the changes of the cone photoreceptors in the human eyes. About eight percent of the male population is color vision deficient (Ching & Sabudin, 2010; Lee & dos Santos, 2011; Semary & Marey, 2014). One type of inherited color vision deficiency is dichromacy, which occurs when one type of cone photoreceptors is absent or not functioning. People with dichromacy are also known as dichromats. Dichromacy can be classified into three categories: protanopia, deuteranopia, or tritanopia depending on whether the missing cone is the L-cone, M-cone, or S-cone respectively (Neitz & Neitz, 2011). Protanopia and deuteranopia are also called red-green deficiencies (Moreira, Alvaro, Melnikova, & Lillo, 2018). People with either protanopia and deuteranopia have difficulty in distinguishing between these two colors (Ching & Sabudin, 2010; Judd, 1949). Another type of dichromacy is called tritanopia with which people have difficulty distinguishing shades of blue and yellow. However, people with tritanopia constitute less than one percent of the male population (Moreira et al., 2018).

To simulate dichromatic color perception, various algorithms have been proposed in Brettel, Vienot, and Mollon (1997), Capilla, Diez-Ajenjo, Luque, and Malo (2004), Capilla, Luque, and Diez-Ajenjo (2004), Lee and dos Santos (2011), Machado, Oliveira, and Fernandes (2009), Meyer and Greenberg (1988), Rodriquez-Pardo and Sharma (2011), Vienot, Brettel, and Mollon (1999), and Wachtler, Dohrmann, and Hertel (2004). Due to its mathematical simplicity and its usability in expressing color discrimination of the people with dichromacy, Brettel's algorithm (Brettel et al., 1997; Vienot et al., 1999) is the most accepted model in modeling dichromatic color perception.

Based on Brettel's algorithm, researchers have proposed image recoloring methods to improve the color perception of people with dichromacy, in particular, red-green deficiency. Many strategies have been utilized for the image recoloring and these methods have been presented in Anagnostopoulos, Tsekouras, Anagnostopoulos, and Kalloniatis (2007), Doliotis, Tsekouras, Anagnostopoulos, and Athitsos (2009), Huang, Chen, Jen, and Wang (2009), Huang, Tseng, Wu, and Wang (2007), Ichikawa et al. (2003), Jefferson and Harvey (2006), Kuhn, Oliviera, and Fernandes (2008), Ma, Gu, and Wang (2006), Machado and

Oliveira (2010), Rasche, Geist, and Westall (2005a), Rasche, Geist, and Westall (2005b), Ribeiro and Gomes (2013), Rigden (1999), Suetake, Tanaka, Hashii, and Uchino (2012), Wakita and Shimamura (2005), and Yang and Ro (2003).

Although all the aforementioned methods for elderly and red-green deficients color perception enable us to understand more about their color perception, there are certain issues that need to be addressed.

1.2 Problem Statement

In the field of elderly color perception, non-uniform yellowing pigmentation has been utilized to simulate their color perception. Recently, results in clinical studies (Artigas et al., 2012; Romano et al., 2011) of elderly color perception confirm that uniform yellowing pigmentation occurs on human crystalline lenses. However, the uniform yellowing pigmentation has not been represented mathematically, and this creates a gap in the research of elderly color perception. Hence, it has becomes a motivation to develop a mathematical model of the uniform yellowing pigmentation and assess the color perception experienced by the elderly.

Meanwhile, most of the recolored images for red-green deficients lose their naturalness when viewed by those with normal color vision (Huang et al., 2007; Jeong, Kim, Wang, & Yoon, 2011). Thus, the recolored images are not suitable for use in advertisements, signboards, and maps in public places such as airports, shopping malls, and train stations. Some of the image recoloring methods may also change all the colors of the original image. As consequence, the recolored images tend to look unnatural to the red-green deficients as well (Kuhn et al., 2008).

In addition, apart from lack of naturalness preservation, several of the recoloring algorithms for red-green deficiency may not be suitable for practical use due to complex and iterative algorithms (Doliotis et al., 2009; Ichikawa et al., 2003), high computational time (Rasche et al., 2005a, 2005b), recoloring process performed in the reduced color space of dichromats (Kuhn et al., 2008), and limited color options in their recoloring process (Rigden, 1999; Wakita & Shimamura, 2005). Hence, there are opportunities for improvement for the enhancement of the color perception for people with color vision deficiency, in particular the elderly people and the red-green deficients.

1.3 Objectives

The main aim of this research is to enhance the color perception for people with color vision deficiency. In order to achieve this aim, this thesis has two objectives. The objectives of this thesis are:

1. *To improve the computerized simulation method of elderly color perception by introducing a mathematical representation of the uniform yellowing pigmentation to mimic elderly color perception*

   It is shown in medical reports that elderly people suffer from certain degrees of color perception loss. Previous works on elderly color perception utilized a non-uniform yellowing pigmentation method. However, results from recent medical studies show that uniform yellowing pigmentation occurs on human crystalline lens as human age increases. This provides motivation and new opportunities to expand the research work in elderly color perception. Thus, a mathematical representation of the uniform yellowing pigmentation is formulated to improve the computerized simulation method of elderly color perception. The simulated uniform yellowing pigmentation is used to mimic the color perception of elderly (Chapter 3).

2. *To improve the image recoloring method for the red-green deficients by proposing a naturalness preservation image recoloring method*

Although there are various image recoloring methods that enhance the visual details and improve the color perception of the red-green deficients, the recolored images may look non-pleasing to people with normal color vision. This may happen in public places such as airports, shopping malls, and train stations where color images used in maps and advertisements are viewed by everyone. Moreover, the recolored images may look unnatural to the red-green deficients as well since all the colors of the original images are changed during the recoloring process. To overcome this issue, a naturalness preservation image recoloring method is introduced which enhances visual details while maintaining the naturalness of the recolored images as much as possible (Chapter 4).

1.4 Organization of the Thesis

This thesis, as was pointed out earlier in this chapter, describes improved methods to enhance the color perception for people with color vision deficiency. A uniform yellowing pigmentation method is introduced to simulate the color perception of the elderly. An image recoloring method that enhances the color perception of the red-green deficients and also maintains the naturalness of the image is also introduced.

The following is a summary of the content of each chapter.

Chapter 2: Human Color Vision. This chapter presents an overview of human color vision. Information on the human visual system is described here. The developments of the CIE color matching functions that corresponds to the response of the human eye are presented. Based on the CIE color matching functions, *XYZ* color space was formulated. The basic formulation of the *XYZ* tristimulus values and its chromaticity diagram are described in this chapter. *XYZ* color space is utilized as the main working domain for the methods proposed in this thesis. Moreover, the mathematical relationship between *XYZ* and *RGB* color spaces is also presented in this chapter. This information is essential as all color images utilized in the proposed methods are transformed from *RGB* color space to *XYZ* color space. The types of color vision deficiencies are also described in this chapter.

Chapter 3: Color Perception of the Elderly. This chapter discusses the research developments in elderly color perception. Findings from earlier research works show that the color perception of the elderly people is degraded due to yellowing pigmentation that occurs on the human crystalline lens. In addition, reduction in the human pupil size also affects the ability of elderly people to differentiate colors. To mimic color perception of the elderly, previous works utilized the non-uniform yellowing pigmentation method. However, results from recent clinical studies have shown that uniform yellowing pigmentation occurs on the human crystalline lens. To study the effects of the uniform yellowing pigmentation on the color perception of the elderly, a mathematical method representing the uniform yellowing pigmentation is proposed. Using the uniform yellowing pigmentation, color perception of the elderly is simulated, and the experimental results are compared with the results from medical studies for validation. In addition, results from experimental studies show that the proposed method produces images that are closer to the results from medical studies and perform better than the results from the non-uniform yellowing pigmentation method.

Chapter 4: Color Perception of Red-green Deficients. This chapter presents an overview of the color perception of red-green deficients. A simulation method to reproduce their color perception is described in this chapter. Some of the research done with the specific aim of improving the color perception of the red-green deficients is briefly discussed in this chapter. Although previous works enhance the color perception of red-green deficients, the recolored images lose their naturalness. These color images used in advertisements in public places may look non-pleasing to the people with normal color vision as well as to red-green deficients. Thus, the chapter proposes a naturalness preserving recoloring method that enhances the color perception of the red-green deficients and also maintains the naturalness of the recolored images to both parties. Experimental results are presented to validate this claim, and a comparison between the state-of-the-art method and two other existing methods show that the proposed recoloring method achieves better objective and subjective scores.

Chapter 5: Conclusion. The thesis is concluded, summarizing the contents of the thesis and discussing the possibilities of future work in this direction.

1.5 Contributions

One of the contributions of this thesis is that it proposes a mathematical representation of the uniform yellowing pigmentation that occurs on the human crystalline lens. The simulated uniform yellowing pigmentation is utilized to model the color perception of the elderly. This work has been published in Hassan, Paramesran, Tanaka, and Tanaka (2018). The proposed method is essential in order for us to really understand the difficulties faced by the elderly. Moreover, it is imperative to consider a good visual presentation through color in order to enable the elderly to experience the surrounding environment safely and with confidence. Based on the proposed method, improvements such as the usage of better color schemes to represent information can be considered, thus avoiding miscommunication and misinterpretation. This, in turn, can improve the quality of life of the elderly. Therefore, the proposed method contributes to the development of the field of color perception of the elderly.

Some of the current image recoloring methods for red-green deficients may potentially change all the colors of the original image. As a result, the recolored image may look non-pleasing to both red-green deficients as well as people with normal color vision. Therefore, the second contribution of this thesis is the construction of a naturalness preserving recoloring method for red-green deficients. This work has been published in

Hassan and Paramesran (2017). The proposed method takes into consideration the needs of red-green deficients as well as people with normal color vision. By maintaining the luminance and the hue of the original image, the proposed method enhances the color perception of the red-green deficients and maintains the naturalness of the recolored images to both parties. This is important for images used in public places such as airports, shopping malls, and train stations where color images such as maps and advertisements are viewed by everyone.

CHAPTER 2: HUMAN COLOR VISION

This chapter presents an overview of human color vision. A description of the human visual system is briefly represented. Research developments on color matching functions that correspond to the response of the human eyes are also discussed. All the color sensations that a human perceives can be encompassed using *XYZ* color space. Thus, information on the *XYZ* color space and its chromaticity diagram are also described in this chapter. However, due to the non-uniformity of the *XYZ* color space, for color reproduction in digital world, transformation to *RGB* color space is required. Hence, the chapter describes the *RGB* color space and the mathematical transformation process between the two color spaces. Lastly, the chapter presents the types of color vision deficiencies.

2.1 Introduction

The human visual system (HVS) consists of the human eyes, part of the brain, and the pathway connecting them. It is part of the human central nervous system which interprets information from the visible light spectrum to form a visual perception of the surrounding world. The human eye can be thought of as an optical path and is the main recipient of the visible light spectrum. Thus, human visual perception is initiated and strongly influenced by the anatomical structure of the human eyes. Figure 2.1 shows a schematic illustration of the optical structure of the human eye.

Some of the key components of the human eye shown in Figure 2.1 are briefly described below (Fairchild, 2005; Malacara, 2011):

1. The Cornea

   The cornea is the transparent outer surface in front of the eye through which light passes. Its normal ideal shape is nearly spherical.

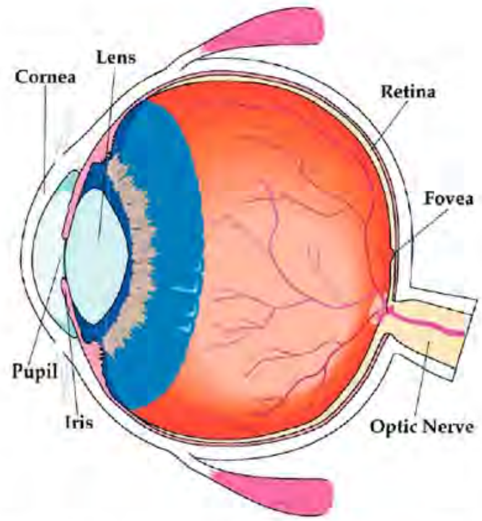

Figure 2.1: Schematic diagram of the human eye (Fairchild, 2005)

2. The Pupil

   This is the circular opening in front of the eye, which is surrounded by the iris. The pupil increases or decreases its diameter to control the amount of light entering the eye. The maximum diameter of the pupil, with low illumination levels, is around 6–8 mm, and the minimum diameter, with high illumination levels, is between 1 and 2 mm. Its average diameter is about 3.5–4 mm.

3. The Iris

   The iris is the sphincter muscle that controls pupil size. The iris is pigmented, giving us our specific eye color.

4. The Lens

   Also called the crystalline lens, the flexible lens varies in index of refraction. The shape and its optical power can be modified by means of the ciliary muscles. The ciliary muscles increase the power (accommodation) to focus on near objects and relaxes its shape to focus on distant objects. The crystalline lens contains a yellow pigment with strong absorption in the ultraviolet region, near a wavelength of 365 nm, with almost perfect transparency 550–650 nm.

5. The Retina

   The optical image formed by the eye is projected onto the retina. The retina is formed by several layers: cell and fiber nerves are in the internal layer while rods and cones are in the last layer. Rods and cones are photoreceptors that serve to transduce the information present in the optical image into chemical and electrical signals. These signals are then transmitted to the later stages of the HVS.

6. The Fovea

   The fovea is the arc on the retina where we have the best spatial and color visions. The fovea contains only cones in a dense random array. Outside the fovea the main light-sensitive elements are the rods, which are responsible for scotopic vision.

7. The Optic Nerve

   The optic nerve is made up of the axons of the ganglion cells, the last level of neural processing in the retina.

As mentioned above, the retina includes several layers of neural cells. Among the cells, there are two photoreceptors: the rods and the cones. The names are derived from their prototypical shapes. There are about 100 million rods and 5 million cones in each human eye (Wandell, 1995). There is only one type of rod receptor with a peak spectral responsivity at approximately 510 nm (Fairchild, 2005). There are three types of cones that are denoted as long (L), medium (M), and short (S) cones. Each cone is sensitive to red, green, and blue stimulation respectively. The three cones enable color vision while the rods are incapable of color vision. Thus, at low luminance levels ($< 0.003\ cd/m^2$), the rods are active; this is referred to as scotopic vision. When the cones are active in high luminance levels ($> 3\ cd/m^2$), vision is referred to as photopic vision. In intermediate luminance levels, both rods and cones are active, and this is referred to as mesopic vision.

The different types of visions and their respective luminance levels are illustrated in Fig 2.2.

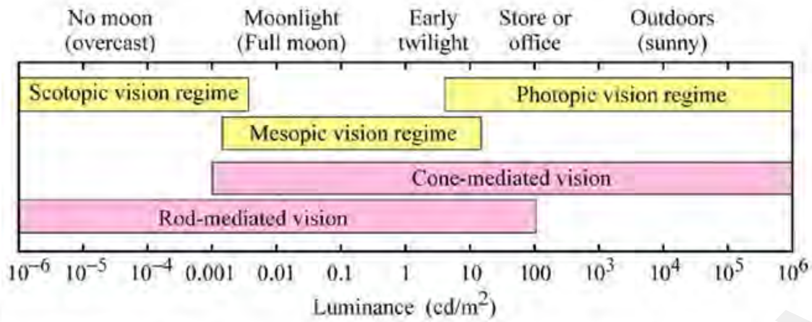

Figure 2.2: Type of visions and its respective luminance levels (Schubert, 1996)

The rest of the chapter is organized as follows. Section 2.2 describes the developments of color matching functions. Section 2.3 and 2.4 describe the XYZ and RGB color spaces respectively and the mathematical transformation process between the two color spaces. The types of color vision deficiencies are presented in Section 2.5. Section 2.6 concludes the chapter.

2.2 Trichromacy and Color Matching Functions

Trichromacy is a condition in which the HVS has three independent channels to convey information about color. These three independent channels are the three types of cones in the human eye. Humans with trichromacy vision are called trichromats. With the establishment of a standardized system of colorimetry, it is necessary to obtain a reliable estimate of the average color matching functions that correspond to the response of the human eye.

Thus, two sets of independent experiments (Wright, 1928; Guild, 1932) were completed to estimate the average color matching functions. These experiments employed the 2° field of view as the viewing condition of standard observers. 2° was chosen as they believed that all the color-sensing cones of the human eyes are located within a 2° arc of the fovea.

The color matching experiments were conducted in a dark room environment where a white screen was divided into two regions: test and reference regions. Red, green, and blue lights of different primary wavelengths were placed in the test region. Meanwhile, in the reference region, a light source of equal energy monochromatic light covering the visible spectrum was placed. This is illustrated in Figure 2.3.

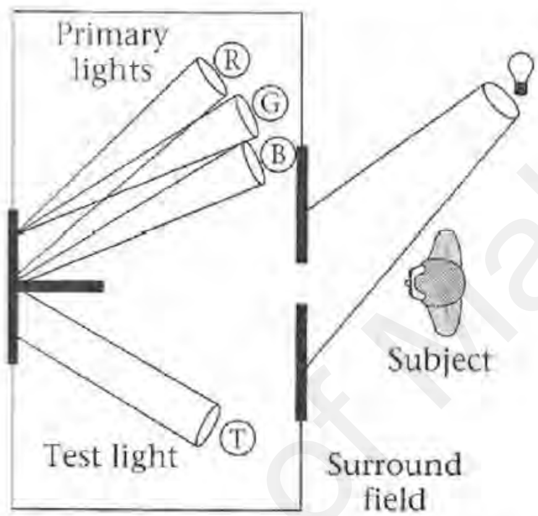

Figure 2.3: Color matching experiment (Wandell, 1995)

During the experiment, the observers had to adjust the red, green, and blue lights until they produced the same light as in the reference region. If the observers could not get a match, the same set of primaries were used in the reference field, and the observers used them to find a match. In this case, negative coefficients of the primaries were obtained. The results from both set of experiments (Wright, 1928; Guild, 1932) were adopted by the International Commission on Illumination (CIE) and are called the color matching functions $\bar{r}(\lambda)$, $\bar{g}(\lambda)$, and $\bar{b}(\lambda)$ for CIE 2° Standard Observer. However, since negative values could not be physically implemented, a set of all positive functions were obtained through a series of transformations and these functions are called the CIE1931 color matching functions $\bar{x}(\lambda)$, $\bar{y}(\lambda)$, and $\bar{z}(\lambda)$.

However, by the 1960s, it was realized that the cones were present in a larger area of the eye than previously believed, and so in 1964, the 10° Standard Observer was developed. The difference between the two viewing angles is that at a viewing distance of 50 cm, a 2° field of view would be a circle with diameter equal to approximately 1.7 cm while a 10° field of view would be a circle with diameter equal to approximately 8.8 cm.

Thus, another color matching functions experiment based the 10° Standard Observer was conducted by Stiles and Burch (Stiles & Burch, 1959, 1955a). From this experiment, CIE adopted another set of color matching functions $\bar{x}_{10}(\lambda)$, $\bar{y}_{10}(\lambda)$, and $\bar{z}_{10}(\lambda)$ for 10° Standard Observer also known as CIE1964 color matching functions. Both sets of color matching functions are illustrated in Figure 2.4.

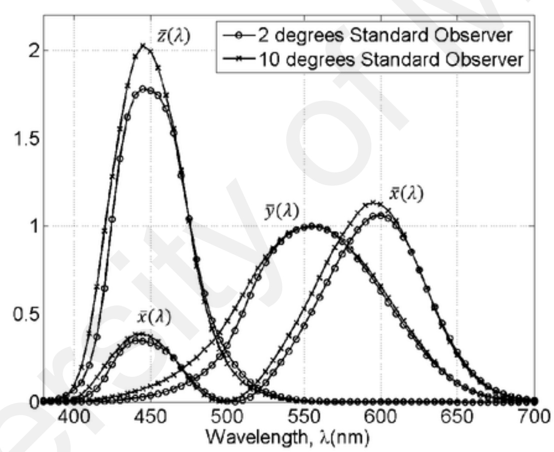

Figure 2.4: CIE color matching functions

Since the color matching functions are intended to correspond to the response of the human eye, both the CIE1931 and CIE1964 color matching functions have profoundly affected the development of modern imaging systems and applications. The CIE1931 color matching functions are used, almost exclusively in color appearance models (Fairchild, 2005).

2.3 *XYZ* Tristimulus Values and Chromaticity Diagram

Utilizing the color matching functions, *XYZ* tristimulus values were formulated. The *XYZ* tristimulus values were formulated so that the *Y* value has a spectral sensitivity that corresponds to the lightness sensitivity of human vision (Poynton, 1995). When the *Y* value is augmented with the *X* and *Z* values, they embed the spectral properties of human color vision (Poynton, 1995).

The *XYZ* tristimulus values for colored stimuli are calculated generally using the equations below (Fairchild, 2005)

$$X = k \int_{\lambda} \Phi(\lambda)\bar{x}(\lambda)d\lambda \tag{2.1}$$

$$Y = k \int_{\lambda} \Phi(\lambda)\bar{y}(\lambda)d\lambda \tag{2.2}$$

$$Z = k \int_{\lambda} \Phi(\lambda)\bar{z}(\lambda)d\lambda \tag{2.3}$$

where $\Phi(\lambda)$ is the spectral power distribution of the stimulus, $\bar{x}(\lambda)$, $\bar{y}(\lambda)$, and $\bar{z}(\lambda)$are the color matching functions, and k is a normalizing constant which is defined as

$$k = \frac{100}{\int_{\lambda} E(\lambda)\bar{y}(\lambda)d\lambda} \tag{2.4}$$

where $E(\lambda)$ is the relative spectral power distribution of the light source or illuminant (Fairchild, 2005).

For reflective objects, the *XYZ* tristimulus values are represented as

$$X = k \int_{\lambda} E(\lambda)\rho(\lambda)\bar{x}(\lambda)d\lambda \tag{2.5}$$

$$Y = k \int_{\lambda} E(\lambda)\rho(\lambda)\bar{y}(\lambda)d\lambda \tag{2.6}$$

$$Z = k \int_{\lambda} E(\lambda)\rho(\lambda)\bar{z}(\lambda)d\lambda \tag{2.7}$$

where $\Phi(\lambda)$ from Eqs. (2.1) to (2.3) is defined as the product of the spectral reflectance factor of the object, $\rho(\lambda)$ and the relative spectral power distribution of the light source or illuminant, $E(\lambda)$ (Fairchild, 2005). The most common illuminant used in colorimetric application is the CIE Illuminant D65 which represents average daylight with a correlated color temperature of 6504 K.

Utilizing the *XYZ* tristimulus values, the color of a stimulus can be represented. However, to provide a convenient two-dimensional representation of colors in term of conceptual understanding and computation, a chromaticity diagram was developed (Fairchild, 2005; Poynton, 1995). To accomplish this, a standardized procedure for normalizing the *XYZ* tristimulus values were performed using the projective transformation shown below.

$$x = \frac{X}{X+Y+Z} \tag{2.8}$$

$$y = \frac{Y}{X+Y+Z} \tag{2.9}$$

$$z = 1 - x - y \tag{2.10}$$

To form the chromaticity diagram, only the x and y values are needed. Thus, the representation of colors is simplified from 3-dimensional to 2-dimensional values. However, the transformation process from *XYZ* tristimulus values to *xyz* representation removes the luminance information represented by the *Y* value (Pascale, 2003). Therefore, it is common practice to report the Y value when dealing with the chromaticity diagram. The xyY chromaticity diagram with Y equal to 100 is illustrated below.

Moreover, using the Y value and the chromaticity coordinates, the other two tristimulus

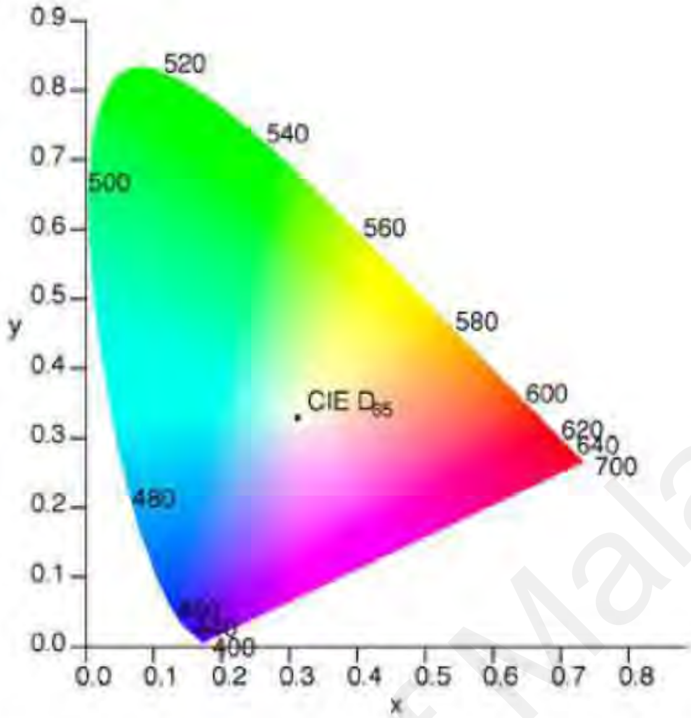

Figure 2.5: Chromaticity diagram with Y equal to 100. (Colantoni, 2004)

values can be obtained using these equations.

$$X = \frac{xY}{y} \tag{2.11}$$

$$Z = \frac{(1 - x - y)Y}{y} \tag{2.12}$$

2.4 *RGB* Color Space and Transformation Matrix

As described in the previous section, the color of stimuli can be represented by the *XYZ* tristimulus values. However, *XYZ* tristimulus values are not realizable in practice since they are not visually uniform (Broadbent, 2017). Therefore, to achieve color reproduction, *XYZ* tristimulus values need to be transformed into a mathematical domain in which physical realizability is not a constraint (Poynton, 1995).

To solve this problem, a mathematical transformation process to *RGB* color space was proposed. The *RGB* color space is an addictive color system in which red, green, and blue lights are added together to reproduce a broad array of colors. This color space is based on human color perception, and the main objective is for the representation and display of images in electronic systems such as televisions and computers. Thus, *RGB* color space is a device dependent color space that will have different coordinates for the same color for various output media (Pascale, 2003).

There are various *RGB* color spaces proposed in the last decades. One of the *RGB* color spaces that is practical and commonly used is the standard Red Green Blue (*sRGB*) color space. *sRGB* was created cooperatively by HP and Microsoft in 1996 for use on monitors, printers and the Internet, and subsequently standardized by the International Electrotechnical Commission (IEC) as IEC 61966-2-1:1999 (Pascale, 2003). Since then, it has often been used as the default color space for images in the digital world.

CIE XYZ color space can be transformed to and from any *RGB* color spaces by a 3×3 transformation matrix. Transformation from *CIE XYZ* into *RGB* can be performed using the transformation matrix as below.

$$\begin{bmatrix} R \\ G \\ B \end{bmatrix} = \begin{bmatrix} \alpha_{11} & \alpha_{12} & \alpha_{13} \\ \alpha_{21} & \alpha_{22} & \alpha_{23} \\ \alpha_{31} & \alpha_{32} & \alpha_{33} \end{bmatrix} \begin{bmatrix} X \\ Y \\ Z \end{bmatrix} \tag{2.13}$$

Meanwhile, the value of *RGB* can be transformed back to *CIE XYZ* using the inverse transformation matrix of Eq. (2.13) as below.

$$\begin{bmatrix} X \\ Y \\ Z \end{bmatrix} = \begin{bmatrix} \alpha_{11} & \alpha_{12} & \alpha_{13} \\ \alpha_{21} & \alpha_{22} & \alpha_{23} \\ \alpha_{31} & \alpha_{32} & \alpha_{33} \end{bmatrix}^{-1} \begin{bmatrix} R \\ G \\ B \end{bmatrix} = \begin{bmatrix} \beta_{11} & \beta_{12} & \beta_{13} \\ \beta_{21} & \beta_{22} & \beta_{23} \\ \beta_{31} & \beta_{32} & \beta_{33} \end{bmatrix} \begin{bmatrix} R \\ G \\ B \end{bmatrix} \tag{2.14}$$

2.5 Color Vision Deficiency

Color vision deficiency arises from the differences in the pigmentation of the cones in the human eye (Wandell, 1995). The vision of trichromats is characterized by three types of cones which collectively allow the reception of long (L), medium (M), and short (S) wavelengths of the visible spectrum. These long (L), medium (M), and short (S) wavelengths exhibits bluish, greenish, and reddish sensitivities respectively (Hunt, 2004; Pascale, 2003). However, people with color vision deficiency are unable to process the three wavelengths and thus, they cannot distinguish certain shades of colors.

Color vision deficiency can be categorized as either acquired or inherited color vision deficiencies (Verriest, 1963; Simunovic, 2016). In acquired color vision deficiency, color perception loss is due to medication, aging, disease or accidents. Meanwhile, in inherited color vision deficiency, color loss occurs due to changes in the cones in the human eye. Inherited color vision deficiency can be further classified into three types: dichromacy, monochromacy, and anamolous trichromacy.

Dichromacy occurs when one of the cones is absent or not functioning, and colors are reduced to two dimensions. The rarest type of inherited color vision deficiency is monochromacy. It occurs when two or three cones are absent or not functioning. Thus, people with monochromacy (monochromats) can only see shades of gray ranging from black to white. Anamolous trichromacy occurs in people with altered cones. Although all three cones exist, one of the cones is slightly out of alignment. This misalignment affects the way they perceive colors depending on which cone is misaligned.

2.6 Summary

In the chapter, a theoretical overview of the human visual system and color perception have been given. Research developments in color matching functions are also described in this chapter. The formulation and relationship between *XYZ* and *RGB* color spaces are described as well. Both color spaces are utilized in the formulation of the proposed methods to improve the color perception of people with color vision deficiency in this thesis.

CHAPTER 3: COLOR PERCEPTION OF THE ELDERLY

This chapter provides an overview of the color perception of the elderly. Fundamental theorems for color perception of the elderly are also described. The earlier works considered a non-uniform yellowing pigmentation model to mimic the color perception of the elderly. Recently, two clinical studies have shown that uniform yellowing pigmentation occurs on the human crystalline lens. Thus, a mathematical model of the uniform yellowing pigmentation is proposed in this chapter.

3.1 Introduction

Color images used by highly visual applications and services on websites and smartphone applications play an important role in distributing information to users of various ages (Soundararajan & Bovik, 2013; Yamazaki & Eto, 2015). As humans age, the functional ability of the eyes wane (Lerman, 1983; Salvi, Akhtar, & Currie, 2006; Weale, 1961a, 1961b; Werner et al., 1990) especially the ability to discriminate colors (Ball & Pollack, 1989; Fiorentini, Porciatti, Morrone, & Burr, 1996; Roy, Podgor, Collier, & Gunkel, 1991; Ruddock, 1965a, 1965b; Shinomori, 2005; Verriest, 1963; Werner et al., 1990). Color perception ability is the ability to recognize the set of signals that are produced when the three cones that are sensitive in the red, green, and blue spectral range in the human eye react with the incoming wavelength light (Hunt, 2004). The red, green, and blue spectral range are generally represented by the long (L), medium (M), and short (S) wavelengths respectively.

Throughout human life, the lens thickness continues to grow, and the accumulation of yellow pigmentation occurs (Artigas et al., 2012; Norren & Vos, 1974; Pokorny et al., 1986; Romano et al., 2011; Ruddock, 1965a; Said & Weale, 1959; Weale, 1961a). Norren and Vos (1974) state that the yellowing pigmentation process occurs after the age of 30. The yellow pigmentation contributes to a gradual reduction in the transparency of the human crystalline lens (Alio et al., 2005). Due to the yellowing pigmentation, the lens absorbs more short wavelength which reduces the amount of blue light entering the eyes (Fiorentini et al., 1996; K. Ishihara et al., 2001; Ruddock, 1965a; Salvi et al., 2006; Shinomori, 2005; Tanaka et al., 2011; Verriest, 1963; Xu et al., 1997). In addition, light scattering in the human lens of the elderly is much higher compared to the young (Boettner & Wolter, 1962). To describe the effect of the yellowing pigmentation to the human lens-density spectrum, several models were introduced: the two-factor model (Pokorny et al., 1986), the exponential model (Weale, 1988), and the linear model (Savage et al., 1993). A comparative experiment between the three models shows that the two-factor model produces better results (Xu et al., 1997).

In addition to yellowing, the size of the human pupil also reduces with age (Applegate et al., 2007; Birren et al., 1950; Bitsios et al., 1996; Kadlecova et al., 1958; Ortiz et al., 2013; Said & Sawires, 1972; Winn et al., 1994). Birren et al. (1950) investigated pupil size measurements and formulated a parabola relation between the pupil diameter and human age. Measurements performed by Said and Sawires show that pupil size reduces linearly with age (Said & Sawires, 1972). The concept of a linear relation between pupil size and human age is further strengthen by Winn et al. (1994) when they formulated mathematical linear relations between pupil size and human age. The reduced pupil size causes the effective light reaching the retina to reduce proportionally (Sloan, 1939; Weale, 1961a, 1961b; Werner et al., 1990). Moreover, the pupil's reflexive response also reduces with age (Bitsios et al., 1996) which in turn increases the reaction time of the elderly (T. Suzuki et al., 2012, 2005).

In Malaysia, the number of people aged 65 and above is expected to increase from 4.5% in 2009 to 7% by 2020 (Chua et al., 2015). The increase in the number of elderly people is also reflected globally (Hegde & Bishop, 2018). One of the areas of concern that needs to be addressed in order to eliminate barriers in terms of physical capabilities for the elderly is their color perception (Hassan et al., 2015; Hegde & Bishop, 2018). To understand the difficulties faced by the elderly due to the yellowing of the human crystalline lens, computerized simulation methods have been proposed in order to simulate the color perception of the elderly. Using the two-factor model (Pokorny et al., 1986), Okajima and Takase (2001) conducted computerized simulations using Munsell color chips to investigate the effect of yellowing on the color perception of the elderly. Meanwhile, (Tanaka et al., 2011) proposed a non-uniform yellowing pigmentation method to simulate the color perception of the elderly by implementing the two-factor model and taking into consideration the effect of retinal illuminance (Winn et al., 1994).

In the non-uniform yellowing pigmentation method, at a particular age, the different colors in the image are multiplied by the different levels of yellowing pigmentation. On the other hand, in the uniform yellowing pigmentation method, the colors in the image are multiplied by the same level of yellowing pigmentation. Figure 3.1 shows two examples of the yellowing pigmentation methods for people aged 80 years old and the simulated images as perceived by an 80-year-old.

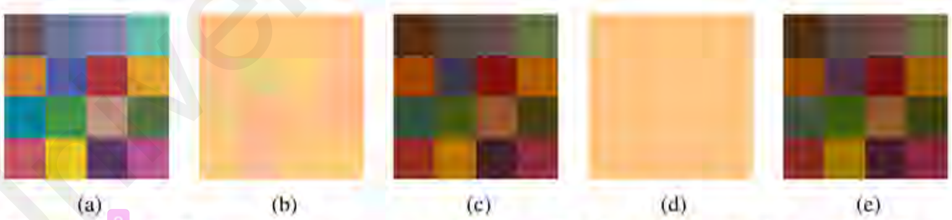

Figure 3.1: Difference between non-uniform yellowing pigmentation and uniform yellowing pigmentation methods (a) Original image formed using color patches from Macbeth ColorCheckers; (b) Non-uniform yellowing pigmentation for people aged 80 years old from Tanaka's method; (c) Simulated image as perceived by an 80-year-old using Tanaka's method; (d) Proposed uniform yellowing pigmentation for people aged 80 years old; (e) Simulated image as perceived by an 80-year-old using the proposed method

The idea of uniform yellowing pigmentation on human crystalline lens was first initiated and implemented in Weale (1961a). Using this idea, Weale calculated the effective pathlength of the human crystalline lens. Said and Weale (1959) found that the white point in the chromaticity diagram moves nearer to the spectrum locus as humans age. It was stated in Werner and Steele (1988) that all three types of cones lose overall sensitivity at a similar rate; this is further supported in experiments performed by Nguyen, Overbury, and Faubert (2003).

Several experiments using artificial uniform yellowing filters that mimic the color vision of the elderly have been conducted (K. Ishihara, Ishihara, Nagamachi, & Osaki, 1997; K. Ishihara et al., 2001; Schneck et al., 1993; Yoshida & Sakuraba, 1996). Schneck et al. designed a three-layer filter that consists of a neutral density filter, a spectral filter and a scratched plastic sheet (Schneck et al., 1993). This 'sandwich' filter reduces the blue-yellow chromatic perception and mimics the color vision loss of the elderly. Yoshida et al. (Yoshida & Sakuraba, 1996) and Ishihara et al. (K. Ishihara et al., 1997, 2001), on the other hand, designed a yellowing filter using yellow films to study the effect of yellowing on the color perception of the elderly. When young observers wore the yellowing filter, they had difficulty differentiating colors due to the confusion that occurred when looking at multiple colored objects. Recently, clinical studies using enucleated human eyes performed by Artigas et al. (Artigas et al., 2012) and Romano et al. (Romano et al., 2011) showed that as human age increases, the chromaticity of the human crystalline lens shifts towards the yellow region of the chromaticity diagram.

Results from recent clinical studies (Artigas et al., 2012; Romano et al., 2011) have shown that uniform yellowing pigmentation occurs on the human crystalline lens. However, the uniform yellowing pigmentation is not represented mathematically. Hence, this has become the main motivation for developing a mathematical model of the uniform yellowing pigmentation and assessing the color perception experienced by the elderly. By understanding the process of color perception of the elderly, website designers and smartphone application developers can factor this consideration when choosing suitable color schemes to represent their information and avoid misinterpretation by the elderly. Moreover, it is also important for designers and architects to consider a good visual color presentation in order to enable the elderly to experience the built environment safely and with confidence. The chapter is therefore organized as follows. Section 3.2 describes the fundamental theorems used in the color perception of the elderly. Section 3.3 shows the proposed uniform yellowing pigmentation method. The performance of the proposed method and comparisons with the non-uniform yellowing pigmentation are shown and discussed in Section 3.4. Section 3.5 concludes this chapter.

3.2 Fundamental Theorems in Color Perception of the Elderly

This section describes the two fundamental theorems that are used in the study of the color perception of the elderly. The two fundamental theorems are the two-factor model and the retinal illuminance model.

3.2.1 Two-factor model

One of the fundamental models used in elderly color perception methods is the two-factor model proposed by Pokorny et al. (1986). This model describes the optical density of humans lens as a function of wavelength, λ and age, A and expresses it using the age-dependent TL_1 and age-independent components, TL_2 as below:

$$L(\lambda, A)= \begin{cases} [1.00 + 0.02(A - 32)]TL_1 + TL_2 & \text{for } 20 \leq A \leq 60 \\ [1.56 + 0.0667(A - 60)]TL_1 + TL_2 & \text{for } A > 60 \end{cases} \quad (3.1)$$

where TL_1 is the portion changed by aging after age 20 and TL_2 is the portion independent of age.

The optical density $L(\lambda, A)$ can also be expressed in terms of the spectral intensities as below:

$$L(\lambda, A) = log_{10}\left(\frac{I_i(\lambda)}{I_t(\lambda)}\right) \tag{3.2}$$

where $I_i(\lambda)$ and $I_t(\lambda)$ are the intensity of incident light and transmitted light respectively. Thus, the spectral transmittance of the human lens can be described as

$$\tau(\lambda, A) = \frac{I_i(\lambda)}{I_t(\lambda)} = 10^{-L(\lambda,A)} \tag{3.3}$$

Spectral transmittance of the human lens for several ages are illustrated in Figure 3.2.

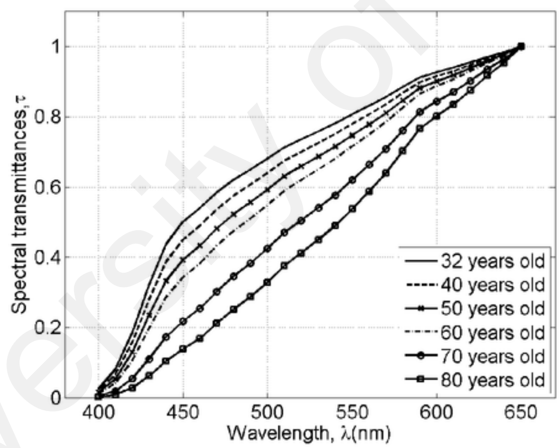

Figure 3.2: Spectral transmittances of human lens for several ages

In order to simulate the lens transmittance of an elderly person of aged A as seen by a young observer of age 32, the spectral transmission factor of the human lens can be derived from Eq. (3.3) as below:

$$F(\lambda, A, 32) = \frac{\tau(\lambda, A)}{\tau(\lambda, 32)} = \frac{10^{-L(\lambda,A)}}{10^{-L(\lambda,32)}} \tag{3.4}$$

Age 32 years old is chosen as a standard age for young people because it was the mean age used in the color matching experiment by Stiles and Burch (Stiles & Burch, 1955b).

3.2.2 Retinal Illuminance Model

Another model that is considered in elderly color perception methods is the retinal illuminance model. The model is based on the relation between pupil size and human age proposed in Winn et al. (1994). According to Winn et al., pupil size decreases linearly with age at all illuminance levels as shown in Figure 3.3. Thus, pupil size can be expressed in terms of age, A as below:

$$d(A) = -0.011A + 1.557 \tag{3.5}$$

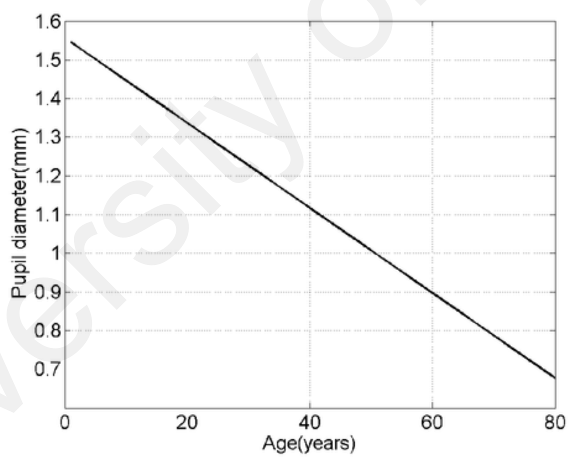

Figure 3.3: Pupil size decreases by aging

As in Tanaka et al. (2011), the rate of retinal illuminance of the elderly aged A as compared to the young observer aged 32 years old can be computed as below:

$$S(A, 32) = \frac{d(A)}{d(32)} = \frac{-0.011A + 1.557}{1.205} \tag{3.6}$$

3.3 Proposed Method - Uniform Yellowing Pigmentation Method

This section proposes a new method that utilizes the uniform yellowing pigmentation of the human crystalline lens to simulate the color perception of the elderly. The proposed method implements the same basic mathematical framework related to elderly color perception as applied in Tanaka et al. (2011). In Tanaka's method, 9 components called effective components were formulated to compute the non-uniform yellowing pigmentation (Hassan et al., 2015; Tanaka et al., 2011). Using this approach, at a particular age, the *RGB* components of the original image lose their overall sensitivity at a different rate. Thus, the non-uniform yellowing pigmentation formulated varies depending on the colors in the original image as shown in Figure 3.1(b).

Meanwhile, in the proposed method, the uniform yellowing pigmentation is formed using 3 components called the effective tristimulus ratios. In this approach, at a particular age, the *RGB* components in the original image lose their overall sensitivity at a similar rate which is in agreement with the results found in Nguyen et al. (2003) and Werner and Steele (1988). Figure 3.1(d) shows the uniform yellowing pigmentation in a person aged 80 years old. The simulated images as perceived by an elderly person of 80 years old using both methods are also illustrated in Figure 3.1.

In the proposed method, the original image is converted to *CIE XYZ* color space. *CIE XYZ* color space encompasses all the color sensations that a human perceives and is formulated based on the *RGB* version of the human eyes (Fairchild, 2005). Meanwhile, the measured transmittance functions and the spectral transmission factor (Pokorny et al., 1986) are utilized to compute the total tristimulus values at a particular age. Based on these values, the effective tristimulus ratios are computed. The uniform yellowing pigmentation is simulated using the effective tristimulus ratios. To simulate the color perception of the elderly, the *XYZ* tristimulus values of the original image are multiplied with the effective tristimulus ratios of the uniform yellowing pigmentation and the rate of retinal illuminance (Tanaka et al., 2011; Winn et al., 1994). The overall process of the proposed method is summarized in Figure 3.4.

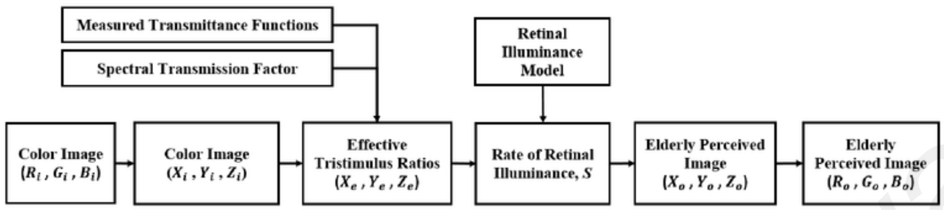

Figure 3.4: Overall process flow of the proposed method

Generally, the tristimulus values of reflected light can be represented as

$$X = k \sum_{\lambda=400}^{650} E(\lambda)\bar{x}(\lambda)\rho(\lambda) \tag{3.7}$$

$$Y = k \sum_{\lambda=400}^{650} E(\lambda)\bar{y}(\lambda)\rho(\lambda) \tag{3.8}$$

$$Z = k \sum_{\lambda=400}^{650} E(\lambda)\bar{z}(\lambda)\rho(\lambda) \tag{3.9}$$

where $E(\lambda)$ is the spectral energy for wavelength, $\bar{x}(\lambda)$, $\bar{y}(\lambda)$ and $\bar{z}(\lambda)$ are the standard CIE color matching functions, $\rho(\lambda)$ is the spectral reflectance, k is the normalization factor and the wavelength interval of 10nm.

However, since the image is presented on the Liquid Crystal Display (LCD), and the backlight of the LCD is observed through red, green, and blue filters, the proposed method utilizes the transmittance functions for red f_r, green f_g, and blue f_b filters of the LCD. The transmittance functions of the LCD are measured using a spectral luminance radiometer in a darkroom environment.

In the proposed method, the spectral reflectance $\rho(\lambda)$ in Eq. (3.7) to Eq. (3.9) are replaced with the respective transmittance functions and the spectral transmission factor

$F(\lambda, A, 32)$ as given in Eq. (3.4) (Pokorny et al., 1986).

Thus, the tristimulus values through the red, green, and blue filters for any given age A can be expressed as

$$X_m(A) = k \sum_{\lambda=400}^{650} E(\lambda)\bar{x}(\lambda) f_m(\lambda) F(\lambda, A, 32) \tag{3.10}$$

$$Y_m(A) = k \sum_{\lambda=400}^{650} E(\lambda)\bar{y}(\lambda) f_m(\lambda) F(\lambda, A, 32) \tag{3.11}$$

$$Z_m(A) = k \sum_{\lambda=400}^{650} E(\lambda)\bar{z}(\lambda) f_m(\lambda) F(\lambda, A, 32) \tag{3.12}$$

where $f_m(\lambda)$ is the transmittance functions of the LCD and $m = r, g, b$. Then, the total tristimulus values X, Y, Z for any given age, A can be computed using the summation of tristimulus value of each light component represented in Eq. (3.10) to (3.12).

$$X(A) = X_r(A) + X_g(A) + X_b(A) \tag{3.13}$$

$$Y(A) = Y_r(A) + Y_g(A) + Y_b(A) \tag{3.14}$$

$$Z(A) = Z_r(A) + Z_g(A) + Z_b(A) \tag{3.15}$$

The effective tristimulus ratios X_e, Y_e, and Z_e for the elderly aged A as compared to the young observer aged 32 years old can be expressed as

$$X_e = \frac{X(A)}{X(32)} \tag{3.16}$$

$$Y_e = \frac{Y(A)}{Y(32)} \tag{3.17}$$

$$Z_e = \frac{Z(A)}{Z(32)} \tag{3.18}$$

Finally, the tristimulus values of the elderly aged A are computed as

$$X_o(A) = X_e S X_i \tag{3.19}$$

$$Y_o(A) = Y_e S Y_i \tag{3.20}$$

$$Z_o(A) = Z_e S Z_i \tag{3.21}$$

where S is the rate of retinal illuminance as given in Eq. (3.6), X_e, Y_e, Z_e are the effective tristimulus ratios, and X_i, Y_i, Z_i are the tristimulus values of the color image converted using the *sRGB* to *CIE XYZ* transformation matrix as shown below.

$$\begin{bmatrix} X_i \\ Y_i \\ Z_i \end{bmatrix} = \begin{bmatrix} 0.4124 & 0.3576 & 0.1805 \\ 0.2126 & 0.7152 & 0.0722 \\ 0.0193 & 0.1192 & 0.9505 \end{bmatrix} \begin{bmatrix} R_i \\ G_i \\ B_i \end{bmatrix} \tag{3.22}$$

To simulate the image perceived by the elderly, $X_o(A)$, $Y_o(A)$, and $Z_o(A)$ are transformed to *RGB* values using the inverse of Eq. (3.22).

3.4 Experimental Studies

A number of experimental studies were performed to evaluate the proposed method. The transmittance functions of the LCD were measured to model the uniform yellowing pigmentation and then verified with the results from previous works. Using several type of images, the transition of the color perception of the elderly from different age groups were also observed. Lastly, an artificial SPP3 color perception test was conducted to young subjects and comparisons were made with the results from the clinical color perception test provided by eye doctors (Tanaka et al., 2011).

Prior to the experimental studies, the LCD was calibrated using X-Rite i1Display 2 based on sRGB color space and white point of D65. The gamma correction parameter, γ was set to 2.2. The calibration process ensures that the preciseness of color reproduction on the LCD is within a very small range of error (Tanaka et al., 2011).

3.4.1 Simulation of Uniform Yellowing Pigmentation

In this experiment, firstly, the transmittance functions of the LCD DELL S2440L were measured using a Konica Minolta CS-2000 spectral luminance radiometer in a darkroom environment. It should be noted here, the transmittance functions may vary slightly depending on the LCDs (Gibson & Fairchild, 2000). The normalized transmittance functions of the LCD are shown in Figure 3.5.

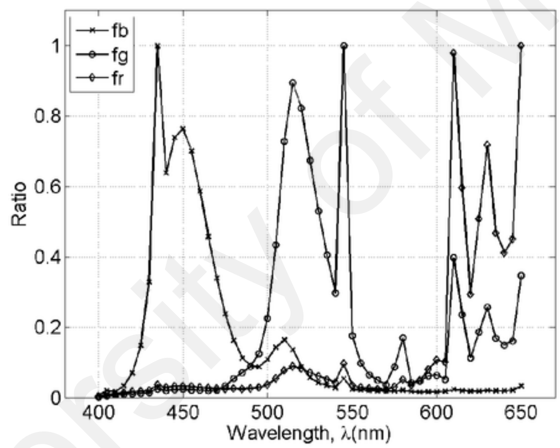

Figure 3.5: Normalized transmittance functions of LCD used in the experiment

Utilizing the values of the transmittance functions, the D65 spectral energy distribution, and the *CIE1931* color matching functions, the effective tristimulus ratios were computed. Then, the effective tristimulus ratios were converted into the effective *RGB* values. The effective *RGB* values computed represent the simulated image of the proposed uniform yellowing pigmentation. The simulated images of the uniform yellowing pigmentation are illustrated in Figure 3.6. It can be observed that as age increases, the simulated uniform yellowing pigmentation becomes yellower, which is consistent with the results found in Artigas et al. (2012) and Romano et al. (2011).

Figure 3.6: The simulated uniform yellowing pigmentation for age (a) 40 years old; (b) 45 years old; (c) 50 years old; (d) 55 years old; (e) 60 years old; (f) 65 years old; (g) 70 years old; (h) 75 years old; (i) 80 years old

Two tests were then conducted in order to verify that the proposed method has similar characteristics with the yellowing of the human crystalline lens found in previous works. As mentioned in Artigas et al. (2012), Pokorny et al. (1986), and Said and Weale (1959), the amount of blue light penetrating into human eyes decreases significantly after the age of 60. Thus, to compare their results with the proposed method, the effective *RGB* values as shown in Figure 3.7 were plotted. It can be seen that the effective value for blue, B_e

decreases significantly after the age of 60, which is in agreement with the results in Artigas et al. (2012), Pokorny et al. (1986), and Said and Weale (1959).

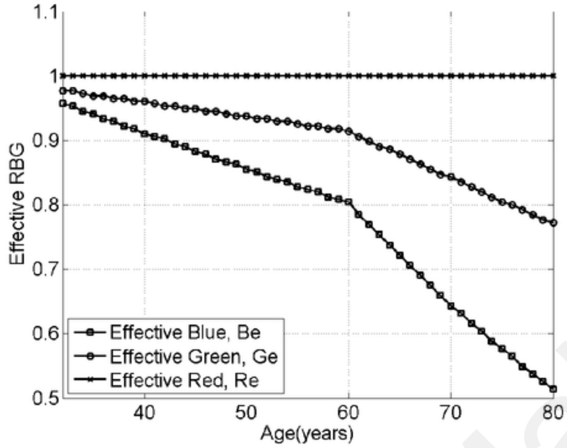

Figure 3.7: Age-related change of the effective *RGB* values for the simulated uniform yellowing pigmentation

The D65 white point was simulated using the proposed method, and the chromaticity points were plotted together with the results from the clinical studies (Artigas et al., 2012; Romano et al., 2011) as shown in Figure 3.8. The results in Artigas et al. (2012) were

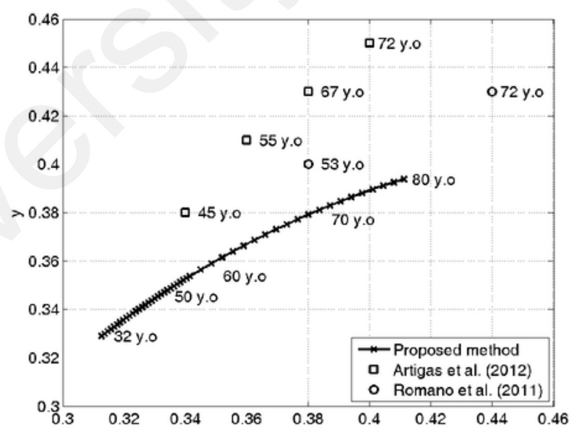

Figure 3.8: Comparison of the chromaticity points of the D65 white point between the proposed method and the results from the clinical studies

obtained from human eyes used for corneal transplants while the results in Romano et al.

(2011) were obtained from freshly enucleated human eyes.

It can be observed that as age increases, the chromaticity of the simulated D65 white point shifts to the yellow region of the chromaticity diagram. This is consistent with the results obtained in Artigas et al. (2012) and Romano et al. (2011). Based on the results of both tests, it can be deduced that the uniform yellowing pigmentation simulated by the proposed method has similar characteristics with the yellowing of the human crystalline lens.

3.4.2 Simulation of the Color Perception of the Elderly

To observe the transition of the color perception of the elderly from different age groups, three Macbeth ColorCheckers color patches (blue sky, green, and moderate red), three synthesized images created using Munsell colors, and three real images from LIVE database (Sheikh, Sabir, & Bovik, 2006) as perceived by the elderly aged 60, 70 and 80 years old were simulated using the proposed method. The original and simulated images are shown in Tables 3.1 to 3.3.

As shown in Table 3.1, as age increases, the blue sky color patch loses its bluish element. This is because the uniform yellowing pigmentation absorbs more blue stimulation than the red and green stimulations of the image. This is similar to the results in Norren and Vos (1974), Pokorny et al. (1986), Ruddock (1965b), and Said and Weale (1959). Their work shows that as human age increases, the amount of blue light that arrives into human eyes is less than green and red light. Moreover, all three color patches become darker as age increases. Other than the uniform yellowing pigmentation, this is also due to the retinal illuminance model in which the reduced pupil size causes the effective light reaching the retina to reduce proportionally (Weale, 1961a, 1961b; Werner et al., 1990).

It can also be observed from Table 3.2 that as age increases, the purple and light blue color blocks from the first synthesized image look like brown and beige respectively. In

Table 3.1: MacBeth ColorCheckers color patches and its simulated images as perceived by 60, 70, and 80-year old elderly using the proposed method

Original image	60 years old	70 years old	80 years old

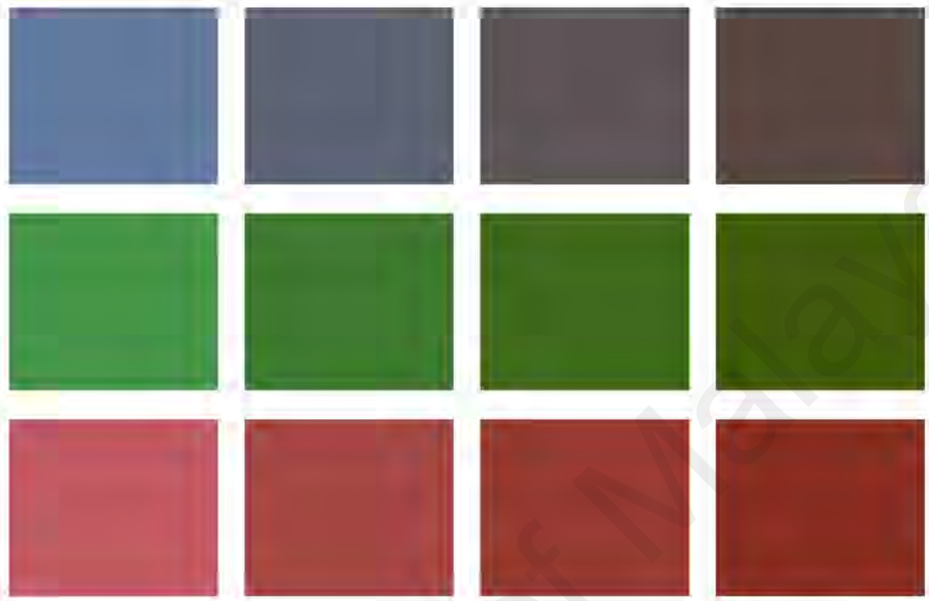

addition, yellow and cream color blocks in the second synthesized image look almost the same in the simulated image of the 80-year-old. Furthermore, the two blue color blocks in the second and third synthesized images lose their blueness and look more greyish as age increases. Thus, these may create confusion in the elderly. As reported in K. Ishihara et al. (2001), elderly may have difficulty finding goods in stores because of the confusion that occurs when looking at the color displays. Moreover, these confusions increase their response time and reduce their response speed in making decisions (T. Suzuki et al., 2005; T. Suzuki, Qiang, Sakuragawa, Tamura, & Okajima, 2006).

For real images, change in color perception can be observed in the first real image as the blue cap looks darker in the simulated image of the 80-year-old. This is illustrated in Table 3.3. The same applies to the red parrot in the second real image. Originally, the wing of the red parrot consists of blue and green colors. However, in the simulated image

Table 3.2: Synthesized images and its simulated images as perceived by 60, 70, and 80-year old elderly using the proposed method

Original image	60 years old	70 years old	80 years old
			
	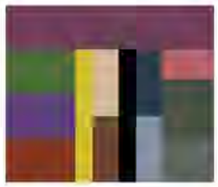		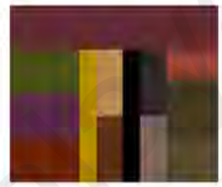
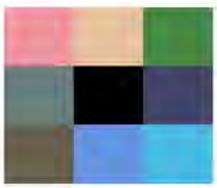	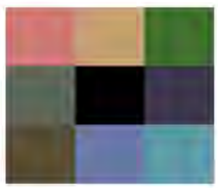	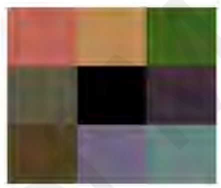	

of the 80-year-old, the wing loses its blueness. In addition, as age increases, the images become yellowish and darker than the original images. These results may cause the elderly to experience color perception loss, and they may face difficulties in differentiating colors in their daily activities, which is also stated in K. Ishihara et al. (2001), Schneck et al. (1993), T. Suzuki et al. (2005), T. Suzuki et al. (2006), and Yoshida and Sakuraba (1996).

Based on these results, the transition of the color perception of the elderly can be simulated using the proposed method. Furthermore, the images produced from the proposed methods have similar effects as shown in previous works (Norren & Vos, 1974; Pokorny et al., 1986; Ruddock, 1965b; Said & Weale, 1959; Weale, 1961a, 1961b; Werner et al., 1990). To further evaluate the effectiveness of the proposed method, further evaluation tests were conducted in the next experiment.

Table 3.3: Real images and its simulated images as perceived by 60, 70, and 80-year old elderly using the proposed method

Original image	60 years old	70 years old	80 years old
			
			
			

3.4.3 Artificial SPP3 Color Perception Tests

The Standard Pseudoisochromatic Plates (SPP) color perception test is an effective screening test to assess the color perception of humans (Haskett & Hovis, 1987). Thus, in order to observe the similarity between the simulated elderly color perception with the actual elderly color perception, an artificial SPP3 color perception test was conducted. The SPP3 color perception test is a combination of the congenital (SPP1) and acquired (SPP2) color blindness test (Haskett & Hovis, 1987). Ten test images from SPP3 color perception test were utilized in the artificial SPP3 color perception test. These images were simulated as perceived by the 80-year old using the proposed method and Tanaka's method (Tanaka et al., 2011). The SPP3 test images and their simulated images are shown in Figures 3.9 to 3.11.

The subjects who attended this experiment were 22 undergraduate students between the

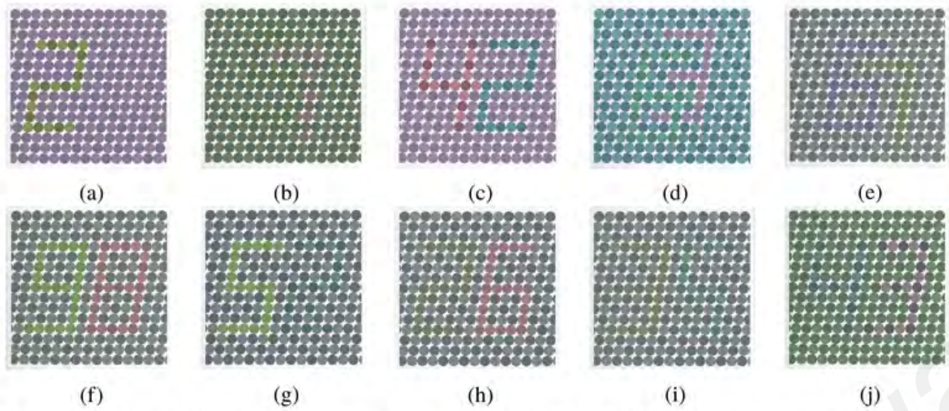

Figure 3.9: The Standard Pseudoisochromatic Plates 3 (SPP3) test images (a) no.1(2); (b) no.2(57); (c) no.3(42); (d) no.4(63); (e) no.5(67); (f) no.6(98); (g) no.7(52); (h) no.8(26); (i) no.9(35); (j) no.10(43)

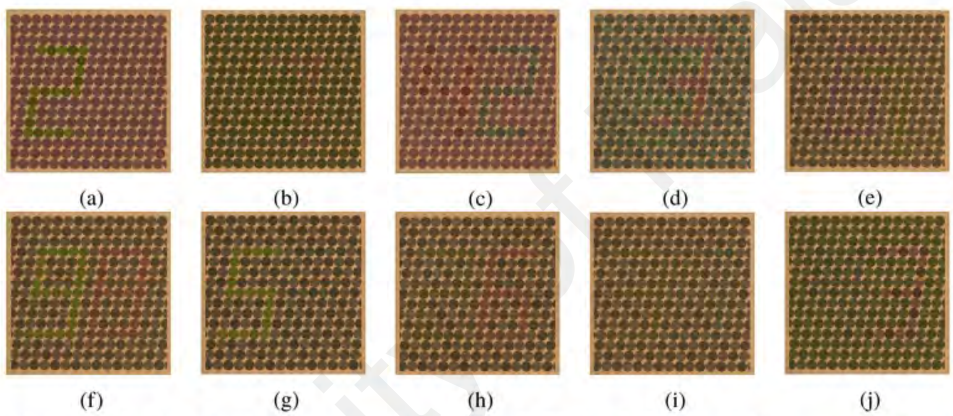

Figure 3.10: The Standard Pseudoisochromatic Plates 3 (SPP3) test images simulated as perceived by the 80-year old using the proposed method (a) no.1(2); (b) no.2(57); (c) no.3(42); (d) no.4(63); (e) no.5(67); (f) no.6(98); (g) no.7(52); (h) no.8(26); (i) no.9(35); (j) no.10(43)

age of 18 and 20 years with a mean age of 18.77. Experiments using young subjects to study the color perception of the elderly have been conducted in previous works (K. Ishihara et al., 2001; Okajima & Takase, 2001; T. Suzuki et al., 2006; Tanaka et al., 2011). As adopted in Tanaka et al. (2011), the color constancy hypothesis was not taken into consideration during the artificial color perception test. By adopting this, the yellowing pigmentation from Tanaka's method and the proposed method change the luminosity and the chromaticity of the color perception of the elderly.

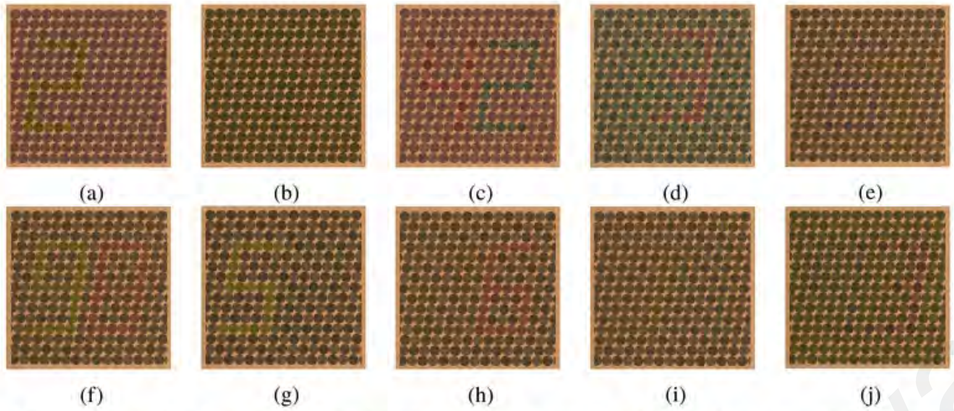

Figure 3.11: The Standard Pseudoisochromatic Plates 3 (SPP3) test images simulated as perceived by the 80-year old using Tanaka's method (a) no.1(2); (b) no.2(57); (c) no.3(42); (d) no.4(63); (e) no.5(67); (f) no.6(98); (g) no.7(52); (h) no.8(26); (i) no.9(35); (j) no.10(43)

The artificial color perception test was conducted in a darkroom environment. The distance between the subject and the LCD was approximately 60 cm. Each test image was displayed for 2 seconds and the interval between test images was 2 seconds. The conditions of the artificial color perception test are summarized in Table 3.4.

Table 3.4: Conditions of artificial color perception test

Item	Condition
Distance between LCD and subject	60 cm
Display time for each test image	2 seconds
Interval time between test images	2 seconds
Location of test image on LCD	Center
Size of test image	512×512 pixel (0.27 mm/pixel)
Background surrounding test image	Gray
Environmental condition	Darkroom

During the artificial color perception test, the test images were shown one at a time to each subject. Moreover, for each method, the test was conducted over two rounds. In the first round, the 10 images shown had the same numbers and background of SPP3 test images. In the second round, the 10 images shown had different numbers, and were presented in a different order from the previous round. This was to avoid habituation by the subjects.

Subjects had to recognize the numbers shown on the images whose colors had been simulated as perceived by the 80-year old. Each time a subject failed to recognize a number shown on a test image, it was considered as one error for that particular number. The average error ratio obtained from the experiment for both methods are shown in Figure 3.12 and compared with the results from the clinical color perception test obtained from eye doctors (Tanaka et al., 2011).

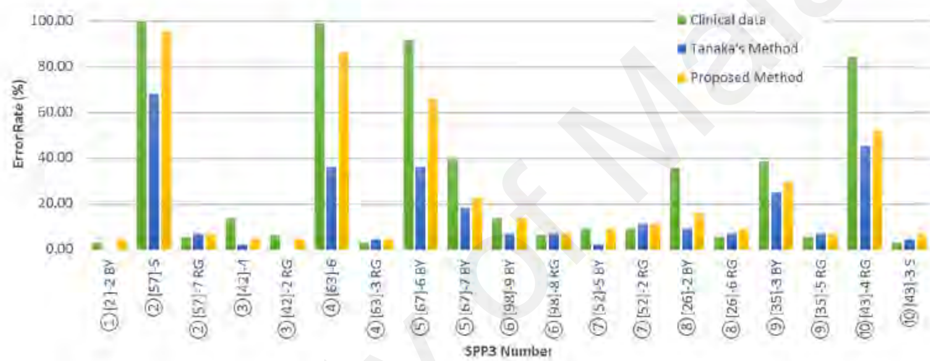

Figure 3.12: Average error ratio of the SPP3 color perception test

From Figure 3.12, it can be observed that the results from the proposed method are closer to the results of the clinical color perception test than the results from the Tanaka's method (Tanaka et al., 2011). This shows that the accuracy of mimicking the color perception of the elderly is fairly improved using the proposed method.

Based on Figure 3.12, results from the clinical data show that the elderly had difficulty recognizing the first number on test image no.2(57). The same thing happened to the subjects of the SPP3 artificial color perception test. Subjects had difficulty recognizing number 5 on the simulated images since the color looks similar to the background as shown in Figures 3.10 and 3.11. The error rates for the first number in the test images no.4(63), no.5(67), and no.10(43) were also high due to this reason.

On the other hand, for the test image no.6(98), the error rate was low because the colors of the numbers on the simulated images are slightly different from the background and could still be recognized by the subjects. As shown in Figures 3.10 and 3.11, both numbers 9 and 8 can still be differentiated from the background. Due to the same reason, the error rates for the test images no.1(2), no.3(42), no.6(98), and no.7(52) were also low.

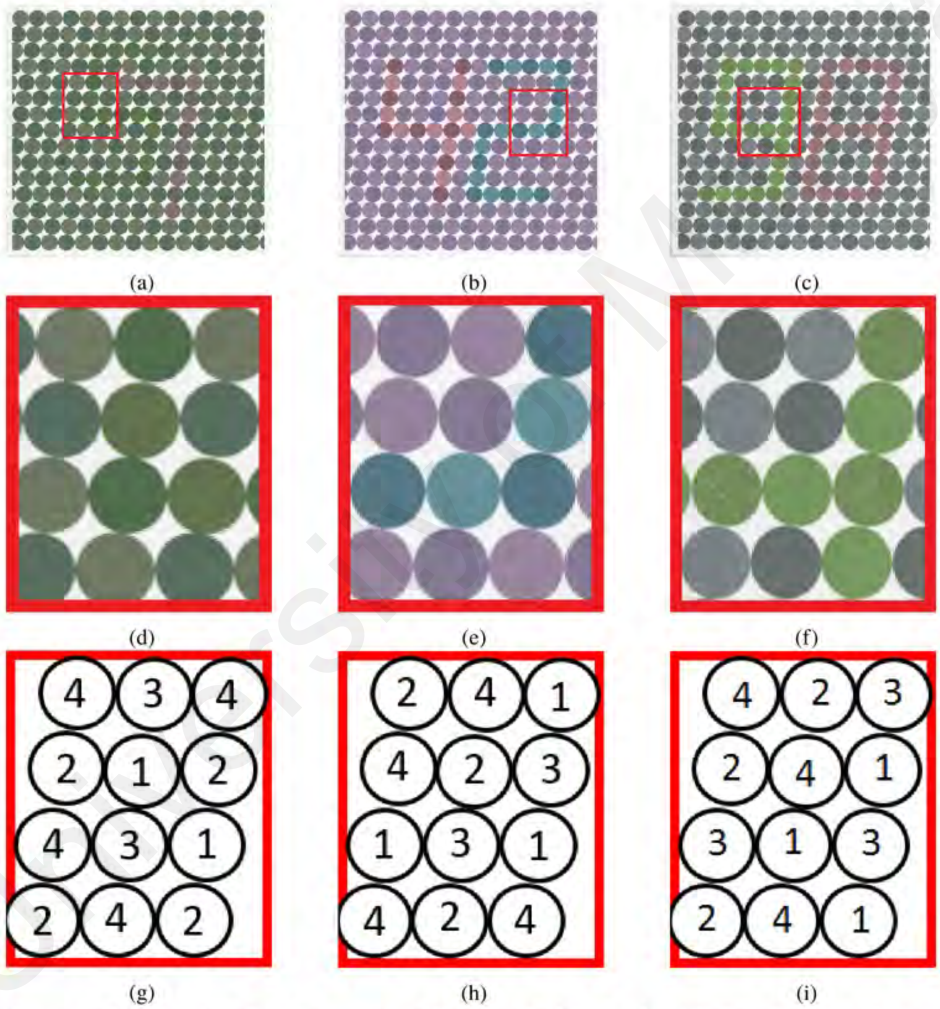

Figure 3.13: (a)-(c) Test images no.2(57), no.3(42), and no.6(98) showing the rectangular section; (d)-(f) Rectangular sections of the respective test images; (g)-(i) Rectangular sections of the respective test images with numbering

A further experiment was conducted to investigate the difference between the simulated images from the proposed method and Tanaka's method (Tanaka et al., 2011). As shown in Figure 3.13, a rectangular section from number 5 on the test image no.2(57), number 2 on the test image no.3(42), and number 9 on the test image no.6(98) were cut and the circles were numbered according to their color. Circles 1 and 3 represent the colors of the number on the test images while circles 2 and 4 represent the background colors.

The rectangular sections were simulated as perceived by the 80-year-old using both methods and the CIEDE2000 color difference, ΔE_{00} (Sharma, Wu, & Dalal, 2005) of the adjacent circles were computed. Tables 3.5 to 3.7 show the color difference values between the adjacent circles for both simulated images.

Table 3.5: Color difference ΔE_{00} of the adjacent circles of the rectangular section from test image no.2(57)

Circles	Proposed method	Tanaka's method
1 and 2	**3.8443**	5.2762
1 and 3	**2.2282**	3.8877
1 and 4	5.1708	**4.7688**
2 and 3	4.9888	**4.3213**
2 and 4	**5.8732**	6.9330
3 and 4	**7.0896**	8.1193

Table 3.6: Color difference ΔE_{00} of the adjacent circles of the rectangular section from test image no.3(42)

Circles	Proposed method	Tanaka's method
1 and 2	**12.9225**	15.7776
1 and 3	4.4172	**4.0841**
1 and 4	**19.9488**	20.8867
2 and 3	**15.4046**	16.0424
2 and 4	**3.6512**	4.9521
3 and 4	19.7509	**17.7028**

Table 3.7: Color difference ΔE_{00} of the adjacent circles of the rectangular section from test image no.6(98)

Circles	Proposed method	Tanaka's method
1 and 2	**16.5334**	16.7848
1 and 3	**2.0988**	3.6148
1 and 4	**4.4597**	18.1432
2 and 3	**10.1937**	10.6438
2 and 4	4.0640	**3.3931**
3 and 4	18.9405	**15.6612**

It can be seen from the tables that most of the color differences ΔE_{00} between horizontal adjacent circles of the proposed method are smaller than those of Tanaka's method. This means that the colors of circles 1 and 3 are almost similar to the colors of circles 2 and 4. It is more difficult for the subjects to recognize number 5, number 2, and number 9 on the simulated test images from the proposed method than the simulated test images from Tanaka's method. Therefore, the error rate of the proposed method is higher than the error rate of Tanaka's method. Moreover, the results from the proposed method are closer to the results of the clinical color perception test.

3.5 Summary

Currently, color images are extensively used to showcase information via websites and smartphone applications. Due to the yellowing on the human crystalline lens, the ability of humans to differentiate colors reduces as age increases, and this may cause confusion and misinterpretation of information by the elderly. Hence, understanding color perception of the elderly is essential in order to minimize this problem. Previous works on color perception of the elderly utilized the non-uniform yellowing pigmentation method. However, recent clinical studies have shown that a uniform yellowing pigmentation occurs on the human crystalline lens. Therefore, in this chapter, we have proposed a mathematical model of the uniform yellowing pigmentation to mimic the color perception experienced by the elderly.

Results obtained from the experimental studies conducted are in agreement with the results obtained from previous works on color perception of the elderly. In the artificial color perception test, the proposed method performed better than the non-uniform yellowing pigmentation method. Moreover, the results from the proposed method are also closer to the results of the clinical color perception test. Based on these results, the effect of the uniform yellowing pigmentation on the color perception of the elderly has been identified. Therefore, implementing the inverse computation of the proposed method, website designers and smartphone application developers can choose better color schemes to represent their information. Thus, misinterpretation of information by the elderly can be avoided. Moreover, designers and architects can produce better visual color representations for the elderly to experience the built environment safely and with confidence.

CHAPTER 4: COLOR PERCEPTION OF RED-GREEN DEFICIENTS

This chapter presents an overview of the color perception of red-green deficients. Mathematical algorithms that model their color perception are also described. Some of the image recoloring methods for red-green deficients are briefly discussed. However, each method has its own disadvantages, especially in preserving the naturalness of the recolored images. Therefore, this chapter proposes a simple and efficient recoloring method that enhances color perception and also maintains the naturalness of the images perceived by red-green deficients.

4.1 Introduction

Color vision, which interprets information from the visible light to form the visual color perception of the surrounding world, is one of the process carried out by the human central nervous system. People with normal color vision, or trichromats, have three independent channels to convey information of colors (Vienot, Brettel, Ott, M'Brek, & Mollon, 1995). These three independent channels are cone photoreceptors which are sensitive in the red, green, and blue spectral range in human eyes, and they are generally represented by the long (L), medium (M), and short (S) cone respectively (Hassan et al., 2015; Hunt, 2004; Vienot et al., 1995). About eight percent of the male population have some kind of inherited color vision deficiencies (Ching & Sabudin, 2010; Semary & Marey, 2014). These are caused by alterations in the opsin gene array in the X chromosome (Sharpe, Stockman, Jagle, & Nathans, 1999). Dichromacy is one of the inherited color vision deficiencies, and it occurs when one of the cones is absent or not functioning. Thus, individuals with dichromacy, or dichromats, experience color perception in a two-dimensional color space (Judd, 1949; Vienot et al., 1995).

Dichromacy can be further classified into three categories depending on which cone carries the defect (Neitz & Neitz, 2011). Protanopia, also known as red-deficiency, occurs when the defect is on the L-cone that carries red sensitivities. Deuteranopia also known as green-deficiency, occurs when the M-cone that carries green sensitivities is deficient. People with red-deficiency and green-deficiency are called protanopes and deuteranopes respectively. Both these categories are also called red-green deficiency (Alvaro, Linhares, Moreira, Lillo, & Nascimento, 2017; Moreira et al., 2018). People with red-green deficiency have difficulty in distinguishing between these two colors (Judd, 1949; Ching & Sabudin, 2010); they view red and green as yellow, orange, and beige (Alvaro, Moreira, Lillo, & Franklin, 2015; Alvaro et al., 2017). This creates confusion and may cause misinterpretation of information (Suetake et al., 2012). Another type of dichromacy is called tritanopia, in which the S cone that carries blue sensitivities is deficient. Tritanopia is also known as blue-yellow deficiency where people with tritanopia have difficulty to distinguish shades of blue and yellow. However, people with tritanopia, or tritanopes, comprise less than one percent of the male population (Moreira et al., 2018).

People with dichromacy or any other type of color vision deficiency experience great difficulty with color discrimination that not only affects their social life but may also affect their careers (Cole, 2007; Tagarelli et al., 2004). In order to understand color experience of dichromats, several methods to simulate their color perception have been proposed. Although it seemed impossible at first to know their color perception, a few individuals have been discovered to have one protanopia, deuteranopia, or tritanopia eye and one normal eye. These individuals are known to have unilateral protanopia, unilateral deuteranopia, and unilateral tritanopia respectively. Research on these individuals shows that a stimulus of 575 nm is perceived as the same yellow, and a stimulus of 475 nm as the same blue, by trichromats, protanopes, and deuteranopes (Judd, 1949). In the case of unilateral tritanopia, the corresponding two hues that are viewed similarly by trichromats and tritanopes are a red with a dominant wavelength of 660 nm and a blue-green with a dominant wavelength of approximately 485 nm (Alpern, Kitahara, & Krantz, 1983).

Based on this information, dichromats confusion lines or dichromatic isochromatic lines, exist and converge at a single point for each type of color vision deficiency (Birch, 1972). The confusion line for protanopia, deuteranopia and tritanopia are shown in Figures 4.1(a) to 4.1(c). Colors represented along such a line are perceived as identical if no luminance contrast is present.

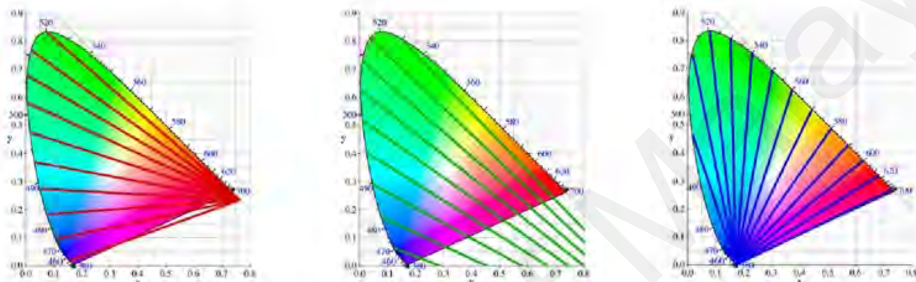

(a) (b) (c)

Figure 4.1: Confusion lines in the CIE 1931 color space for (a) protanopia; (b) deuteranopia; (c) tritanopia (Daniel, 2010)

Based on these findings, Meyer and Greenberg (1988) proposed a color reproduction method by utilizing the CIE color matching functions to produce an image that approximates the image seen by dichromats. Their work is considered a pioneer work in using color television displays and digitally controlling it to identify dichromatic color perception. Brettel et al. proposed a computerized simulation of dichromatic vision (Brettel et al., 1997). Their aims are to reproduce dichromatic color perception and also offer a plausible dichromatic color appearance to trichromats. Moreover, protanopes and deuteranopes confirmed that the colors produced by Brettel's algorithm are accurate. Further experiments on Brettel's algorithm by Vienot et al. produced the linear transformations from trichromatic color perception to dichromatic color perception (Vienot et al., 1999).

Another model to simulate the color perception of dichromats was proposed by Wachtler et al. (2004). The key feature of their model is the processing of the photoreceptor signals in parallel channels with different gains and nonlinearities. Meanwhile, Capilla, Diez-Ajenjo, et al. (2004) introduced an alternative algorithm called the corresponding-pair procedure . However, this procedure can only be applied to color models that fulfill certain conditions. Furthermore, Capilla, Luque, and Diez-Ajenjo (2004) utilized different color vision models to represent dichromatic color perception. In this method, they implemented either a cone-loss model, setting the appropriate cone responses to zero, or a cone-replacement model, in which the L cone becomes an M cone for protanopia and the M cone becomes an L cone for deuteranopia.

A more recent work conducted by Machado et al. (2009) presents a physiologically based model to simulate dichromatic color perception. Their model is based on the stage theory of human color vision and is derived from the data obtained in electrophysiological studies. Their work not only simulates dichromatic color perception, but it can also be utilized to represent anomalous trichromacy. Meanwhile, Lee and dos Santos (2011) modified Brettel's algorithm (Brettel et al., 1997) using an adaptive fuzzy-based system to represent the linear transformation of anamolous trichromacy. Furthermore, a two stage model of dichromatic color perception is introduced by Rodriquez-Pardo and Sharma (2011). Their model consists of a first sensor stage with per-channel gain control and a second opponent encoding stage. However, although their model is in agreement with the perceptual data, they have not performed any psychophysical validation to verify their model. Of all the models discussed above, Brettel's algorithm (Brettel et al., 1997; Vienot et al., 1999) is the most accepted method due to its mathematical simplicity and its usability in expressing dichromatic color perception.

Utilizing Brettel's algorithm to simulate dichromatic color perception, several methods using different strategies have been proposed to enhance the visual details missed by dichromats. Most of the recoloring methods proposed for dichromacy focus on protanopia and deuteranopia. This is due to the fact that protanopia and deuteranopia are from the red-green deficiency group that corresponds to over 99.9 percent of all color vision deficiency cases worldwide (Sharpe et al., 1999). Rigden (1999) created color palette for protanopia and deuteranopia based on the standard 216-color web-safe palette. Another method for website color modification was proposed by Ichikawa et al. (2003). They proposed an automatic color arrangement optimization process using a genetic algorithm known as the robust optimization method. Wakita and Shimamura (2005) proposed a repainting system called SmartColor which replaces the set of colors used in the original documents with another set of colors. However, although these methods help designers plan a proper color scheme for their designs, these methods are not suitable for natural images since they consist of limited colors. Moreover, the use of a limited number of colors may harm a designer's creativity.

To overcome this issue, Yang and Ro (2003) proposed an adaptive recoloring method that allows color adaptation at anytime and anywhere according to the type and severity of the color vision deficiency. Their color adaptation method consists of two stages; hue adaptation and saturation adaptation. Meanwhile, Jefferson and Harvey proposed a recoloring method that selects key colors from the difference between the original image and dichromat perceived image histograms (Jefferson & Harvey, 2006). They utilize four objective functions to preserve brightness, color contrast, colors in available gamut, and color naturalness.

Another recoloring process was proposed in Anagnostopoulos et al. (2007). Their method implemented logical image masking in order to modify the colors that are confused, and to preserved colors that are perceived correctly. To improve the efficiency of this method, Doliotis et al. (2009) added a color clustering process to automatically differentiate between colors that need to be recolored and colors that need to be preserved. However, this method implemented a complex computational algorithm that may not be suitable for practical applications.

Rasche et al. (2005a) proposed an automatic recoloring method that implemented an optimization process using an affine transformation in order to preserve the perceptual color differences between all pairs of colors. However, this method does not capture the color variation along many directions and does not ensure that the mapped colors are all within the available color gamut. To address this limitation, they implemented a constrained multivariate optimization procedure applied to a reduced set of quantized color, which are then used to optimize the entire set of colors (Rasche et al., 2005b). Even though they improved their previous method, they did not take into consideration the problem of naturalness preservation, and the method can arbitrarily change all the colors of the original images.

One of the concerns in the recoloring method for dichromats is to preserve the naturalness of the recolored images. Kuhn et al. (2008) proposed a naturalness-preserving recoloring method by implementing a mass-spring system to optimize the colors in the input image and enhance the color contrast for dichromats. However, this method did not preserve the temporal coherence of the images. Thus, Machado and Oliveira (2010) proposed an automatic image-recoloring technique for enhancing color contrast for dichromats while maintaining the temporal coherence of the images. Moreover, due to this characteristic, it is also suitable for video recoloring. Although this technique is better than Kuhn's method, this method is more suitable to recolor scientific visualization images.

In natural images, the number of colors may be less than the whole range of the color spectrum. Hence, there are a lot of color redundancies that can be utilized. By exploiting the color redundancies, Ma et al. (2006) proposed a nonlinear transformation method.

Their method uses the self-organizing map to change the colors. This method has two advantages: global nonlinearity, which is more effective that linearity or local nonlinearity and adaptability, which makes the practical implementation more viable.

Huang et al. (2007) developed a recoloring process that can automatically construct a transformation process which maintains the visual details for dichromats and preserves the naturalness for trichromats. Their method utilized a rotational process in CIELAB color space to transform the colors in the image while maintaining the luminance of the original image. However, the results from this method may not be depictive enough. In Huang et al. (2009), they proposed another recoloring method that implemented a more depictive strategy: the Gaussian Mixture Model (GMM) together with the Expectation-Maximization (EM) algorithm to represent the colors in the images. Using the optimization process, they determined the optimal mapping to maintain the color contrast between a pair of colors. The optimal mapping functions are then used in the recoloring process.

Recently, Ribeiro and Gomes (2013) proposed a simpler recoloring method by implementing the Hue-Saturation-Value (HSV) color model. Their main objective is to avoid confusion between red and green colors. To achieve that, they remapped the confused colors using trivariate recoloring and hue remapping functions. These functions ensure that any two different colors are mapped into two distinct colors.

Although all the aforementioned recoloring methods enhance the visual details and improve the color perception of the red-green deficients, the recolored images may look nonpleasing to trichromats (Huang et al., 2007; Jeong et al., 2011). Moreover, the recoloring methods may potentially change all the colors of the original images and thus, may make the recolored images look unnatural to the red-green deficients as well (Kuhn et al., 2008). If the recoloring method focuses only on the needs of red-green deficients, these recolored images may appear awkward to trichromats. On the other hand, if the needs of the red-green deficients are not taken into consideration, they may face difficulties when looking at the images. This may happen in public places such as in airports, shopping malls, and train stations where color images used in advertisements and maps are observed by both trichromats and red-green deficients. Thus, it is important to have a recoloring method that takes into consideration the needs of both parties.

Therefore, this chapter proposes a simple and efficient recoloring method that improves visual details and color perception of the red-green deficients and also preserves the naturalness of the recolored images for both trichromats and red-green deficients. The main advantage of the proposed method is that it recolors the colors confused by the red-green deficients with colors that have the same hue as the original. Moreover, the recolored images have the same luminance as the original images. The proposed method consists of two main parameters: error parameters and a rotation parameter. These parameters are used to compute the modified error parameters that will be distributed back into the original colors. The rest of the chapter is organized as follows. Section 4.2 describes the fundamental algorithm of the color perception of dichromats. The proposed recoloring method is described in Section 4.3. The performance of the proposed recoloring method and comparison with other recoloring methods are discussed in Section 4.4. Lastly, the chapter conclusion is presented in Section 4.5.

4.2 Dichromatic Color Perception Model

Of all the models that represent the dichromatic color perception, Brettel's algorithm (Brettel et al., 1997; Vienot et al., 1999) is the most accepted model due to its mathematical simplicity and its usability in expressing the color discrimination of dichromats. Hence, this section describes Brettel's algorithm.

4.2.1 Brettel's Algorithm

Brettel's algorithm (Brettel et al., 1997; Vienot et al., 1999) represents color stimuli as a vector in a three-dimensional LMS color space. The LMS color space is specified by the peak responses of the three types of cones for the human eye, which are named after the human eyes cone photoreceptors which are long (L), medium (M), and short (S).

Thus, to implement Brettel's algorithm, color images need to be transformed to the LMS color space. This is done first by transforming the RGB color space to the XYZ color space using the transformation matrix obtained via Judd-Vos colorimetric modification (Travis, 1991; Vienot et al., 1999)

$$\begin{bmatrix} X \\ Y \\ Z \end{bmatrix} = \begin{bmatrix} 40.9568 & 35.5041 & 17.9167 \\ 21.3389 & 70.6743 & 7.98680 \\ 1.86297 & 11.4620 & 91.2367 \end{bmatrix} \begin{bmatrix} R \\ G \\ B \end{bmatrix} \tag{4.1}$$

Then, the XYZ color space is transformed to LMS color space according to Smith and Pokorny (1995)

$$\begin{bmatrix} L \\ M \\ S \end{bmatrix} = \begin{bmatrix} 0.15514 & 0.54312 & -0.03286 \\ -0.15514 & 0.45684 & 0.03286 \\ 0 & 0 & 0.01608 \end{bmatrix} \begin{bmatrix} X \\ Y \\ Z \end{bmatrix} \tag{4.2}$$

For simplification, these computations can be combined as shown below:

$$\begin{bmatrix} L \\ M \\ S \end{bmatrix} = \begin{bmatrix} 17.8824 & 43.5161 & 4.11935 \\ 3.45565 & 27.1554 & 3.86714 \\ 0.0299566 & 0.184309 & 1.46709 \end{bmatrix} \begin{bmatrix} R \\ G \\ B \end{bmatrix} \tag{4.3}$$

To understand the algorithm more clearly, a geometric representation of the algorithm is shown in Figures 4.2 and 4.3. As shown in Figures 4.2 and 4.3, in dichromatic vision, the

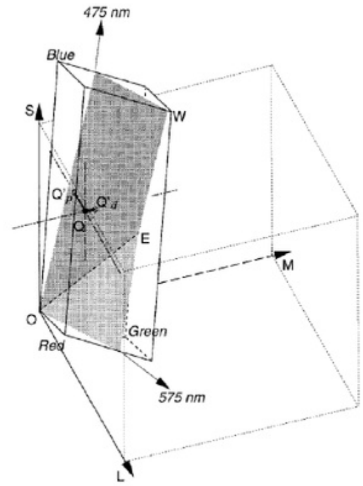

Figure 4.2: Geometric representation of the reduced stimuli surface for protanopia and deuteranopia (Brettel et al., 1997; Vienot et al., 1999)

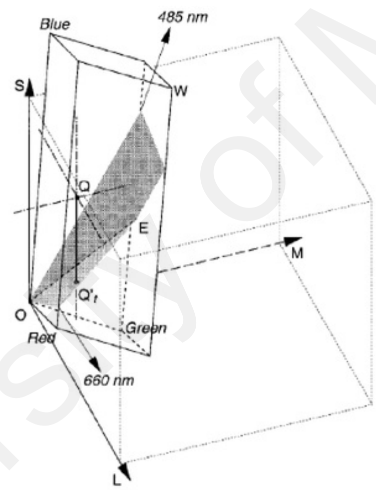

Figure 4.3: Geometric representation of the reduced stimuli surface for tritanopia (Brettel et al., 1997; Vienot et al., 1999)

LMS color space is reduced to two color domains which include the origin **O**, the nominal white stimulus **W**, and the neutral color stimulus **E**. In these figures, OE represents the neutral stimuli for dichromats as well as for trichromats. The neutral axis OE divides the surface of the reduced stimuli into two half-planes, each of which is anchored on a point specifying an invariant hue for a given type of dichromat.

The wings from OE toward the 475 nm and 575 nm locations represent the reduced stimuli surface for protanopia and deuteranopia stimulation as shown in Figure 4.2. Meanwhile, the wings from OE toward the 485 nm and 660 nm locations represent the reduced stimuli surface for tritanopia as shown in Figure 4.3. For any given stimulus **Q** located on the LMS color space, Brettel's algorithm replaces the undetermined component of a dichromat by the value corresponding to the projection of **Q** onto the wing, parallel to the direction of the missing fundamental axis.

Using vector algebra, the equation for any given stimulus **Q'** on a plane defined by the origin **O**, the monochromatic anchor stimulus **A** with coordinates of (L_A, M_A, S_A) and stimuli **E** with coordinates of (L_E, M_E, S_E) is given as

$$(\mathbf{E} \times \mathbf{A})\mathbf{Q'} = 0 \tag{4.4}$$

since **Q'** is always orthogonal to the normal vector $\mathbf{E} \times \mathbf{A}$ of the plane. Solving the plane relation gives the linear equation of the stimulus **Q'** with coordinates (L_Q, M_Q, S_Q) as

$$\alpha L_Q + \beta M_Q + \gamma S_Q = 0 \tag{4.5}$$

with

$$\alpha = M_E S_A - S_E M_A \tag{4.6}$$

$$\beta = S_E L_A - L_E S_A \tag{4.7}$$

$$\gamma = L_E M_A - M_E L_A \tag{4.8}$$

From these relations, the reduction of the normal color domain to the dichromatic color domain maintains the unaffected values that correspond to the existing photoreceptors.

Thus, the replacement tristimulus values corresponding to the missing photoreceptor is, for the protanopia

$$L_p = \frac{-(\beta M + \gamma S)}{\alpha} \tag{4.9}$$

for the deuteranopia,

$$M_d = \frac{-(\alpha L + \gamma S)}{\beta} \tag{4.10}$$

and for the tritanopia

$$S_t = \frac{-(\alpha L + \beta M)}{\gamma} \tag{4.11}$$

where L, M, S are the values obtained in Eq. (4.3).

Further experiments by Vienot et al. produced the linear transformation from trichromatic vision to the red-green deficiency using the following transformation matrices (Vienot et al., 1999). For protanopia,

$$\begin{bmatrix} L_p \\ M_p \\ S_p \end{bmatrix} = \begin{bmatrix} 0 & 2.02344 & -2.52581 \\ 0 & 1 & 0 \\ 0 & 0 & 1 \end{bmatrix} \begin{bmatrix} L \\ M \\ S \end{bmatrix} \tag{4.12}$$

and for deuteranopia,

$$\begin{bmatrix} L_d \\ M_d \\ S_d \end{bmatrix} = \begin{bmatrix} 1 & 0 & 0 \\ 0.494207 & 0 & 1.24827 \\ 0 & 0 & 1 \end{bmatrix} \begin{bmatrix} L \\ M \\ S \end{bmatrix} \tag{4.13}$$

Finally, to form the image viewed by protanopes and deuteranopes, the LMS values obtained from Eq. (4.12) and Eq. (4.13) are transformed back to the RGB color space using the inverse of Eq. (4.3).

Table 4.1 illustrates the color perception of protanopes and deuteranopes using Brettel's algorithm for natural images taken from Kuhn et al. (2008), Martin, Fowlkes, Tal, and Malik (2001), and Rasche et al. (2005b).

Table 4.1: Color perception of the red-green deficiency

Original image	Protanopia	Deuteranopia
		
		
		
		

4.3 Proposed method - Naturalness Preservation Recoloring Method

This section proposes a simple and efficient recoloring method that enhances visual details and improves the color perception of the red-green deficients. The proposed method also maintains the naturalness of the recolored image for both trichromats and red-green deficients. To achieve these objectives, the proposed method adopts two premises. First, the luminance of the recolored image is the same as the luminance of the original image. Second, the recolored image has the same hue as the original image.

In the proposed method, the original image and the image perceived by the red-green deficients are converted into the XYZ color space. The XYZ color space is chosen as the working domain because it encompasses all color sensations that a human can perceive and is formulated based on the RGB version of the human eye (Fairchild, 2005). Moreover, the XYZ color space can be easily mapped to many alternative RGB color spaces by simply choosing any point of the chromaticity diagram.

To maintain the same luminance, the XYZ tristimulus values for both images are normalized. The error parameters and rotation parameter are then computed. These parameters are used to compute the modified error parameters. To obtain the recolored image, the modified error parameters are distributed back to the original image but in such a way that it increases the blue stimulation of the recolored image while maintaining the same hue as the original image. The overall process of the proposed method is summarized in Figure 4.4.

To start the recoloring process, the original image, R_o, G_o, B_o and the image perceived by red-green deficients R_s, G_s, B_s are converted to X_o, Y_o, Z_o and X_s, Y_s, Z_s respectively using Eq. (4.1). Next, both sets of tristimulus values are normalized so that the value of the luminance Y_o and Y_s are set to 100. This is so that the luminance of the recolored image can be maintained as similar to the original one. Thus, the normalized tristimulus

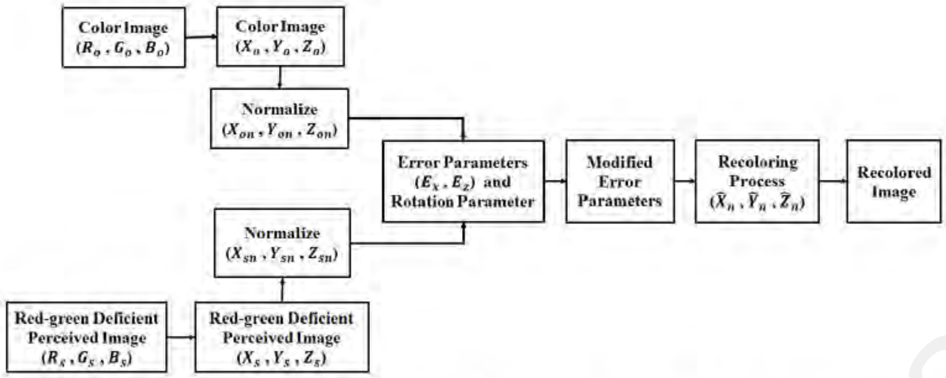

Figure 4.4: Overall process flow of the proposed image recoloring method

values of the original image and the image perceived by red-green deficients are given as X_{on}, Y_{on}, Z_{on} and X_{sn}, Y_{sn}, Z_{sn} respectively.

Based on Brettel's algorithm (Brettel et al., 1997; Vienot et al., 1999), it is evident that the red-green deficients have difficulty discriminating colors and thus changing their color perception. Hence, the error parameters are defined as the absolute difference between the normalized tristimulus values of the original image and the image perceived by the red-green deficients. Since Y_{on} and Y_{sn} have the same value, there are only two error parameters that need to be computed, E_x and E_z.

$$E_x = |X_{on} - X_{sn}| \tag{4.14}$$

$$E_z = |Z_{on} - Z_{sn}| \tag{4.15}$$

In the proposed method, we modified the error parameters by adopting a rotation operation in the XZ plane in order to transform the information of X onto the Z-axis. The rotation operation is performed according to the value of the rotation parameter, ϕ. In order to compute the rotation parameter, ϕ, the normalized X and Z values of both the original image and the image perceived by red-green deficients are plotted on the XZ plane as illustrated in Figure 4.5.

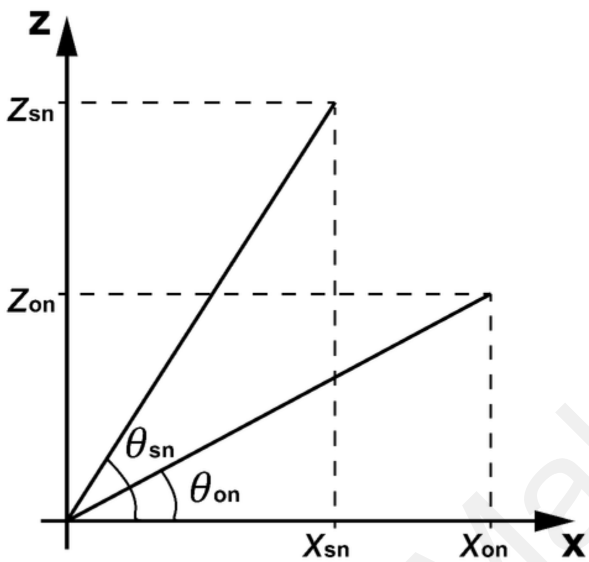

Figure 4.5: Angles of elevation of the normalized X and Z values

Based on Figure 4.5, the angles of elevation from the X-axis are computed for both points and they are defined as

$$\theta_{on} = tan^{-1}\left(\frac{Z_{on}}{X_{on}}\right) \tag{4.16}$$

$$\theta_{sn} = tan^{-1}\left(\frac{Z_{sn}}{X_{sn}}\right) \tag{4.17}$$

Hence, the rotation parameter, ϕ, is defined as the absolute difference between the angles of elevation, θ_{on} and θ_{sn}.

$$\phi = |\theta_{on} - \theta_{sn}| \tag{4.18}$$

As illustrated in Figure 4.6, the error parameters are plotted on the XZ plane and the point is rotated according to the rotation parameter, ϕ. The rotation operation increases the value of E_z which is related to the error of the blue stimulation and simultaneously decreases the value of E_x. From the rotation operation, the value of E_x and E_z are

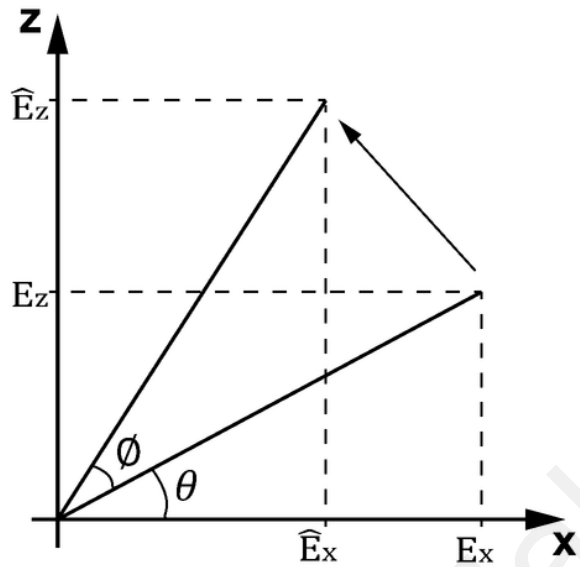

Figure 4.6: Rotation operation of the error parameters

modified to $\widehat{E}_x$ and $\widehat{E}_z$ respectively. Mathematically, $\widehat{E}_x$ and $\widehat{E}_z$ can be formulated as matrix multiplication.

$$\begin{bmatrix} \widehat{E}_x \\ \widehat{E}_z \end{bmatrix} = \begin{bmatrix} cos\phi & -sin\phi \\ sin\phi & cos\phi \end{bmatrix} \begin{bmatrix} E_x \\ E_z \end{bmatrix} \tag{4.19}$$

The modified error parameters $\widehat{E}_x$ and $\widehat{E}_z$ are distributed back to the normalized tristimulus values of the original image X_{on}, Y_{on}, Z_{on} as shown below.

$$\widehat{X}_n = X_{on} + \widehat{E}_x \tag{4.20}$$

$$\widehat{Y}_n = Y_{on} \tag{4.21}$$

$$\widehat{Z}_n = Z_{on} + \left(\widehat{E}_x + \widehat{E}_z\right) \tag{4.22}$$

The $\widehat{E}_x$ and $\widehat{E}_z$ are both added into Z_{on} in order to increase the blue stimulation of the recolored image so as to enhance the color perception of the red-green deficients. Moreover, the distribution process recolored the original image with the colors of the same hue so as to preserve the naturalness of the original image from a trichromat's point of view.

Finally, the recolored tristimulus values $\widehat{X}_n$, $\widehat{Y}_n$, $\widehat{Z}_n$ are un-normalized and converted back to the *RGB* values using the inverse relation of Eq. (4.1). The recolored image perceived by red-green deficients can be observed using Brettel's algorithm (Brettel et al., 1997; Vienot et al., 1999).

4.4 Experimental Studies

In this section, two experimental studies were performed to evaluate the proposed method. The naturalness error, E_{nat} (Huang et al., 2007; Jeong et al., 2011) and the Feature Similarity chrominance (FSIMc) index (Zhang, Zhang, Mou, & Zhang, 2011) were computed to objectively evaluate the effectiveness of the proposed method and other recoloring methods in preserving the naturalness of the recolored images. Moreover, a visual comparison of the protanopic and deuteranopic views of the recolored images was also performed.

Lastly, paired comparison tests (Thurstone, 1927) were conducted with trichromats and red-green deficients in order to evaluate the performance of the proposed method in terms of the naturalness preservation of the recolored images and the overall preference.

Prior to the studies, the LCD was calibrated using X-Rite i1Display 2 based on sRGB color space and white point of D65. The gamma correction parameter, γ was set to 2.2. The calibration process ensures that the preciseness of color reproduction on LCD display is within a very small range of error (Tanaka et al., 2011).

4.4.1 Objective Evaluations

In this experiment, 6 natural images taken from Kuhn et al. (2008), Martin et al. (2001), and Rasche et al. (2005b) were utilized. The proposed method was compared with two recoloring methods: Huang's (Huang et al., 2009) and Ribeiro's methods (Ribeiro & Gomes, 2013). These two methods were chosen for comparison because they implemented a similar recoloring framework as the proposed method in which the original images are recolored instead of the images perceived by the red-green deficients.

The images were recolored using the proposed method, Huang's method (Huang et al., 2009), and Ribeiro's method (Ribeiro & Gomes, 2013). Then, to observe how protanopes and deuteranopes view the recolored images, the recolored images were simulated using Brettel's algorithm (Brettel et al., 1997; Vienot et al., 1999). To objectively evaluate the performance of these three recoloring methods, the naturalness error, E_{nat} (Huang et al., 2007; Jeong et al., 2011) of the recolored images was computed. The naturalness error is defined as

$$E_{nat} = \sum_{i} \left\| C_i - \hat{C}_i \right\|^2 \tag{4.23}$$

where i ranges over the colors contained in the images, C is the original image and $\hat{C}$ is the recolored image. Table 4.2 shows that the proposed method produced recolored images that have the smallest naturalness errors. This means that the proposed method produces recolored images that have a better degree of correspondence with the original images than the other two recoloring methods.

Table 4.2: Naturalness error, E_{nat} of the recolored images

Original image	Proposed method	Huang's method	Ribeiro's method
Red Berries	**1,817**	2,772	3,093
Apples	**4,138**	4,180	6,746
Red Flowers	**3,051**	9,915	4,049
Orange Flower	**2,275**	7,024	2,374
Peppers	**2,408**	3,702	3,761
Flowers	**4,259**	8,198	7,129

In addition, the chrominance information of the recolored images with respect to the original images was computed using Feature Similarity chrominance (FSIMc) index (Zhang et al., 2011). Higher FSIMc index shows that the chrominance information of the recolored images is closer to the chrominance information of the original images. Hence, the recolored images with a higher FSIMc index look almost similar to the original images from a trichromat's point of view. As shown in Table 4.3, the recolored images from the proposed method obtained the highest FSIMc index as compared to the other two recoloring methods.

Table 4.3: Feature Similarity (FSIMc) index of the recolored images

Original image	Proposed method	Huang's method	Ribeiro's method
Red Berries	**0.9855**	0.9738	0.9648
Apples	**0.9744**	0.8892	0.9202
Red Flowers	**0.9610**	0.9487	0.9442
Orange Flower	**0.9877**	0.9282	0.9726
Peppers	**0.9897**	0.9870	0.9318
Flowers	**0.9668**	0.9526	0.9166

Next, a visual comparison was conducted between the recolored images of the proposed method and the other two recoloring methods. As shown in Tables 4.4 and 4.5, the recolored images from the proposed method look more similar to the original images than the recolored images from the other two recoloring methods. This is in agreement with the results obtained in Tables 4.2 and 4.3. Since the proposed method recolors the red-green deficients confused colors with colors that have the same hue as the original, the recolored images maintain the naturalness of the original images as much as possible.

On the other hand, in Huang's and Ribeiro's methods, the recolored images lose their naturalness as the red-green deficients' confused colors are recolored with colors that have different hues. Moreover, Huang's method has the tendency to recolor colors

Table 4.4: Recolored images and images perceived by the red-green deficients

Original image	Perceived by protanopes	Perceived by deuteranopes
		
	Proposed method	
Recolored image	Perceived by protanopes	Perceived by deuteranopes
		
	Huang's method	
Recolored image	Perceived by protanopes	Perceived by deuteranopes
		
	Ribeiro's method	
Recolored image	Perceived by protanopes	Perceived by deuteranopes
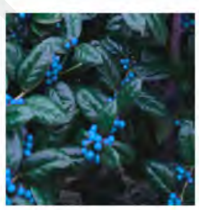	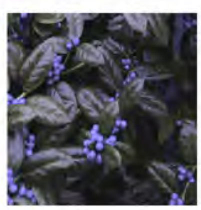	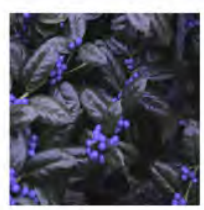

whose differences are perfectly visible to trichromats to colors that look identical to them (Simon-Liedtke & Farup, 2016). Therefore, their recolored images may look weird and

Table 4.5: **Recolored images and images perceived by the red-green deficients**

Original image	Perceived by protanopes	Perceived by deuteranopes
		
Proposed method		
Recolored image	Perceived by protanopes	Perceived by deuteranopes
		
Huang's method		
Recolored image	Perceived by protanopes	Perceived by deuteranopes
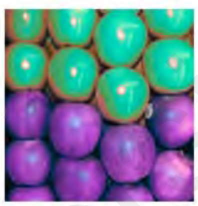		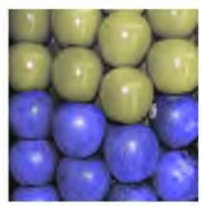
Ribeiro's method		
Recolored image	Perceived by protanopes	Perceived by deuteranopes
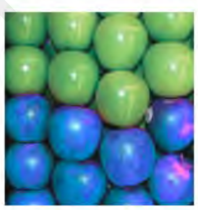	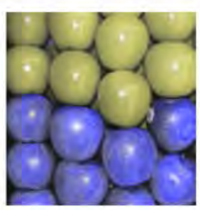	

unnatural. This can be observed from Table 4.4 where the color of the red berries are recolored to orange and light blue by Huang's and Ribeiro's methods respectively. The same happened to the color of the red apples in Table 4.5 where Huang's and Ribeiro's methods recolored the red apples with purple and blue respectively.

Images perceived by red-green deficients can also be observed in Tables 4.4 and 4.5. From the results, it can be observed that all three methods enhance the visual details of the original images. Moreover, compared to the original images perceived by red-green deficients, all the recolored images improve the color perception of the red-green deficients. As shown in Table 4.4, the red berries of the recolored images perceived by red-green deficients are more visible as compared to the original image perceived by them. In addition, the recolored images perceived by red-green deficients in Table 4.5 show the difference between the green and red apples more clearly than the original image perceived by them. However, in order to further evaluate the effectiveness of the proposed method and other recoloring methods, subjective evaluations were conducted in the next experiment.

4.4.2 Paired Comparison Tests

In this experiment, paired comparison tests (Thurstone, 1927) were conducted with trichromats and red-green deficients. The main objective of this experiment is to evaluate the performance of the proposed method with Huang's (Huang et al., 2009) and Ribeiro's methods (Ribeiro & Gomes, 2013) in terms of the naturalness preservation of the recolored images and the overall preference by the trichromats and red-green deficients. Twenty-four test images were utilized for protanopia and deuteranopia paired comparison tests and these images are shown in Table 4.6.

There were a total of 36 pairs of test images for each paired comparison test and these images were arranged side-by-side; *(Or, P), (Or, H), (Or, R), (P, H), (P, R),* and *(H, R)* where *Or* stands for original image, *P* for the image recolored by the proposed method, *H* for Huang's method, and *R* for Ribeiro's method. To avoid habituation, the order of the images in each pair, as well as the order of each pair were defined randomly. These images

Table 4.6: Images used in the paired comparison test

Original image	Recolored images for protanopia test			Recolored images for deuteranopia test		
	Proposed method	Huang's method	Ribeiro's method	Proposed method	Huang's method	Ribeiro's method

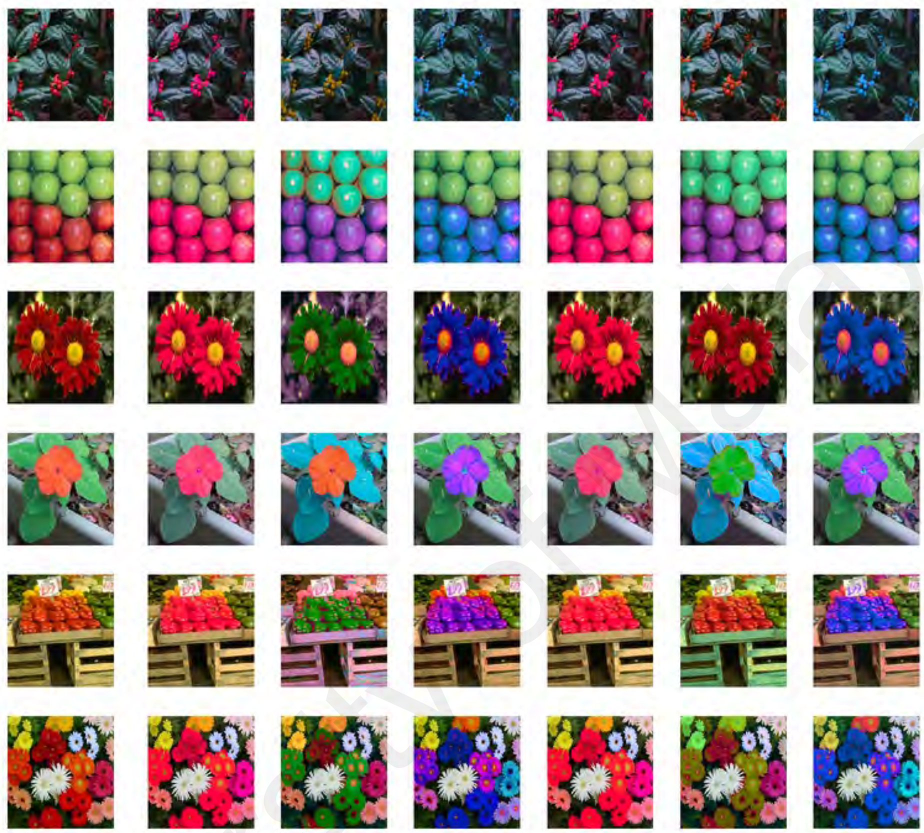

were displayed on a DELL S2440L LCD display at approximately 60 cm from the subject.

The trichromat subjects consisted of 15 volunteers between the ages of 20 and 34 years with a mean age of 26.33. Meanwhile, for red-green deficients, the subjects consisted of 11 male volunteers who declared themselves as color vision deficient. Their age ranged between 11 and 37 years with a mean age of 27.64. The color vision deficient volunteers were subjected to the Ishihara test (S. Ishihara, 1979) to confirm their color vision deficiency. Based on the outcome of the Ishihara test, the 11 male volunteers were classified as deuteranopes. It should be noted here that the Ishihara test cannot achieve a precise diagnosis of protanopia and deuteranopia. In order to obtain precise results, they would have been required to submit to an anomaloscope test.

The subjects were then grouped into two groups; trichromats and deuteranopes. Each subject is the trichromats group underwent two paired comparison tests. The first paired comparison test was to evaluate the protanopia recolored images and the second one was to evaluate the deuteranopia recolored images. Each subject in the deuteranopes group underwent the paired comparison test for deuteranopia recolored images. During the paired comparison test, each subject was asked to indicate their binary preference in terms of the naturalness and their overall preference for the images.

The results obtained for the paired comparison tests were analyzed using Thurstone's Law of Comparative Judgment (Thurstone, 1927). Case V Law of Comparative Judgment is a classical tool that ranks items based on subjective choices, which allows one to measure individuals' preference orderings for some stimuli from a set of discrete binary choices (Kuhn et al., 2008). Moreover, we used the maximum a posteriori estimation method in our analysis. The maximum a posteriori estimation method was chosen because it is an optimal approach to estimation and can be solved efficiently as a convex optimization problem (Tsukida & Gupta, 2011). We also computed the corresponding 95% confidence intervals using the formulation in Montag (2006). The 95% confidence intervals are shown as vertical bars in Figures 4.7 to 4.9.

The preference scores of protanopia paired comparison test by trichromats are shown in Figure 4.7(a) for naturalness and Figure 4.7(b) for overall preference. Since the original images are recolored to match the reduced color gamut of protanopia, it can be observed that trichromats preferred the original images more than the recolored images in terms of naturalness and overall preference. However, between the recolored images, the results show that trichromats preferred images recolored using the proposed method.

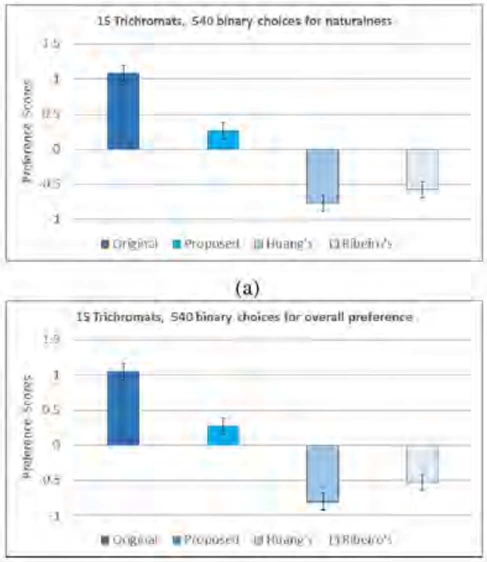

(b)

Figure 4.7: Preference scores of protanopia paired comparison test by trichromats, (a) Naturalness, (b) Overall preference

The same thing was observed from the results of the deuteranopia paired comparison test by trichromats. They preferred the original images more than the recolored images in terms of naturalness and overall preference. Images recolored using the proposed method achieved slightly higher preference scores than images recolored using Huang's method and significantly higher preference scores than images recolored using Ribeiro's method. Figure 4.8(a) shows preference for naturalness and Figure 4.8(b) for overall preference. Thus, these results show that the proposed method maintained the naturalness of the original images, and enhanced the visual details better than the two other recoloring methods for both protanopia and deuteranopia recolored images.

The preference scores for the deuteranopia paired comparison test by deuteranopes are shown in Figure 4.9(a) for naturalness and Figure 4.9(b) for overall preference. It can be deduced that most of the deuteranopes preferred the original images in terms of naturalness and overall preference. This is because they are used to their color perception when looking at natural images such as flowers and fruits (Oliveira, 2013). Moreover, deuteranopes

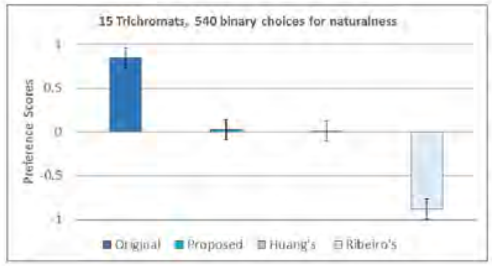

(a)

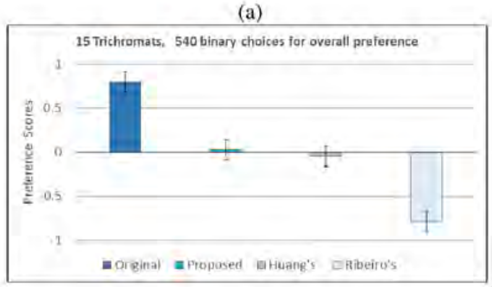

(b)

Figure 4.8: Preference scores of deuteranopia paired comparison test by trichromats, (a) Naturalness, (b) Overall preference

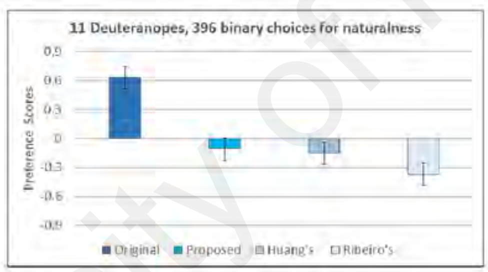

(a)

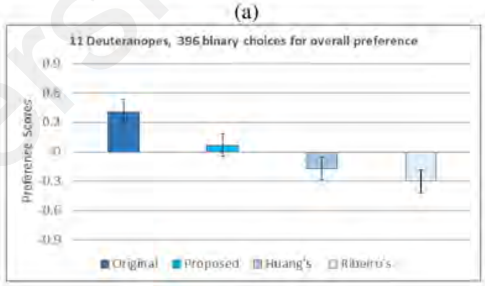

(b)

Figure 4.9: Preference scores of deuteranopia paired comparison test by deuteranopes, (a) Naturalness, (b) Overall preference

prefer saturated yellow compared to other colors (Alvaro et al., 2015). As such, most of the recolored images used in this test did not look natural to them. However, among the three recoloring methods, in terms of naturalness and overall preference, deuteranopes preferred the recolored images from the proposed method more than the other two recoloring methods. Hence, these results show that the proposed method produced images that look natural to deuteranopes and also enhanced their visual details better than Huang's and Ribeiro's methods.

In addition, a second paired comparison test was conducted to evaluate the proposed method with the recoloring method that recolored the images perceived by the red-green deficients instead of the original images. Applying the same setup as the previous paired comparison test, we compared the effectiveness of the proposed method with Kuhn's method (Kuhn et al., 2008) in terms of the naturalness preservation of the recolored images and the overall preference. Since in Kuhn's method the recolored images remained in the reduced color space of red-green deficients, the second paired comparison test was only conducted to the deuteranopes.

Here, the same set of the original and recolored images from the proposed method used in the previous deuteranopia paired comparison test and the recolored images from Kuhn et al. (2008) as shown in Figure 4.10 were utilized. Hence, there were a total of 18 pairs of test images for the second deuteranopia paired comparison test and these images were arranged side-by-side; *(Or, P)*, *(Or, K)*, and *(P, K)* where *Or*, *P*, and *K* stand for original image, image recolored by the proposed method and Kuhn's method respectively.

Applying Thurstone's Law of Comparative Judgment (Thurstone, 1927) with the maximum a posteriori estimation method and the corresponding 95% confidence intervals (Montag, 2006), the preference scores for naturalness and overall preference are shown in Figure 4.11. The 95% confidence intervals are shown as vertical bars.

Similar to the previous deuteranopia paired comparison test, most of the deuteranopes preferred the original images more than the recolored images from both methods due to their previous color experiences. However, the proposed method has slightly higher

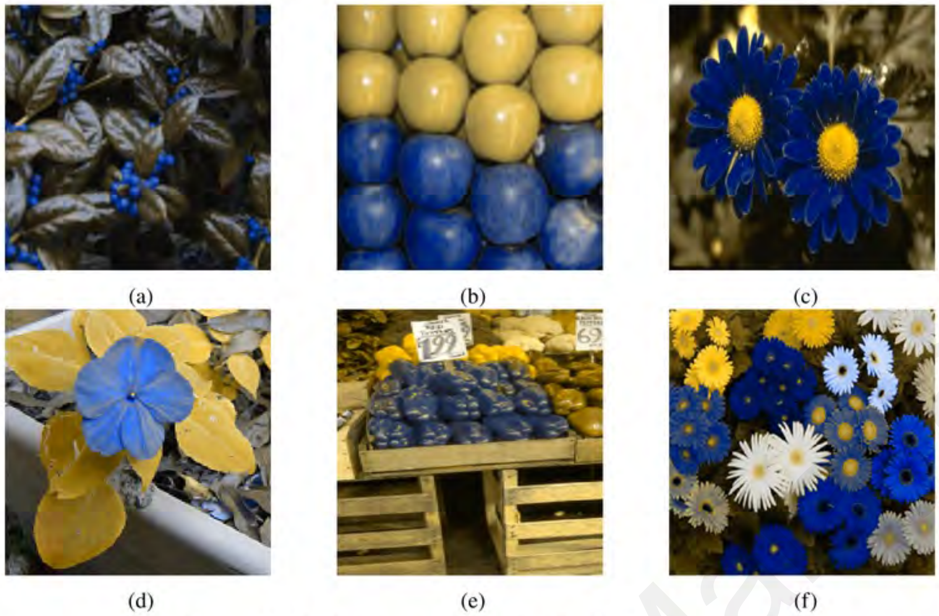

Figure 4.10: Images recolored using Kuhn's method

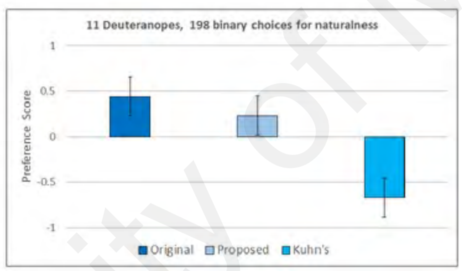

(a)

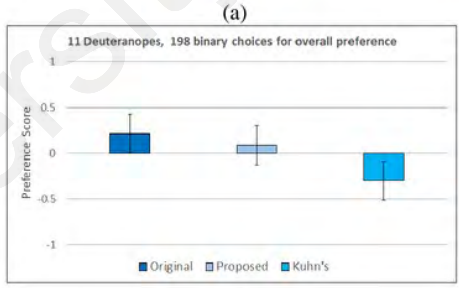

(b)

Figure 4.11: Preference scores of the second deuteranopia paired comparison test by deuteranopes, (a) Naturalness, (b) Overall preference

preference scores than Kuhn's method for both naturalness and overall preference.

4.5 Summary

Color images in public places such as in airports, shopping malls, and train stations are observed by everyone. However, loss of information may occur when the images are viewed by red-green deficients. Various recoloring methods have been proposed to overcome this problem. However, the recolored images may look non-pleasing to trichromats. Moreover, the recoloring methods may change all the colors of the images, and as a result, the recolored images may look unnatural to the red-green deficients as well. Therefore, it is essential that recoloring methods take into consideration the needs of both trichromats and red-green deficients.

Thus, in this chapter, a simple and efficient recoloring method that considers the needs of both trichromats and red-green deficients is proposed. The proposed method improves visual details and enhances the color perception of the red-green deficients while preserving the naturalness of the recolored images for both trichomats and red-green deficients. The main advantage of the proposed method is that it recolors the colors confused by the red-green deficients with the colors that have the same hue as the original ones. Moreover, the recolored images have the same luminance as the original images.

Results obtained from the experimental studies show that the proposed method performed better than three other existing methods. The proposed method not only improves visual details and enhances the color perception of the red–green deficients, but it also preserves the naturalness of the recolored images for both trichromats and red–green deficients.

CHAPTER 5: CONCLUSIONS

Color vision deficiency is the inability to discriminate certain shades of colors. This inability arises from the differences in the pigmentation of the cones in the human eye. Color vision deficiency can be categorized as acquired or inherited color vision deficiencies. In acquired color vision deficiency, elderly people suffer from certain degrees of color perception loss while some people with inherited color vision deficiency have difficulty in distinguishing between red and green colors. Thus, people with color vision deficiency may experience some difficulty in performing their daily activities. In order to improve their quality of life and ease their physical limitations, this thesis describes research on human color perception that has been conducted. The main objectives of this thesis are to propose a mathematical formulation of the uniform yellowing pigmentation to model the color perception of the elderly, and to introduce an image recoloring method for red-green deficients that enhances the visual details and preserves the naturalness of the original image.

Previous studies in color perception of the elderly utilized the non-uniform yellowing pigmentation model. However, recent clinical studies indicate that uniform yellowing pigmentation occurs on the human lens as human age increases. Therefore, to understand the effect of the uniform yellowing pigmentation on the color perception of the elderly, a mathematical formulation of the uniform yellowing pigmentation is proposed in Chapter 3. It uses three effective tristimulus ratios to form the uniform yellowing pigmentation. Experimental studies verified that the uniform yellowing pigmentation is in agreement with the results from clinical studies. In the experiments, the color perception of the elderly is simulated using the uniform yellowing pigmentation. The artificial SPP3 color perception test was conducted to compare the proposed method with the non-uniform yellowing pigmentation method and the clinical data. Results from the artificial SPP3 color perception test show that the proposed method performed better than the non-uniform yellowing pigmentation method. In addition, the results from the proposed method are closer to the clinical data.

In Chapter 4, a naturalness preserving recoloring method for the red-green deficients is proposed. The proposed method considers the needs of both trichromats and red-green deficients. The main advantages of the proposed method are that it recolors the confused colors with the colors that have the same hue as the original ones, and the recolored images have the same luminance as the original ones. Therefore, the proposed method improves the visual details of the recolored image and also preserves the naturalness from both trichromats' and red-green deficients' points of view. In objective evaluations, recolored images from the proposed method obtained better scores in term of naturalness preservation and chrominance similarity index than the other two recoloring methods that implemented similar recoloring framework. Moreover, in the paired comparison tests, the proposed method achieved higher preference scores than three other recoloring methods.

5.1 Future Research Directions

There are still many possibilities for extensions of the proposed methods and improvement for the applications discussed in this thesis. In the study of the color perception of the elderly, one possible future research direction is to formulate an image enhancement method to mitigate the effect of the uniform yellowing pigmentation on color perception of the elderly. Moreover, non-natural color images such as scientific visualization (SciVis) and information visualization (InfoVis) require contrast enhancement for the red-green deficients. In future research, the proposed naturalness preservation recoloring method can be extended to cater to this requirement of color contrast enhancement. In addition, both of the methods proposed in this thesis can also be extended to video recoloring.

REFERENCES

Alio, J. L., Schimchak, P., Negri, H. P., & Montes-Mico, R. (2005). Crystalline lens optical dysfunction through aging. *Ophthalmology*, *112*(11), 2022 - 2029.

Alpern, M., Kitahara, K., & Krantz, D. H. (1983). Perception of colour in unilateral tritanopia. *The Journal of Physiology*, *335*(1), 683 - 697.

Alvaro, L., Linhares, J., Moreira, H., Lillo, J., & Nascimento, S. (2017). Robust colour constancy in red-green dichromats. *PLos ONE*, *12*(6).

Alvaro, L., Moreira, H., Lillo, J., & Franklin, A. (2015). Color preference in red-green dichromats. *Proceedings of the National Academy of Sciences*, 9316 - 9321.

Anagnostopoulos, C. N., Tsekouras, G., Anagnostopoulos, I., & Kalloniatis, C. (2007). Intelligent modification for the daltonization process of digitized paintings. *International Conference on Computer Vision Systems*.

Applegate, R. A., Donnelly, W. J., Marsack, J. D., & Koenig, D. E. (2007). Three-dimensional relationship between high-order root-mean-square wavefront error, pupil diameter, and aging. *Journal of the Optical Society of America*, *24*(3), 578 - 587.

Artigas, J. M., Felipe, A., Navea, A., Fandino, A., & Artigas, C. (2012). Spectral transmission of the human crystalline lens in adult and elderly persons: color and total transmission of visible light. *Investigative Ophthalmology & Visual Science*, *53*(7), 4076 - 4084.

Ball, L. J., & Pollack, R. H. (1989). The effects of color and preretinal aging on embedded figures test performance: a failure to replicate. *Experimental Aging Research*, *15*(4), 177 - 180.

Birch, J. (1972). Dichromatic convergence points obtained by subtractive colour matching. *Vision Research*, *13*, 1755 - 1765.

Birren, J. E., Casperson, R. C., & Botwinick, J. (1950). Age changes in pupil size. *Journal of Gerontology*, *5*(3), 216 - 221.

Bitsios, P., Prettyman, R., & Szabadi, E. (1996). Changes in autonomics function with age: a study of pupipupil kinetics in healthy young and old people. *Age and Ageing*, *25*, 432 - 438.

Boettner, E. A., & Wolter, J. (1962). Transmission of the ocular media. *Investigative Ophthalmology & Visual Science*, *1*(6), 776 - 783.

Brettel, H., Vienot, F., & Mollon, J. D. (1997). Computerized simulation of color appearance for dichromats. *Journal of the Optical Society of America*, *14*(10), 2647 - 2655.

Bright, K., & Egger, V. (2008). Using visual contrast for effective, inclusive environments. *Information Design Journal*, *16*(3), 178 - 189.

Broadbent, A. D. (2017). Colorimetry, methods. *Encyclopedia of Spectroscopy and Spectrometry (Third Edition)*, 321 - 327.

Capilla, P., Diez-Ajenjo, M. A., Luque, M. J., & Malo, J. (2004). Corresponding-pair procedure: a new approach to simulation of dichromatic color perception. *Journal of the Optical Society of America A*, *21*(2), 176 - 186.

Capilla, P., Luque, M. J., & Diez-Ajenjo, M. A. (2004). Looking for the dichromatic version of a colour vision model. *Journal of Optics A Pure and Applied Optics*, *6*, 906 - 919.

Ching, S. L., & Sabudin, M. (2010). A study of color transformation on website images for the color blind. *World of Academy of Science, Engineering and Technology*, *4*(2), 684 - 687.

Chua, J.-L., Chang, Y. C., & Lim, W. K. (2015). A simple vision-based fall detection technique for indoor video surveillance. *Signal, Image and Video Processing*, *9*(3), 623 - 633.

Colantoni, P. (2004). *Color space transformations.* Retrieved from `http://faculty.kfupm.edu.sa/ics/lahouari/Teaching/colorspacetransform-1.0.pdf`

Cole, B. L. (2007). Assessment of inherited colour vision defects in clinical practice. *Clinical and Experimental Optometry*, *90*(3), 157 - 175.

Daniel. (2010). *There is not one color blindness.* Retrieved from http://www.daltonize.org/2010/05/there-is-not-just-one-color-blindness.html

DesMarais, C. (2013). *Facebook's instagram says it has 90 million monthly active users.* Retrieved from https://www.pcworld.com/article/2025801/facebooks-instagram-says-it-has90-million-monthly-active-users.html

Doliotis, P., Tsekouras, G., Anagnostopoulos, C. N., & Athitsos, V. (2009). Intelligent modification of color in digitized paintings for enhancing the visual perception of color-blind viewers. *Artificial Intelligence Applications and Innovations III*, *296*, 292 - 301.

Fairchild, M. D. (2005). *Color appearance models*. John Wiley & Sons, Ltd.

Fiorentini, A., Porciatti, V., Morrone, M. C., & Burr, D. C. (1996). Visual ageing: unspecific decline of the responses to luminance and colour. *Vision Research*, *36*(21), 3557 - 3566.

Gibson, J. E., & Fairchild, M. D. (2000). Colorimetric characterization of three computer displays (lcd and crt). *Munsell Color Science Laboratory Technical Report*.

Guild, J. (1932). The colorimetric properties of the spectrum. *Philosophical Transactions of the Royal Society of London. Series A, Containing Papers of a Mathematical or Physical Character*, *230*, 149 - 187.

Haskett, M. K., & Hovis, J. K. (1987). Comparison of the standard pseudoisochromatic plates to the ishihara color vision test. *American Journal of Optometry and Physiological Optics*, *46*(3), 211 - 216.

Hassan, M. F., Kugimiya, T., Tanaka, Y., Tanaka, K., & Paramesran, R. (2015). Comparative analysis of the color perception loss for elderly people. *Asia-Pacific Signal and Information Processing Association (APSIPA) Annual Summit and Conference*, 1176 - 1181.

Hassan, M. F., & Paramesran, R. (2017). Naturalness preserving image recoloring method for people with red-green deficiency. *Signal Processing: Image Communication*, *57*, 126 - 133.

Hassan, M. F., Paramesran, R., Tanaka, Y., & Tanaka, K. (2018). A method using uniform yellowing pigmentation to model the color perception of the elderly people. *Signal, Image and Video Processing*, *12(6)*, 1019 - 1026.

Hegde, A. L., & Bishop, N. (2018). Saturation based color appearance of objects: a comparison between healthy elderly, young adults, and young adults wearing goggles simulating cataract. *Building and Environment*, *127*, 148 - 156.

Huang, J. B., Chen, C. S., Jen, T. C., & Wang, S. J. (2009). Image recolorization for the colorblind. *IEEE International Conference on Acoustics, Speech and Signal Processing*, 1161 - 1164.

Huang, J. B., Tseng, Y. C., Wu, S. I., & Wang, S. J. (2007). Information preserving color transformation for protanopia and deuteranopia. *IEEE Signal Processing Letters*, *14*(10), 711 - 714.

Hunt, R. W. G. (2004). *The reproduction of colour*. John Wiley & Sons.

Ichikawa, M., Tanaka, K., Kondo, S., Hiroshima, K., Ichikawa, K., Tanabe, S., & Fukami, K. (2003). Web-page color modification for barrier-free color vision with genetic algorithm. *Genetic and Evolutionary Computation - GECCO*, *2724*, 2134 - 2146.

Ishihara, K., Ishihara, S., Nagamachi, M., Hiramatsu, S., & Osaki, H. (2001). Age-related decline in color perception and difficulties with daily activities-measurement, questionnaire, optical and computer-graphics simulation studies. *International Journal of Industrial Ergonomics*, *28*, 153 - 163.

Ishihara, K., Ishihara, S., Nagamachi, M., & Osaki, H. (1997). Difficulties for elderly people caused by age-related yellowing vision. *Proceedings of Trienniel Congress of the International Ergonomics Association*, *5*, 579 - 581.

Ishihara, S. (1979). *Tests for colour-blindness*. Tokio: Kanehara Shuppan Co. Ltd.

Jefferson, L., & Harvey, R. (2006). Accomodating color blind computer users. *Proceedings of the 8th international ACM SIGACCESS Conference on Computers and Accessibility*, 40 - 47.

Jeong, J. Y., Kim, H. J., Wang, T. S., & Yoon, Y. J. (2011). An efficient re-coloring method with information preserving for the color-blind. *IEEE Transactions on Consumer Electronics*, *57*(4), 1953 - 1960.

Judd, D. B. (1949). The color perceptions of deuteranopic and protanopic observers. *Journal of the Optical Society of America*, *39*(3), 252 - 256.

Kadlecova, V., Peleska, M., & Vasko, A. (1958). Dependance on age of the diameter of the pupil in the dark. *Nature*, *182*, 1520 - 1521.

Kuhn, G. R., Oliviera, M. M., & Fernandes, L. A. F. (2008). An efficient naturalness-preserving image-recoloring method for dichromats. *IEEE Transactions on Visualization and Computer Graphics*, *14*(6), 1747 - 1754.

Lee, J., & dos Santos, W. P. (2011). An adaptive fuzzy-based system to simulate, quantify and compensate color blindness. *Integrated Computer-Aided Engineering*, *18*, 29 - 40.

Lerman, S. (1983). An experimental and clinical evaluation of lens transparency and aging. *Journal of Gerontology*, *38*(3), 293 - 301.

Ma, Y., Gu, X. D., & Wang, Y. Y. (2006). A new color blindness cure model based on bp neural network. *Advances in Neural Networks - ISNN 2006*, *3973*, 740 - 745.

Machado, G. M., & Oliveira, M. M. (2010). Real-time temporal-coherent color constrast enhancement for dichromats. *Proceedings of the 12th Eurographics / IEEE - VGTC conference on Visualization*, 933 - 942.

Machado, G. M., Oliveira, M. M., & Fernandes, L. A. F. (2009). A physiologically-based model for simulation of color vision deficiency. *IEEE Transactions on Visualization and Computer Graphics*, *15*(6), 1291 - 1298.

Malacara, D. (2011). *Color vision and colorimetry: Theory and applications*. SPIE Press.

Martin, D., Fowlkes, C., Tal, D., & Malik, J. (2001). A database of human segmented natural images and its application to evaluating segmentation algorithms and measuring ecological statistics. *IEEE International Conference on Computer Vision*, *2*, 416 - 423.

Meyer, G. W., & Greenberg, D. P. (1988). Color-defective vision and computer graphics displays. *IEEE Computer Graphics and Applications*, *8*(5), 28 - 40.

Montag, E. D. (2006). Empirical formula for creating error bars for the method of paired comparison. *Journal of Electronic Imaging*, *15*(1).

Moreira, H., Alvaro, L., Melnikova, A., & Lillo, J. (2018). Colorimetry and dichromatic vision, colorimetry and image processing carlos travieso-gonzalez. In (p. 1 - 21). IntechOpen.

Neitz, J., & Neitz, M. (2011). The genetics of normal and defective color vision. *Vision Research*, *51*, 633 - 651.

Nguyen, D. T., Overbury, O., & Faubert, J. (2003). The role of lenticular senescence in age-related color vision changes. *Investigative Ophthalmology and Visual Science*, *44*(8), 3698 - 3704.

Norren, D. V., & Vos, J. J. (1974). Spectral transmission of the human ocular media. *Vision Research*, *14*, 1237 - 1244.

Okajima, K., & Takase, M. (2001). Computerized simulation and chromatic adaptation experiments based on a model of aged human lens. *Optical Review*, *8*(1), 64 - 70.

Oliveira, M. M. (2013). Towards more accessible visualizations for color-vision-deficient individuals. *Computing in Science and Engineering*, *15*(5), 80 - 87.

Ortiz, E., Bowyer, K. W., & Flynn, P. J. (2013). A linear regression analysis of the effects of age related pupil dilation change in iris biometrics. *IEEE International Conference on Biometrics: Theory, Applications and Systems (BTAS)*, 1 - 6.

Pascale, D. (2003). *A review of rgb color spaces ... from xyy to r'g'b'*. The BabelColor Company.

Pokorny, J., Smith, V. C., & Lutze, M. (1986). Aging of the human lens. *Applied Optics*, *26*(8), 1437 - 1440.

Poynton, C. A. (1995). A guided tour of colour space. *New Foundation for Video Technology: The SMPTE Advanced Television and Electronic Imaging Conference*.

Rasche, K., Geist, R., & Westall, J. (2005a). Detail preserving reproduction of color images for monochromats and dichromats. *IEEE Computer Graphics and Applications*, *25*(3), 22 - 30.

Rasche, K., Geist, R., & Westall, J. (2005b). Re-coloring images for gamuts of lower dimension. *Computer Graphics Forum*, *24*(3), 423 - 432.

Ribeiro, M. G., & Gomes, A. J. P. (2013). A skillet-based recoloring algorithm for dichromats. *International Conference on e-Health Networking, Applications and Services*, 702 - 706.

Rigden, C. (1999). The eye of the beholder - designing for colour-blind users. *British Telecommunications Engineering*, *17*, 2 - 6.

Rodriquez-Pardo, C. E., & Sharma, G. (2011). Dichromatic color perception in a two stage model: testing for cone replacement and cone loss models. *IEEE IVMSP Workshop*, 12 - 17.

Romano, G., Mercatelli, L., Fusi, F., Guasti, A., Favuzza, E., Monici, M., & Mencucci, R. (2011). Colorimetric comparison of light-filtering intraocular lelens and human crystalline lenses at various ages. *Journal of Cataract and Refractive Surgery*, *37*(4), 758 - 762.

Roy, M. S., Podgor, M. J., Collier, B., & Gunkel, R. D. (1991). Color vision and age in a normal north american population. *Graefe's Archive for Clinical and Experimental Ophthalmology*, *229*, 139 - 144.

Ruddock, K. H. (1965a). The effect of age upon colour vision - ii. changes with age in light transmission of the ocular media. *Vision Research*, *5*, 47 - 58.

Ruddock, K. H. (1965b). The effect of age upon colour vision - i. response in the receptoral system of the human eye. *Vision Research*, *5*, 37 - 45.

Said, F. S., & Sawires, W. S. (1972). Age dependance of changes in pupil diameter in the dark. *Optica Acta*, *19*(5), 359 - 361.

Said, F. S., & Weale, R. A. (1959). The variation with age of the spectral transmissivity of the living human crystalline lens. *Gerontologia*, *3*(37), 213 - 231.

Salvi, S. M., Akhtar, S., & Currie, Z. (2006). Ageing changes in the eye. *Postgraduate*

Medical Journal, *82*(971), 581 - 587.

Savage, G. L., Haegerstrom-Portnoy, G., Adams, A. J., & Hewlett, S. E. (1993). Age changes in the optical density of human ocular media. *Clinical Vision Science*, *8*, 97 - 108.

Schneck, M. E., Adams, A. J., Huie, K., & Lee, E. (1993). A filter for simulating color and spatial vision of the elderly. *Colour Vision Deficiencies XI*, 357 - 364.

Schubert, E. F. (1996). *Light-emitting diodes*. Cambridge University Press.

Semary, N. A., & Marey, H. M. (2014). An evaluation of computer based color vision deficiency test: Egypt as a study case. *International Conference on Engineering and Technology (ICET)*, 1 - 7.

Sharma, G., Wu, W., & Dalal, E. N. (2005). The ciede2000 color-difference formula: Implementation notes, supplementary test data and mathematical observations. *COLOR Research and Application*, *30*(1), 21 - 30.

Sharpe, L. T., Stockman, A., Jagle, H., & Nathans, J. (1999). *Color vision: From genes to perception*. Cambrigde University Press.

Sheikh, H. R., Sabir, M. F., & Bovik, A. C. (2006). A statistical evaluation of recent full reference quality assessment algorithms. *IEEE Transactions on Image Processing*, *15*(11), 3440 - 3451.

Shinomori, K. (2005). Ageing effects on colour vision changed and unchanged perception . *Congress of the International Colour Association*, 7 - 12.

Simon-Liedtke, J. T., & Farup, I. (2016). Evaluating color vision deficiency daltonization method using a behavorial visual-search method. *Journal of Visual Communication and Image Representation*, *35*, 236 - 247.

Simunovic, M. P. (2016). Acquired color vision deficiency. *Survey of Ophthalmology*, *61*, 132 - 155.

Sloan, L. L. (1939). Instruments and techniques for the clinical testing of light sense. *Archives of Ophthalmology*, 258 - 270.

Smith, V., & Pokorny, J. (1995). Spectral sensitivity of the foveal cone photopigments between 400 and 500 nm. *Vision Research*, *15*, 161 - 171.

Soundararajan, R., & Bovik, A. C. (2013). Survey of information theory in visual quality assessment. *Signal, Image and Video Processing*, *7*(3), 391 - 401.

Stiles, W. S., & Burch, J. M. (1955a). Interium report to the cie, zurich, 1955, on the national physical laboratory's investigation of colour-matching. *Optica Acta*, *2*, 168 - 181.

Stiles, W. S., & Burch, J. M. (1955b). Interium report to the cie, zurich, 1955, on the national physical laboratory's investigation of colour-matching. *Optica Acta*, *2*, 168 - 181.

Stiles, W. S., & Burch, J. M. (1959). N.p.l. colour-matching investigation: final report (1958). *Optica Acta*, *6*(1).

Suetake, N., Tanaka, G., Hashii, H., & Uchino, E. (2012). Simple lightness modification for color vision impaired based on craik-o'brien effect. *Journal of Franklin Institute*, *349*, 2093 - 2107.

Suzuki, R., Tanaka, Y., Aguirre, H., Tanaka, K., Yokoyama, S., Nakamura, H., ... Tanabe, S. (2012). Color compensation method to display images looking similar to their original ones for elderly people. *Proceedings of the IIEEJ Image Electronics and Visual Computing Workshop*.

Suzuki, T., Okajima, K., & Funai, T. (2012). Optical simulation of reduced retinal illuminance caused by senile miosis. *Optical Review*, *19*(3), 174 - 181.

Suzuki, T., Qiang, Y., Sakuragawa, S., Tamura, H., & Okajima, K. (2006). Age-related changes of reaction time and p300 for low-contrast color stimuli: effects of yellowing of the aging human lens. *Journal of Physiological Anthropology*, *25*(2), 179 - 187.

Suzuki, T., Yi, Q., Sakuragawa, S., Tamura, H., & Okajima, K. (2005). Comparing the visibility of low-contrast color landolt-cs: Effect of aging human lens. *Color Research and Application*, *30*, 5 - 12.

Tagarelli, A., Piro, A., Tagarelli, G., Lantieri, P. B., Risso, D., & Olivieri, R. L. (2004). Colour blindness in everyday life and car driving. *Acta Ophthalmologica Scandinavica*, *82*(4), 436 - 442.

Tanaka, Y., Tanaka, K., Yokoyama, S., Nakamura, H., Ichikawa, K., & Tanabe, S. (2011). An improved simulation method of color perception by elderly people based on measured luminescence spectrum and color constancy relaxation. *Journal of the Institute of Image Electronics Engineers of Japan*, *40*(1), 86 - 95.

Thomas, O. (2012). *Facebook: Users upload 300 million images a day (so please let us buy instagram).* Retrieved from `http://www.businessinsider.com/facebook-images-a-day-instagram-acquisition-2012-7/?IR=T`

Thurstone, L. L. (1927). A law of comparative judgment. *Psychological Review*, *34*(4), 273 - 286.

Travis, D. (1991). *Effective color display, theory and practice*. Academic Press.

Tsukida, K., & Gupta, M. R. (2011). How to analyze paired comparison data. *UWEE Technical Report*.

Ueda, C., Azetsu, T., Suetake, N., & Uchino, E. (2015a). Gamma correction-based image enhancement for elderly vision. *International Symposium on Communications and Information Technologies*, 141 - 144.

Ueda, C., Azetsu, T., Suetake, N., & Uchino, E. (2015b). Light transform method considering visual feature of elderly vision. *International Symposium on Intelligent Signal Processing and Communication Systems*, 62 - 65.

Ueda, C., Azetsu, T., Suetake, N., & Uchino, E. (2016). Improvement in appearance of colors for elderly persons using lightness transform. *The Optical Society of Japan*, *23*, 917 - 925.

Verriest, G. (1963). Further studies on acquired deficiency of color discrimination. *Journal of the Optical Society of America*, *53*(1), 185 - 195.

Vienot, F., Brettel, H., & Mollon, J. D. (1999). Digital video colourmaps for checking the legibility of displays by dichromats. *COLOR Research and Application*, *24*(4), 243 - 252.

Vienot, F., Brettel, H., Ott, L., M'Brek, A. B., & Mollon, J. D. (1995). What do colour-blind people see? *Nature*, *376*, 127 - 128.

Wachtler, T., Dohrmann, U., & Hertel, R. (2004). Modeling color percepts of dichromats. *Vision Research*, *44*, 2843 - 2855.

Wakita, K., & Shimamura, K. (2005). Smartcolor: disambiguation framework for the colorblind. *Proceedings of the 7th International ACM SIGACCESS Conference on Computers and Accessibility*, 158 - 165.

Wandell, B. A. (1995). *Foundations of vision*. Sinauer Associates.

Weale, R. A. (1961a). Notes on the photometric significance of the human crystalline lens. *Vision Research*, *1*, 183 - 191.

Weale, R. A. (1961b). Retinal illumination and age. *Lighting Research and Technology*, *26*(2), 95 - 100.

Weale, R. A. (1988). Age and the transmittance of the human crystalline lens. *Journal of Physiology*, *395*, 577 - 587.

Werner, J. S., Peterzell, D. H., & Scheetz, A. J. (1990). Light, vision, and aging. *Optometry and Vision Science*, *67*(3), 214 - 229.

Werner, J. S., & Steele, V. G. (1988). Sensitivity of the human foveal color mechanisms throughout the life span. *Journal of the Optical Society of America*, *5*, 2122 - 2130.

Winn, B., Whitaker, D., Elliott, D. B., & Phillips, N. J. (1994). Factors affecting light-adapted pupil size in normal human subjects. *Investigative Ophthalmology & Visual Science*, *35*(3), 1132 - 1137.

Wright, W. D. (1928). A re-determination of the trichromatic coefficients of the spectral colours. *Transactions of the Optical Society*, *30*(4), 141 - 161.

Xu, J., Pokorny, J., & Smith, V. C. (1997). Optical density of the human lens. *Journal of the Optical Society of America*, *14*(5), 953 - 960.

Yamazaki, A. K., & Eto, K. (2015). A preliminary experiment to investigate the effects of blue backgrounds on a tablet screen for elderly people. *International Conference in Knowledge Based and Intelligent Information and Engineering Systems*, *60*, 1490 - 1496.

Yang, S., & Ro, Y. M. (2003). Visual contents adaptation for color vision deficiency. *International Conference on Image Processing*, *1*, 453 - 456.

Yoshida, C. A., & Sakuraba, S. (1996). The use of films to simulate age-related decline in yellow vision. *Journal of Occupational Rehabilitation*, *6*(2), 119 - 134.

Zhang, L., Zhang, L., Mou, X., & Zhang, D. (2011). Fsim: a feature similarity index for image quality assessment. *IEEE Transactions in Image Processing*, *20*(8), 2378 - 2386.